



EG0900028

Ain Shams University
Faculty of Science
Chemistry Department

**Radiation Effects on Some Polymeric
Materials and Their Utilization for
Possible Practical Applications**

Thesis
Submitted To
Faculty of Science
Ain Shams University

**In partial fulfillment of the requirements
Of the Master Degree in Chemistry
(MSc.)**

By

**Ahmed Mohamed Elbarbary Ahmed Refaee
(BSc. 2002)
(2008)**

Radiation Effects on Some Polymeric Materials and Their Utilization for Possible Practical Applications

THESIS ADVISORS:

Approved

Prof. Dr. El-Sayed Ahmed Soliman Abd El-Aziz

Prof. Dr. Naeem Mohamed El-Sawy

Prof. Dr. Hassan Ahmed Abd El-Rehim

Head of Chemistry

Department

Prof. Dr. El-Sayed A. Soliman

Radiation Effects on Some Polymeric Materials and Their Utilization for Possible Practical Applications

By

Ahmed Mohamed Elbarbary Ahmed Refaee

(B.Sc. 2002)

This Thesis for M.Sc. Degree has been approved by:

Prof.Dr / Abo Elkhair B. Mostafa

Prof.Dr / Maher Zaki Elsabee

Prof. Dr / El-Sayed Ahmed Soliman Abd El-Aziz

Prof. Dr / Naeem Mohamed El-Sawy

Date of Examination: 20/07/2008

Contents

Aim of Work.....

List of Figures.....

List of Tables.....

List of Abbreviation.....

<i>Chapter I Introduction</i>	
I.1- Radiation Processing of Polymeric Materials	1
I.2- Naturally Occurring Polymers	2
I.2.1- Cellulose and Cellulose Ether CarboxyMethylCellulose - Sodium Salt (CMC- Na)	3
I.2.2- Chitosan	4
I.2.3- Sodium Alginate	5
I.3- Radiation Processing of Natural Occurring Polymers	5
I.4- Combined Radiation and Conventional Processes for Efficient Processing of Natural Polymers	6
I.5- Specific Advantages of Radiation Processing Over Other Chemical Alternatives	7
I.6- Applications of Radiation Processed Natural Polymers	8
I.6.1- Induction of Biological Activities	8
I.6.1.1- Anti-microbial Activity	8
I.6.1.2- Phytoalexin Elicitor Activity	9
I.6.1.3- Suppression of Environmental Stress on Plants	9
I.6.1.4- Enhancement of Antioxidant Activity	10
I.6.2- Bio-medical Applications	10
I.6.3- Development of Biodegradable Plastics	11
I.6.4- Development of Hybrid Technologies for Processing of Cellulose Based Materials	11
I.6.5- Adsorption of Metal Ions	12
I.6.6- Removal of Dyes	12

I.7- Radiation Processed Low Molecular-Weight Polysaccharides for Use as a Growth Promoters in Agricultural Purposes	12
II. Radiation Graft Copolymerization of VAc/HEMA Binary Monomer Onto poly(tetraflouroethylene-perflourovinyl ether) (PFA) Films	14
II.1. Principles of Copolymerization Grafting	14
II.2. Radiation Grafting Technique	16
II.3. Methods of Radiation Induced Grafting	16
II.3.1. Simultaneous (Direct or Mutual) Irradiation Method	17
II.3.2. Pre-irradiation Method (Post-irradiation Grafting)	17
I.4. Applications of Grafted Membranes	18
II.4.1. Hemodialysis and Bioapplications	18
II.2.4.2. Metal-Complex Membranes	20
<i>Chapter II Literature Review</i>	
II.1- Radaition Degradartion Process of Naturally Occurring polymers	23
II.2 Thermal and Chemical Degradartion Processes of Naturally Occurring polymers	39
II.3- Possible Applications of Degraded Naturally Occurring Polymers	49
II.4- Radiation-Induced Graft Copolymerization and Their Possible Applications	60
<i>Chapter III Experimental</i>	87
III.1-Materials	87

III.2. Apparatus and Methods	88
III.2.1-Gamma Radiation Source	88
III.2.2- Preparation of Low Molecular Weights of Naturally Occurring Polymers	89
III.2.2.1- Gamma Irradiation Method	89
III.2.2.2- Chemical and Thermal Treatment Method	89
III.2.3- Determination the Intrinsic Viscosity of Degraded Naturally Occurring Polymers	89
III.2.4- Determination the Molecular Weight of Degradable Naturally Occurring Polymers	90
III.2.4.1- The Viscometric Method	90
III.2.4.2- Gel permeation chromatography (GPC) Method	91
III.2.5. Separation of Water Soluble Chitosan	92
III.2.6- Plantation	92
III.2.7- Radiation-Induced Graft Copolymerization of VAc / HEMA Binary Monomers onto PFA Films	93
III.2.8- Synthesis of Metal-doped Graft Copolymer	93
III.2.9- Platelet Adhesion Assessment	94
III.2.10- pH Measurements	94
III.2.11- Infra - red Spectroscopy (FTIR)	94
III.2.12- Ultra Violet Spectroscopy (UV-Vis)	95
III.2.13- X-ray Fluorescence Measurements	95
III.2.14- Mechanical Measurements	95
III.2.15- Differential Scanning Calorimetry (DSC)	95
III.2.16- Thermal Gravimetric Analysis (TGA)	96
III.2.17- X-Ray Diffraction (XRD)	96
III.2.18- Scanning Electron Microscopy (SEM)	96
III 2.19- Electron Spin Resonance (ESR)	96
III.2.20- Electrical Conductivity Measurement	96
<i>Chapter IV</i> <i>Results and Discussion</i>	
IV.I- Controlling the Radiation Degradation Process of Some Naturally Occurring Polymers	97
IV.I.1- Effect of Gamma Irradiation on Polymeric	97

Materials	
IV.I.2- Effect of Gamma Irradiation on the Degradation process of Some Natural Polymers in the Presence of Some Initiators	100
IV.I.3- Effect of Initiator Concentration on Degradation of Natural Polymers Induced by Gamma Irradiation	106
IV.I.4- Degradation of Chitosan, Sodium Alginate and CMC by Gamma Irradiation in Comparison with Thermal Treatments Using Initiators	110
IV.I.5- Effect of Irradiation Dose on Degradation of Natural Polymers: Determination of the Molecular Weight and the Synergetic Effect	115
IV.I.5.1- Viscometric Method	115
IV.I.5.2- Gel Permeation Chromatography (GPC) Method	122
IV.I.6- Characterization of Degraded Naturally Occurring Polymers	130
IV.I.6.1- UV-Vis Spectroscopy	130
IV.I.6.2- XRD Analysis	135
IV.I.6.3- TGA Analysis	140
IV.I.6.4- ESR Analysis	146
IV.I.7- Applications of Degraded Naturally Occurring Polymers as Growth Promoters in Agricultural Purposes	150
IV.II- Radiation Graft Copolymerization of VAc/HEMA Binary Monomer Onto poly(tetraflouroethylene-perflourovinyl ether) (PFA) Films	164
IV.II.1- Effect of Preparation Conditions on the Grafting Yield	164
IV.II.1.1- Effect of Solvent	164
IV.II.1.2- Effect of Inhibitor Concentration	165
II.1.3- Effect of Monomer and Comonomer Concentrations	168

IV.II.1.3.1- Effect of Monomer Concentration	168
IV.II.1.3.2. Effect of Comonomer Concentration	168
IV.II.1.4- Effect of Comonomer Composition	172
IV.II.1.5- Effect of Irradiation Dose	172
IV.II.2- Characterization of the Grafted Membranes	176
IV.II.2.1- FTIR Spectroscopy	176
IV.II.2.2- Mechanical Analysis	176
IV.II.2.3- Thermal Gravimetric Analysis (TGA)	181
IV.II.2.4- Morphological Structure	183
IV.II.3- Applications of Grafted Membranes	185
IV.II.3.1- Platelet Adhesion Assessment	185
IV.II.3.2- Polymer Metal - Complex Membranes	189
IV.II.3.2.1- FTIR Spectroscopy	189
IV.II.3.2.2- UV- Vis Measurements	189
IV.II.3.2.3- X-ray Fluorescence Measurements	193
IV.II.3.2.4- Electron Spin Resonance (ESR)	193
IV.II.3.2.5- TGA Analysis	196
IV.II.3.2.6- Electrical Conductivity Measurements	198
IV.II.3.2.7- - Surface Morphology	199
<i>Summary and Conclusion</i>	202
<i>References</i>	208

Aim of the Work

In recent years, naturally occurring polymers are being looked at again with renewed interest because of their unique characteristics like inherent biocompatibility, biodegradability and easy availability. Polysaccharides such as cellulose, starch, chitin/ chitosan and their water-soluble derivatives have a variety of application in many fields. A further progress in natural polymers processing is foreseen.

Naturally occurring polymers or their derivatives under normal conditions of irradiation undergo chain scission reaction. In this respect, the present study is interested with controlling the degradation process of chitosan, sodium alginate and CMC by gamma ray from a ^{60}Co - source in presence of some initiators such as ammonium per-sulfate and hydrogen peroxide. The factors affecting the degradation process such as irradiation dose, initiator type and its concentration will be studied. The molecular weight of degraded polymers is determined by viscometric method and GPC technique. Characterization of degraded natural polymer by UV-Vis spectroscopy, XRD, TGA and ESR analysis will be examined. The possibility of using such degraded natural polymers in the field of agriculture will be investigated.

Radiation grafting is one of the most promising methods because of the easy handling at room temperature, large

penetration in polymer matrix, rapid and uniform formation of active sites for initiating grafting throughout the matrix under appropriate experimental conditions for homogeneous diffusion of monomer in the polymer *Mukherjee and Gupta (1985)*. The objective of the modification of polymers by radiation-induced grafting are: (1) Preparation and development of new materials more efficient and stimuli-responsive for many applications such as in separation and purification purposes. (2) The selection of reactive groups may lead to stimuli-responsive and purification purposes in different applications; such as in industrial and biomedical applications. (3) The applicability of the polymers for removal, separation and purification of some bio-molecules.

In this respect, the direct radiation grafting of Vac / HEMA binary monomers onto PFA copolymer membranes was used to synthesize graft copolymer membranes of complexing ability with some selected transition metal ions such as Cu^{2+} and Cr^{3+} ions in aqueous solution. Physiochemical characterizations of the prepared graft copolymers were carried out by FTIR, UV-Vis, XRF, ESR and TGA analysis. Mechanical properties and SEM were investigated. The possibility of these graft copolymer membranes can be used in the field of blood biocompatibility and in waste treatment of some heavy metals in the environmental industrial wastes.

List of Figures

<i>Caption</i>	<i>Page No.</i>
Figure (1): Changes in the viscosity average molecular weights of (●) chitosan, (○) CMC and (▼) sodium alginate (solid form) when exposed to gamma irradiation.	99
Figure (2): The effect of some initiators on degradation process of sodium alginate induced by gamma irradiation at 80 kGy or thermal heating at 70°C.	102
Figure (3): The effect of some initiators on degradation process of chitosan induced by gamma irradiation at 80 kGy or thermal heating at 70°C..	103
Figure (4): The effect of some initiators on degradation process of CMC induced by gamma irradiation at 80 kGy or thermal heating at 70°C.	104
Figure (5): The effect of ammonium per-sulfate concentration on degradation of sodium alginate (paste) induced by gamma irradiation at 80 kGy as a function of the change in viscosity average molecular weight,	107
Figure (6): The effect of ammonium per-sulfate concentration on degradation process of chitosan (paste) induced by gamma irradiation at 80 kGy as a function of the change in viscosity average molecular weight.	108
Figure (7): The effect of ammonium per-sulfate concentration on degradation process of CMC (paste) induced by gamma irradiation at 80 kGy as a function of the change in viscosity average molecular weight.	109
Figure (8): Effect of treatment time on the degradation of chitosan (paste) as a function of the changes in its viscosity average molecular weight in the presence of	112

<p>initiators using gamma irradiation or thermal heating at 70°C. (●) γ-irradiation only (○) 10% H₂O₂ (v/w) at 70 °C (▼) 10% APS (w/w) at 70 °C, (Δ) 10% H₂O₂ (v/w) γ-irradiation and (■) 10% APS (w/w) γ-irradiation.</p>	
<p>Figure (9): Effect of treatment time on the degradation of sodium alginate (paste like condition) as a function of the change in its viscosity average molecular weight in presence of initiators using gamma irradiation or thermal heating at 70°C. (●) γ-irradiation only (○) 10% H₂O₂ (v/w) at 70 °C (▼) 10% APS (w/w) at 70 °C, (Δ) 10% H₂O₂ (v/w) γ-irradiation and (■) 10% APS (w/w) γ-irradiation.</p>	113
<p>Figure (10): Effect of treatment time on the degradation of CMC (paste) as a function of the change in its viscosity average molecular weight in presence of initiators using gamma irradiation or thermal heating at 70°C. (●) γ-irradiation only (○) 10% H₂O₂ (v/w) at 70 °C (▼) 10% APS (w/w) at 70 °C, (Δ) 10% H₂O₂ (v/w) γ-irradiation and (■) 10% APS (w/w) γ-irradiation.</p>	114
<p>Figure (11): The changes in the viscosity average molecular weight of pure chitosan when exposed to gamma irradiation: (●) γ-irradiation only and that mixed with (○) 10% H₂O₂ (v/w) (▼) 20% H₂O₂ (Δ) 10% KPS and (■) 10% APS (w/w).</p>	118
<p>Figure (12): The changes in the viscosity average molecular weight of pure sodium alginate on exposure to gamma irradiation (●) γ-irradiation only and that mixed with (○) 10% H₂O₂ (v/w) (▼) 20% H₂O₂, (Δ) 10% KPS and (■) 10% APS (w/w).</p>	119
<p>Figure (13): The changes in the viscosity average molecular weight of pure CMC on exposure to gamma irradiation (●) γ-irradiation only and that mixed with (○) 10% H₂O₂ (v/w) (▼) 20% H₂O₂, (Δ) 10% KPS and (■) 10% APS (w/w).</p>	120

Figure (14): GPC elution curves of sodium alginates as a function of retention time (a) blank, (b) irradiated at 120 kGy, (c) treated by 10% APS at 120 kGy and (d) treated by 10% H ₂ O ₂ at 120 kGy.	123
Figure (15): The changes in the number average molecular weight of chitosan measured by GPC when exposed to gamma irradiation and that mixed with 10% H ₂ O ₂ (v/w) or 10% APS (w/w) beside gamma irradiation (●) after irradiation and (○) after storing for 2 months.	126
Figure (16): The changes in the number average molecular weight of sodium alginate measured by GPC when exposed to gamma irradiation and that mixed with 10% H ₂ O ₂ (v/w) or 10% APS (w/w) beside gamma irradiation (●) after irradiation and (○) after storing for 2 months.	127
Figure (17): The changes in the number average molecular weight of CMC measured by GPC when exposed to gamma irradiation and that mixed with 10% H ₂ O ₂ (v/w) or 10% APS (w/w) beside gamma irradiation (●) after irradiation and (○) after storing for 2 months.	128
Figure (18): UV-Vis spectra of (a) pure chitosan and that mixed with 10 (wt%) ammonium per-sulfate at different irradiation doses of (b) 40 kGy, (c) 80 kGy, (d) 120 kGy, (e) 160 kGy and (f) 200 kGy.	132
Figure (19): UV-Vis spectra of (a) pure sodium alginate and that mixed with 10 (wt%) APS at different irradiation doses of (b) 40 kGy, (c) 80 kGy, (d) 120 kGy, (e) 160 kGy and (f) 200 kGy.	133
Figure (20): UV-Vis spectra of (a) pure CMC and that mixed with 10 (wt%) APS at different irradiation doses of (b) 40 kGy, (c) 80 kGy, (d) 120 kGy, (e) 160 kGy and (f) 200 kGy.	134

Figure (21): XRD spectra of (a) pure chitosan and that mixed with 10 (wt%) ammonium per-sulfate at different irradiation doses of (b) 40 kGy, (c) 120 kGy and (d) 200 kGy.	137
Figure (22): XRD spectra of (a) pure sodium alginate and that mixed with 10 (wt%) ammonium per-sulfate at different irradiation doses of (b) 40 kGy, (c) 120 kGy and (d) 200 kGy.	138
Figure (23): XRD spectra of (a) pure CMC and that mixed with 10 (wt%) ammonium per-sulfate at different irradiation doses of (b) 40 kGy, (c) 120 kGy and (d) 200 kGy.	139
Figure (24): TGA diagram of (—) pure chitosan and that mixed with 10 wt% ammonium per-sulfate at different irradiation doses of (····) 40 kGy, (---) 120 kGy and (·-·-·-·) 200 kGy.	142
Figure (25): TGA diagram of (—) pure sodium alginate and that mixed with 10 (wt%) ammonium per-sulfate at different irradiation doses of (····) 40 kGy, (---) 120 kGy and (·-·-·-·) 200 kGy.	143
Figure (26): TGA diagram of (—) pure CMC and that mixed with 10 (wt%) ammonium per-sulfate at different irradiation doses of (····) 40 kGy, (---) 120 kGy and (·-·-·-·) 200 kGy.	144
Figure (27): ESR spectrum of (a) pure chitosan irradiated at dose of 120 kGy and that mixed with (b) 10 (wt%) APS and (c) 10% H ₂ O ₂ (v/w) at the same dose were measured after 1, 8 and 15 day.	147
Figure (28): ESR spectrum of (a) pure sodium alginate irradiated at dose of 120 kGy and that mixed with (b) 10 (wt%) APS and (c) 10% H ₂ O ₂ (v/w) at the same dose were measured after 1, 8 and 15 day.	148
Figure (29): ESR spectrum of (—) pure CMC irradiated at dose of 120 kGy and that mixed with (...) 10 (wt %) APS and (---) 10% H ₂ O ₂ (v/w) at the same	149

dose were measured after 1, 8 and 15 day.	
Figure (30): Effect of degraded sodium alginate on growth of zea maize plant: (a) control and spraying the plant by 100 ppm of sodium alginate solution in water, (b) pure one, (c) pure one irradiated at 200 kGy and that mixed with 10 % APS at different irradiation doses of (d) 40 kGy, (e) 80 kGy, (f) 120 kGy, (g) 160 kGy and (h) 200 kGy.	154
Figure (31): Growth of zea maize cob yield size (a) control and that sprayed by 100 ppm of sodium alginate (b) irradiated at 200 kGy and (c) mixed with 10% APS at 200 kGy.	155
Figure (32): Effect of degraded chitosan on growth of maize plant: (a) control and spraying the plant by 100 ppm of chitosan solution in water, (b) pure one, (c) pure one irradiated at 200 kGy and that mixed with 10 % APS at different irradiation doses of (d) 40 kGy, (e) 80 kGy, (f) 120 kGy, (g) 160 kGy and (h) 200 kGy.	157
Figure (33): Growth of zea maize cob yield size (a) control and that mixed with 100 ppm of chitosan, (b) irradiated at 200 kGy and (c) treated with 10% APS at 200 kGy.	158
Figure (34): Effect of degraded sodium alginate on growth of soybean plant: (a) control and spraying the plant by 100 ppm of sodium alginate solution in water, (b) pure one, (c) pure one irradiated at 200 kGy and that mixed with 10 % APS at different irradiation doses of (d) 40 kGy, (e) 80 kGy, (f) 120 kGy, (g) 160 kGy and (h) 200 kGy.	160
Figure (35): Effect of degraded chitosan on growth of faba bean plant: (a) control and spraying the plant by 100 ppm of chitosan solution in water, (b) pure one, (c) pure one irradiated at 200 kGy and that mixed with 10 % APS at different irradiation doses of (d) 40 kGy, (e) 80 kGy, (f) 120 kGy, (g) 160 kGy and (h) 200	162

kGy.	
Figure (36): Schematic diagram for the effect of different solvents as a function of the degree of grafting of VAc/HEMA binary monomers onto PFA films using 50% comonomer concentration, (50:50) comonomer composition, irradiation dose 30 kGy, and dose rate 1.85 Gy/s.	166
Figure (37): Effect of inhibitor concentration on the degree of grafting of VAc/HEMA binary monomers onto PFA films using methanol as a solvent, 50% comonomer concentration, (50:50) comonomer composition, irradiation dose 30 kGy, and dose rate 1.85 Gy/s.	167
Figure (38): Effect of monomer concentration on the degree of grafting of (●) VAc and (○) HEMA monomers onto PFA films using methanol as a solvent, 0.1 (wt%) FeCl ₃ as inhibitor, irradiation dose 30 kGy and dose rate 1.85 Gy/s.	170
Figure (39): Effect of comonomer concentration on the degree of grafting of VAc/HEMA binary monomers onto PFA films using methanol as a solvent, 0.1 (wt%) FeCl ₃ as inhibitor, (50:50) VAc/HEMA comonomer composition, irradiation dose 30 kGy and dose rate 1.85 Gy/s.	171
Figure (40): Effect of comonomer composition on the degree of grafting of VAc/HEMA binary monomers onto PFA films using methanol as a solvent, 0.1 (wt %) FeCl ₃ as inhibitor, 50% comonomer concentration, irradiation dose 30 kGy and dose rate 1.85 Gy/s.	174
Figure (41): Effect of irradiation dose on the degree of grafting of VAc/HEMA binary monomers onto PFA films using methanol as a solvent, 0.1 (wt %) FeCl ₃ as inhibitor, 50% comonomer concentration, (70/30) VAc/HEMA comonomer composition, respectively and dose rate 1.85 Gy/s.	175

Figure (42): FTIR spectra of (a) trunk PFA, (b) PFA-g-pVAc, (c) PFA-g-pHEMA and (d) its graft copolymer PFA-g-p(VAc/HEMA).	178
Figure (43): The change in elongation at break percent and tensile strength, respectively with monomer concentration of grafted PFA films by (●) VAc and (○) HEMA using methanol as a solvent, 0.1 (wt%) FeCl ₃ inhibitor and irradiation dose 30 kGy and dose rate 1.85 Gy/s.	179
Figure (44): The change in elongation at break percent and tensile strength, respectively with VAc/HEMA comonomer composition of grafted PFA films using methanol as a solvent, 0.1 (wt%) FeCl ₃ inhibitor, 50% comonomer concentration, irradiation dose 30 kGy and dose rate 1.85 Gy/s.	180
Figure (45): TGA diagram of (a) trunk PFA, (b) PFA-g-pVAc, (c) PFA-g-pHEMA and its graft copolymer (d) PFA-g-p(VAc/HEMA).	182
Figure (46): The SEM micrographs of (a) trunk PFA (b) PFA-g-pVAc, (c) PFA-g-pHEMA and (d) PFA-g-p(VAc/HEMA).	184
Figure (47): The SEM micrographs before treatment by platelet adhesion of (a) trunk PFA and PFA-g-p(VAc/HEMA) with different grafting yield of (b) 5.3, (c) 21.2, (d) 31.5 and (e) 42%, respectively.	187
Figure (48): The SEM micrographs of platelet adherent on (a) trunk PFA and PFA-g-p(VAc/HEMA) with comparison of platelet adhesion at different grafting yield of (b) 5.3, (c) 21.2, (d) 31.5 and (e) 42%, respectively.	188
Figure (49): FTIR spectra of (a) PFA-g-p(VAc/HEMA) and its graft copolymer complexed with (b) Cu ²⁺ and (c) Cr ³⁺ ions, having the same grafting yield of 5.3 %.	191
Figure (50): Change in the relative absorbance with	192

wavelength (nm) for (I) $\text{Cu}(\text{NO}_3)_2$ and (II) $\text{Cr}(\text{NO}_3)_3 \cdot 9\text{H}_2\text{O}$ in aqueous solutions (curve a and b) before and after reactions respectively, and (curve c) PFA-g-p(VAc/HEMA) complexed with Cu^{2+} (Fig.50 I) and Cr^{3+} (Fig.50 II) ions, having the same grafting yield of 42%.	
Figure (51): X-ray fluorescence spectra of PFA-g-p(VAc/HEMA) complexed with (a) Cu^{2+} and (b) PFA-g-p(VAc/HEMA) complexed with Cr^{3+} ions, having the same grafting yield of 42%.	194
Figure (52): ESR spectra of PFA-g-p(VAc/HEMA) complexed with (—) Cu^{2+} ions and (---) PFA-g-p(VAc/HEMA) complexed with Cr^{3+} ions at room temperature, having the same grafting yield of 42%.	195
Figure (53): TGA diagram of (a) PFA-g-p(VAc/HEMA), (b) PFA-g-p(VAc/HEMA) complexed with Cu^{2+} ions and (c) PFA-g-p(VAc/HEMA) complexed with Cr^{3+} ions, having the same grafting yield of 42%.	197
Figure (54): Electrical conductivity of (●) PFA-g-p(VAc/HEMA) and (▼) PFA-g-p(VAc/HEMA) complexed with Cu^{2+} ions and (○) PFA-g-p(VAc/HEMA) complexed with Cr^{3+} ions as a function of degree of grafting.	200
Figure (55): The SEM micrographs of (a) PFA-g-p(VAc/HEMA), (b) PFA-g-p(VAc/HEMA) complexed with Cu^{2+} ions and (c) complexed with Cr^{3+} ions, having the same grafting yield of 42%.	201

List of Tables

Table	Page No.
Table (1): Viscosity average molecular weights of	121

chitosan when exposed to different irradiation doses and in presence of initiators measured by viscometric method.	
Table (2): Viscosity average molecular weights of sodium alginate when exposed to different irradiation doses and in presence of initiators measured by viscometric method.	121
Table (3): Viscosity average molecular weights of CMC when exposed to different irradiation doses and in presence of initiators measured by viscometric method.	121
Table (4): Number-average molecular weights of chitosan on exposure to gamma irradiation and that mixed with different initiators measured by GPC.	129
Table (5): Number-average molecular weights of sodium alginate on exposure to gamma irradiation and that mixed with different initiators measured by GPC.	129
Table (6): Number-average molecular weights of CMC on exposure to gamma irradiation and that mixed with different initiators measured by GPC.	129
Table (7): Weight loss percent for pure chitosan and that mixed with 10 (wt%) ammonium per-sulfate at different irradiation doses of 40, 120 and 200 kGy.	145
Table (8): Weight loss percent for pure sodium alginate and that mixed with 10 (wt%) ammonium per-sulfate at different irradiation doses of 40, 120 and 200 kGy.	145
Table (9): Weight loss percent for pure CMC and that mixed with 10 (wt%) ammonium per-sulfate at different irradiation doses of 40, 120 and 200 kGy.	145
Table (10): Effect of spraying 100 ppm of sodium alginate and that mixed by 10% wt APS at different irradiation doses on crop yield of zea maize plants.	156
Table (11): Effect of spraying 100 ppm of chitosan	159

and that mixed by 10% wt APS at different irradiation doses on crop yield of zea maize plants.	
Table (12): Effect of spraying 100 ppm of sodium alginate and that mixed by 10 (wt%) APS at different irradiation doses on crops yield of faba bean plants.	161
Table (13): Effect of spraying 100 ppm of chitosan and that mixed by 10 (wt%) APS at different irradiation doses on crop yield of faba bean.	163
Table (14): Weight loss (%) for trunk PFA, PFA-g-pVAc, PFA-g-pHEMA and PFA-g-p(VAc/HEMA) in nitrogen atmosphere and heating rate of 10°C/min.	183
Table (15): Weight loss (%) for PFA-g-p(VAc/HEMA), PFA-g-p(VAc/HEMA) complexed with Cu ²⁺ and Cr ³⁺ ions in nitrogen atmosphere, having the grafting yield of 42%.	198

Abbreviations List

<i>Name</i>	<i>Abbr.</i>
2-hydroxyethylmethacrylate	HEMA
Ammonium per-sulfate	APS
Carboxymethylcellulose - Na salt	CMC
Electron Spin Resonance	ESR
Ferric chloride	FeCl ₃
Gamma Irradiation	γ
Gel Permeation Chromatography	GPC
Hydrogen peroxide	H ₂ O ₂
Infra Red Spectroscopy	FTIR
Kilogray (<i>absorbed dose of radiation</i>)	kGy
Molecular Weight	Mwt
Poly(tetrafluoroethylene-perflourovinyl ether)	PFA
Potassium per-sulfate	KPS
Scanning Electron Microscopy	SEM
The inherent viscosity	η_{inh}
The intrinsic viscosity	$[\eta]$
The reduce viscosity	η_{red}
The relative viscosity	η_{rel}
The specific viscosity	η_{sp}
Thermal Gravimetical analysis	TGA
Ultra Violet Spectroscopy	UV-Vis
Vinyl acetate	VAc
X - Ray Diffraction	XRD
X-ray Fluorescence	XRF

Acknowledgment

First of all thanks to GOD for the infinite helps and persistent supply with patience and efforts to accomplish this work successfully.

I would like to express my deep gratitude and thanks to **Prof. Dr. El-Sayed Ahmed Soliman Abd El-Aziz** (prof. of Organic Chemistry - Faculty of Science - Ain Shams University) for his supervision, sponsorship, constructive criticism and deep concern in this work. Deepest thanks and sincere gratitude to **Prof. Dr. Naeem Mohamed El-Sawy** and **Prof. Dr. Hassan Ahmed Abd El-Rehim** (prof. of Radiation Chemistry - Polymer Chemistry department - National Center of Radiation Research and Technology - Atomic Energy Authority) for suggesting the plane point of research, close supervision and cooperation, their interest, valuable discussion and facilities provided during this work.

I am cordially indebted to **Prof. Dr. El-Sayed Abd El-Aziz Hegazy** (Chairman of the National Center for Radiation Research and Technology (NCRRT) - Atomic Energy Authority of Egypt (AEAE). Also, many thanks to **Dr. Eman Abd-Alla Abd El-Hamied Farag** (Lecture in Natural products department - National Center of Radiation Research and Technology- Atomic Energy authority) for her cooperation in the application site. Many thanks to my parents, my wife and all colleagues in hydrogel laboratory and all staff members of Polymer Chemistry Department and groups of irradiation

facilities in National Center for Radiation Research and Technology - Atomic Energy Authority of Egypt (AEAE) for their helps and facilities provided throughout this work.

Chapter I

INTRODUCTION

I.1- Radiation Processing of Polymeric Materials

Radiation treatment of polymers is a fairly recent technology following new applications derived from the nuclear industry. The success of these investigations led to an entirely new industrial activity, the manufacture of electric accelerators to be used as powerful radiation sources. These are now widely spread in industry for radiation processing. The largest productions in the polymer field involve cross-linking of shaped polymer articles and curing of coatings. Sterilization of plastic medical supplies in hospitals is another large-scale application in which the polymers are not modified. This method of sterilization enjoys great popularity for its ease of operation. Smaller-volume applications are found in various fields and involve numerous products. Radiation treatment of polymers is still rapidly expanding, and entirely new applications are expected to come to light in the future.

Radiation is a very convenient tool for the modification of polymeric materials. The irradiation of polymeric materials with ionizing radiation (γ -rays, X-rays, accelerated electrons, ion beams, etc...) lead to the formation of very reactive intermediates, free radicals, ions and excited states. These intermediates can follow several reaction paths that result in disproportion, hydrogen abstraction, arrangements and/or the formation of new bonds. The degree of these transformations depends on the structure of the polymer and the conditions of treatment before, during and after irradiation. Through control of all of these factors facilitates the modification of polymers by radiation processing. Nowadays, the modification of polymers covers radiation crosslinking, radiation-induced graft polymerization, radiation curing and the degradation of polymers.

The success of radiation technology for the processing of synthetic polymers can be attributed to two reasons, namely the easiness of processing in various shapes and sizes and secondly, most of these polymers undergo crosslinking reaction upon exposure to radiation. On the other hand, naturally occurring polymers were difficult to process and degraded when exposed to high energy radiation either in solid state or in dilute aqueous solution *Andrzej et al. (2005)* and *Bin et al. (2000)*.

1.2- Naturally Occurring Polymers

Naturally occurring polymers such as cellulose, starch, chitin / chitosan and their water-soluble derivatives have a

variety of application in many fields owing to their unique structure, distinctive properties, safety, non-toxic and biodegradability. In their utilization many shapes and material properties are required such as hydrogels which have been widely used in the field of biomedicine and pharmacy *Dumitriu (1996)*.

1.2.1- Cellulose and Cellulose Ether

CarboxyMethylCellulose - Sodium Salt (CMC- Na)

Cellulose is a widely occurring polymer in nature and has the formula $(C_6H_{10}O_5)_n$. The main sources of cellulose used in the chemical fibers industry are wood pulps, cotton and other plant materials... It is insoluble in water. Cellulose is made up of chains of D- glucose units each unit joined by a glycoside linkage between C_1 and C_4 . The average molecular weight ranging from 250,000 to 1,000,000 or more contains at least 1500 glycoside unit.

The cellulose modification process can be conducted by chemical, physical or biochemical methods. Alkalization of cellulose is the oldest and most frequently used method of its modification. The process includes treating cellulose with 18-19 wt% aqueous sodium hydroxide. Many chemical reactions and physical processes take place and as results intermolecular bond become weaker and polymerization degree decreases.

Native cellulose has a highly ordered structure. Both swelling and chemical modification are good technique to loosen the ordered structure of cellulose i.e. to improve the accessibility of the molecules. Substitution of original H- atoms of cellulose's hydroxyl groups at C₆ with bulky carboxymethyl groups (-CH₂COO-) results in significant improvement of accessibility; even water solubility can be achieved to give the anionic linear polymer carboxymethylcellulose (CMC-Na) the most utilized cellulose ether contrary to pure cellulose.

Carboxymethylcellulose (CMC-Na) is a derivative of [cellulose](#) formed by its reaction with alkali and chloroacetic acid. CMC is an anionic water soluble natural polymer derivative but retains the biodegradability of its original natural macromolecule. These and other advantageous features are the reason of manufacturing significance of CMC due to its low cost, biodegradability, lack of toxicity and its applications in pharmaceutical **Guo et al. (1998)**, food and other major industries as thickener, stabilizing agent for emulsion and suspensions or water binder **Greenway (1994)**.

1.2.2- Chitosan

Chitosan is a high-molecular-weight with a strong network of inter- and intra-molecular hydrogen bonds polysaccharide derived from the most abundant natural polymer chitin; is composed of 2-amino-2-deoxy-D-glucose and 2-acetamido-2-deoxy-D-glucose units. Chitosan one of the most important marine polysaccharide has many peculiar biological activities such as immunity, nor-cholesterol and antibacterial **Felse and Panda (1999)** and **Chandy and**

Sharma (1992). So it is of increasing interest to degrade chitosan to low molecular weight under appropriate conditions and then compare the relationship between biological activity and molecular weight in order to improve its solubility. The structure of chitosan results in poor solubility in most organic solvent and makes it chemically inert for derivatization. Since only a few chemical modifications can be made in chitosan-carboxylic acid aqueous solution (acetic acid or citric acid) most reactions of chitosan are carried out in heterogeneous systems of organic solvents **Chirachanchai et al. (2001)**.

1.2.3- Sodium Alginate

Sodium alginate is a sodium salt of alginic acid, a naturally occurring non-toxic polysaccharide found in brown algae has molecular formula $(C_6H_7NaO_6)_n$. Alginate is anionic linear biodegradable and biocompatible polysaccharide occurring in large amounts in nature. It is composed of a 1-4-linked block polymer of polyglucuronate (poly-G) and polymannuronate (poly-M) acids or its copolymer bound in a random sequences. The uses of alginates are based on two main properties; the first is their ability when dissolved in water to thicken the resulting solution. The second is their ability to form films and gels when a calcium salt is added to a solution of sodium alginate in water.

1.3- Radiation Processing of Natural Occurring Polymers

Naturally occurring polymers or their derivatives under normal conditions of irradiation undergo chain scission reaction. Polymers such as carboxymethyl cellulose (CM-

cellulose) or carboxymethyl starch can be crosslinked to form a hydrogel material. This offers an opportunity to obtain non-toxic, additive free, totally biodegradable and biocompatible crosslinked hydrogels for many applications. The crosslinked material is now being evaluated as an adsorbent for removing toxic materials from the waste waters. Formation of crosslinked polymer hydrogels from natural polymers and their derivatives offers new avenues for applications of such materials in many areas.

Interactions of high energy radiation with polysaccharides result in dehydrogenation, oxidative degradation and depolymerization reactions and destruction of the basic monomer units. It is known that after irradiation cellulose molecules are altered by breaking of glycosidic linkages and the introduction of carboxyl and carbonyl groups *Nitzel (1984)* with increasing dose there was an increasing formation of these groups and the yields were slightly greater when cellulose was irradiated in air as compared with irradiation in an oxygen-free atmosphere. The degradation of cellulose was studied using different radiation sources. These studies showed that when cellulose is irradiated by γ -radiation, neutrons and also X-rays, chain scission occurs to give rise to carbonyl- and carboxyl groups.

1.4- Combined Radiation and Conventional Processes for Efficient Processing of Natural Polymers

Many processes of radiation treatment of natural polymers, though known for a long time, have not yet been commercialized either because of the high cost of irradiation

(high dose) or because of the reluctance on part of the industry to adapt the radiation technology. It is therefore of importance to consider combining the beneficial effects of conventional technology along with radiation technology to overcome such problems. The use of electron beam processing of cellulose pulp for reducing its degree of polymerization (DP) has been studied very extensively as it offers advantage in terms of reducing the concentration of carbon disulphide in the viscose process. The results presented at the Meeting showed that by suitably combining radiation technology along with the enzymatic treatment it can be used to dissolve cellulose pulp even without addition of the toxic carbon disulphide solvent used in the conventional viscose-rayon process. The developed process utilizes the electron beam treatment for initially reducing the DP to a desired level and enzymatic modification to produce alkali soluble cellulose. The combined process offers many unique advantages over the existing viscose-rayon process, which is now facing stiff environmental regulations due to large pollution associated with the process.

Another concept of combining radiation technology with the conventional technology that has been successfully demonstrated is in the area of converting cellulosic agro byproducts (agro-wastes) material into substrate for growing mushroom and subsequently using it as an animal feed. The process involves radiation pasteurization of cellulosic waste followed by inoculation with desirable fungi to grow mushrooms. The process has been demonstrated to be technically and economically feasible on a large scale using electron beam accelerator to achieve the desired output.

1.5- Specific Advantages of Radiation Processing Over Other Chemical Alternatives

Primarily radiation processing concerns molecular weight increase by radiation induced crosslinking or molecular weight decrease by degradation caused by scission or both. Secondly, it concerns those reactions where no significant change in molecular weight will be observed. Thirdly electron beam processing as an alternate to chemical additives i.e. electron beam processing of crosslinkable plastics has yielded materials with improved dimensional stability, reduced stress cracking, higher service temperature, reduced solvent and water permeability and contributed significant improvement in other thermo-mechanical characteristics *Andrzej et al. (2005)*. The main advantages of radiation processing of polysaccharides over other chemical alternatives are: (1) The degradation process can be performed at room temperature. (2) The degraded polysaccharides can be used without purifications. (3) The simplicity of controlling the whole process. (4) Large scale applications.

1.6- Applications of Radiation Processed Natural Polymers

Naturally occurring polymers or their derivatives are diverse, abundant, possess unique properties and are now being explored for various knowledge-based applications. In a short span of about five years, considerable success has been achieved in some of areas related to health care and agriculture practices by the use of radiation processed polymeric materials. Further efforts are necessary for demonstrating applications on a large scale.

1.6.1- Induction of Biological Activities

1.6.1.1- Anti-microbial Activity

Carbohydrates such as chitosan can be easily degraded by radiation in liquid state and in solid state. Anti-bacterial activity of irradiated chitosan has been tested against *Escherichia coli* B/r ***Matsuhashi and Kume (1997)***. Irradiation of chitosan at 100 kGy in the dry state was effective in increasing the activity, and inhibited the growth of *E. coli* completely at a concentration of 3 µg/ ml.

1.6.1.2- Phytoalexin Elicitor Activity

Phytoalexins are antimicrobial compounds that are both synthesized by and accumulated in plants after exposure to pathogens. Phytoalexins are absent in healthy plants. The molecules that signal plants to synthesize phytoalexin are called elicitors. Thus radiation degraded polysaccharides such as pectin, chitosan exhibited phytoalexin induction effect that is different due to molecular size (or absorbed dose) ***Kume et al. (2002)***. The induction of phytoalexins has been studied by using radiation-degraded carbohydrates. The pectic fragments obtained by irradiation with 1000 kGy (10 kGy/ h) from ⁶⁰Co were the most effective for induction of glyceollins (a phytoalexin in soybean) and induced almost the same amount of glyceollins as pectin-PGase. Pisatin, a phytoalexin induced in peas, was also effectively induced by irradiating pectin and chitosan

1.6.1.3- Suppression of Environmental Stress on Plants

The damages of heavy metals and salts on plants were relatively reduced by the application of radiation degraded polysaccharides. Lignocellulosic materials extracted from oil palm fiber, sugarcane bagasse and sawdust of fagus were increased by radiation ***Lam et al. (2000)***. These extracts in hot water and ethanol show a strong activity that suppresses the heavy metal and salt stress on plants.

1.6.1.4- Enhancement of Antioxidant Activity

Gamma ray irradiation of chitosan gives enough degradation to increase its antioxidant activity as a result of a change in molecular weight where the antioxidant activity of chitosan and its derivatives has attracted the attention. Since they exert strong antioxidant activities and their effects are also similar to those of phenolic antioxidants ***Park et al. (2004)***.

1.6.2- Bio-medical Applications

Natural polysaccharides like chitosan have been demonstrated to be useful materials for biomedical applications such as culture material for skin graft and bone cells. Chitosan also can be used in wound-dressing materials which possess wound healing characteristics besides having good biocompatibility. Chitosan act as a carrier for various active agents including drugs and biologics due to its physicochemical and biological properties. Chitosan has interesting biopharmaceutical characteristics such as pH sensitivity, biocompatibility and low toxicity ***Bersch et al. (1995)***. Moreover, chitosan is metabolised by certain human enzymes, especially lysozyme, and is considered as

biodegradable *Muzzarelli (1997)*. Chitosan grafted systems have great potential to be used in other biomedical applications, such as in the cardio-vascular field *Mao et al. (2004)*.

1.6.3- Development of Biodegradable Plastics

The development of biodegradable plastic for environmental conservation needs to be addressed on an urgent basis as a large amount of non-degradable waste is generated throughout the world especially in the advanced countries. On the other hand, enormous amounts of agro-waste materials are produced in the developing countries, which in various forms can be suitably used as fillers or additives in the plastics to increase the environmental degradability of the composite materials. Besides taking care of the waste generated, this step will impart value addition to the waste and enhance the economic condition of the people engaged in agro-related industries in such countries. Radiation processing can be effectively utilized to develop synthetic-natural polymer based composites that can be crosslinked to impart the desired physico-chemical properties to these materials

1.6.4- Development of Hybrid Technologies for Processing of Cellulose Based Materials

The tightly bound network structure of cellulose necessitates use of very harsh and toxic conditions for solubilizing it. New biotechnological methods have been developed in recent years, which allow dissolution of cellulose in alkali solutions. Radiation technology methods along with such biotechnical methods should be investigated for bringing

economical benefits to the industries where cellulose is used as a raw material for manufacture of products like fibres, films, fibroids and in emerging area of nano structured products. The hybrid technology can also be beneficially utilized to convert cellulosic waste into useful products.

1.6.5- Adsorption of Metal Ions

A great number of chitosan derivatives have been obtained with the aim of adsorbing metal ions by grafting new functional groups on the chitosan backbone. The new functional groups are incorporated with chitosan to increase the density of sorption sites to change the pH range for metal sorption and to change the sorption sites in order to increase sorption selectivity for the target metal.

1.6.6- Removal of Dyes

Chitosan, due to its high contents of amine and hydroxy functional groups, has an extremely high affinity for many classes of dyes including disperse, direct, reactive, anionic, vat, sulfur and naphthol *Martel et al. (2001)*; the only class for which chitosan has low affinity is cationic dyes *Chao et al. (2004)*.

1.7- Radiation Processed Low Molecular Weight Polysaccharides for Use as Growth Promoters in Agricultural Purposes

Recently much attention has been paid to the utilization of radiation processing technology for degradation of natural polysaccharides in agricultural applications due to several reasons for instances: (1) The degradation process can be

performed at room temperature. (2) The degraded polysaccharides can be used without purifications. (3) The simplicity of controlling the whole process. (4) Economic competitiveness to alternatives ***Kume et al. (2002)***. As compared to the conventional techniques like acid or base hydrolysis or enzymatic methods, radiation processing offers a clean one step method for the formation of low molecular weight polysaccharides in aqueous solutions even at high concentrations. Low molecular weight polysaccharides and/or oligosaccharides can be produced by degradation of corresponding polysaccharides including marine polysaccharides such as alginate, chitin/chitosan and carrageenan. Chemical, enzymatic and radiation processing technologies can be applied for degradation process.

A lot of studies have been carried in countries like Japan, Vietnam, China, India and Philippines to investigate the plant growth promotion and plant protection effect of radiation processed polysaccharides in a variety of crops under different environmental conditions. Low molecular weight naturally occurring polysaccharides prepared by conventional methods possessed novel features such as growth-promotion of plants ***Nguyen et al. (2000)***, ***Kume et al. (2002)***, promotion of germination and shoot elongation ***Wanichpongpan et al. (2001)***, stimulation of growth of bifidiobacteria to resist infection of diseases for plants particularly oligochitosan in agriculture as biotic elicitor to enhance defense responses against diseases ***Akiyama et al. (1992)*** and ***Harwiger et al, (2002)*** and suppression of heavy metals stress ***Kume et al. (2002)***. The results of these studies have clearly shown that

radiation processed polysaccharides even at very low concentrations of a few tens of ppm are very effective for use as plant growth promoter. This application offers tremendous opportunity to use them as highly effective organic fertilizers. Their biodegradability will be an additional advantage of using such materials as plant growth promoters.

II. Radiation Graft Copolymerization of VAc/ HEMA Binary Monomer Onto Poly(tetraflouroethylene-perflourovinyl ether) (PFA) Films

II.1. Principles of Copolymerization Grafting

In principle, graft copolymerization is a process which side chain grafts are covalently attached to main chain of a polymer backbone to form branched copolymer. The extent of polymerization grafts is called the degree of grafting (grafting yield) which is gravimetrically determined as the percentage of mass increase. Both the backbone and side chain grafts can be either homopolymer or copolymer reaction. Graft copolymerization takes place as a result of formation of active sites on the polymer backbone. The active sites may be free radicals or ionic chemical groups which initiate polymerization reaction. The formation of active sites on the polymer backbone can be carried out by several methods such as plasma

treatment, ultraviolet (UV) light radiation, decomposition of chemical initiator and high energy radiation. Of all, high energy radiation-induced graft copolymerization method has been widely investigated for membrane preparation as bulk modification of polymer films can be achieved *Hegazy et al., (1999)*.

Grafting process can take place in two different ways, i.e. "Surface grafting" and "bulk grafting". Surface grafting occurs onto the surface of the polymer whereas bulk grafting occurs deep-rooted into the polymer matrix. In case of membranes modification, surface grafting is more suitable than the bulk grafting for biomedical applications. Surface modification of polymers by graft copolymerization has afforded a great number of new materials with unique properties. The surface properties of the grafted polymer are often in stark contrast to the properties of the original polymer. Most industrial polymers are hydrophobic in nature; however through introduction of new functional groups to the surface; properties such hydrophilicity, adhesion, biocompatibility, conductivity, antifogging and anti-fouling may be attained. Surface modification with increasing hydrophilicity is believed to be a useful method for preventing platelet adhesion and protein adsorption *Lee et al. (1995)*.

The improvement in properties of the grafted copolymer depends on the nature, amount and chain length of the grafted branches as well as on the type of distribution of the grafted monomer in the base polymer. The properties which might be incorporated into the base polymer are determined by the

evolution of various parameters as elongation, elasticity, permeability, etc. Moreover the structural changes are also dependent on the nature of the trunk polymer as well as the monomer, the method of graft copolymerization, the medium in which reaction occurs and the extent of graft copolymerization. The properties of the graft copolymer change according to the combination of trunk polymer / monomers and the reaction conditions such as the irradiation dose, dose rate, temperature and concentration of monomer. Therefore, an accumulation of data in this field may be necessary for establishing the reaction condition for the synthesis of the desired membranes by radiation - induced grafting *Sankholkar and Deb (1990)*.

II.2. Radiation Grafting Technique

Radiation is a powerful source of energy for chemical processing applications. Thus it can be applied in different industrial areas and can initiate chemical reactions. Radiation provides a highly advantageous means of grafting. A large concentration of free radicals is produced in the irradiated materials without the use of chemical initiators. Radiation grafting is one of the most promising methods because of the easy handling at room temperature, large penetration in polymer matrix, rapid and uniform formation of active sites for initiating grafting throughout the matrix under appropriate experimental conditions for homogeneous diffusion of monomer in the polymer *Mukherjee and Gupta (1985)*.

The objective of the modification of polymers by radiation-induced grafting are: (1) Preparation and

development of new materials more efficient and stimuli-responsive for many applications such as in separation and purification purposes. (2) The selection of reactive groups may lead to stimuli-responsive and purification purposes in different applications; such as in industrial and biomedical applications. (3) The applicability of the polymers for removal, separation and purification of some biomolecules.

II.3. Methods of Radiation Induced Grafting

Radiation-induced graft copolymerization can be carried out by using two main methods (1) Simultaneous (direct or mutual) irradiation and (2) pre-irradiation (post-irradiation), which can be performed either in presence of air or under vacuum *Nasef and Hegazy (2004)*.

II.3.1. Simultaneous (Direct or Mutual) Irradiation Method

Simultaneous method is the simplest irradiation technique for preparation of graft copolymers involves a single step. In this method a polymer backbone is irradiated in the presence of a monomer available in different forms: vapor, liquid or in bulk solution. Irradiation can be carried out in air, inert atmosphere (e.g. N₂) or preferably under vacuum leading to the formation of active free radicals on both polymer backbone and monomer units. Despite being the most efficient in principal, simultaneous graft copolymerization has a serious limitation arising from the high level of homo-polymer formation. However, a number of conditions can be adopted to overcome this problem and improve the grafting efficiency by keeping the formation of radicals in the polymer backbone at higher rates than that in the monomer units. These conditions include

the addition of polymerization inhibitors such as Fe^{2+} and Cu^{2+} salts, the use of good swelling agents (solvent), the selection of low dose rates to avoid rapid termination of graft growing chains and the addition of the monomer either in vapor or liquid form to the polymer backbone while it is in a solid form.

II.3.2. Pre-irradiation Method (Post-irradiation Grafting)

Pre-irradiation method involves a combination of two steps: (1) Irradiation of the polymer backbone to form active radicals and (2) Contact of the irradiated polymer backbone with monomer. If irradiation step is carried out in air, the generated radicals react with oxygen to form peroxides and hydroperoxides which initiate grafting upon contacting monomer units by thermal decomposition. In practice, the pre-irradiation method has been given much attention because the homopolymer formation is little and the grafting can be carried out at any time away from radiation sources. The main problem of the indirect method is that only a portion of the radicals formed remain trapped after the irradiation. The efficiency of radical retention can be improved by using the radicals immediately after irradiation or by storing the irradiated samples at low temperature prior to use.

II.4. Applications of Grafted Membranes

Many radiation grafted membranes were found to meet the requirements for a variety of applications in the present time and many more are being developed for the future. Perhaps, the most significant applications of these membranes are in separation processes by means of distillation or

recrystallization, electrochemical devices including fuel cells batteries and sensors in addition to biological and biomedical uses, the waste water treatment of heavy and toxic metals from water because the severe problems of environmental pollution.

II.4.1. Hemodialysis and Bioapplications

In recent years there has been a growing interest in the use of polymers in the development of materials for bioapplications. Hemodialysis is one of the most important methods for blood purification. The properties required for a hemodialysis material are excellent ultrafiltration rate, permeability by solutes, mechanical strength and hemocompatibility. Many polymer materials for hemodialysis membranes such as cellulose acetate, polysulfone, polyacrylonitrile, polycarbonate, polyvinylidene fluoride, nylon, polymethylmethacrylate and ethylene-vinyl alcohol copolymer have been investigated to raise the efficiency of hemodialysis *Nunes and Peinemann (2001)*.

Membranes made from unmodified cellulose have been the typical membranes for dialysis for a long time and these membranes are still used worldwide for 85% of hemodialysis. Although the cellulose membranes have good permeability and mechanical strength, their hemocompatibility must be improved further for better hemodialysis. Thus it is necessary to infuse an anticoagulant such as heparin during hemodialysis to maximize blood compatibility *Cheung et al. (1992)*. To enhance the biocompatibility of surfaces is one of the most important aims for the development and use of artificial biomaterial and is a topic which had been studied intensively.

Therefore, various surface modification attempts have been made to optimize these interfacial biological responses with an attempt to develop antithrombogenic materials. Biomaterial surfaces have been modified with various molecules, such as albumin *Kamath et al. (1994)*, heparin *Pekna et al. (1993)*, poly(ethylene glycol) (PEG) *Jo and Park (2000)*, self-assembled monolayer *Prime and Whitesides (1991)* and phospholipids *Iwasaki et al. (1997)*.

In the late 1960s, membranes separation techniques were already being used for oxygen-enriched air and hemodialysis processing utilizing membrane blood dialysis to remove toxic wastes from blood. Blood compatibility of most membranes is not adequate and injections of anticoagulants are required during hemodialysis to prevent clotting. The decrease in membrane transportation of various waste molecules from whole blood is due to changes in membrane permeability which is due to the adhesion of blood cells. In the biosystems, the adhesion of blood cells on the membranes correlates to membrane material properties. Membrane quality depends on many factors including the mode of preparation and surface functionality.

II.2.4.2. Polymer Metal-Complex Membranes

Many potential membrane applications are just entering commercialization and look attractive both technically and economically. These membranes play a very important role in various separation processes. The polymer metal complex is another interesting polymeric material in which certain metal ions are surrounded by enormous polymer chains forming

metal complex containing polymer ligands with remarkably specific structures ***Kaneko and Isuchida (1981)***. Metal complex membranes are often prepared by radiation-induced graft copolymerization of functional monomers such as acrylic acid onto a polymer film followed by chemical treatment with desired aqueous solution of transition metal salts. Based on the polymeric ligands these membranes have interesting and important characteristics including chelating and catalytic activities different from their corresponding ordinary metal complexes of low molecular weight ***Hegazy et al. (1993)***.

Many studies have reported the preparation of chelating membranes using radiation-induced grafting technique with the main focus on improving the adsorption affinity (selectivity) to heavy metals by optimization of the grafting conditions and selection of an appropriate monomer. Various metals ions Fe^{3+} , Co^{2+} , Ni^{2+} , Cr^{3+} , Mn^{2+} , Ag^+ , Cu^{2+} , Cd^{2+} and Rh^{2+} have been complexed by grafting of carboxylate monomers onto various polymer films followed by chemical treatment with metal solution ***El-Sawy (1998, 2000 and 2004)***, ***El-Sawy and Ali (2007)***, ***El-Sawy and Al-Sagheer (2001)***, ***El-Sawy et al. (1994 and 1992)*** and ***Abdel-Ghaffar et al. (1991)***.

Complexation of Cu^{2+} and Cr^{3+} with amidoximated PE-g-poly(acrylonitrile) membrane prepared by radiation-induced grafting of acrylonitrile onto PE films followed amidoximation reaction with hydroxyl amine were also reported by ***El-Sawy (2000)***. Removal of some heavy metals from waste-water of chemical industries including metallurgical and metal finishing

has been receiving an increasing attention in the recent years ***Hegazy et al. (1999)*** this is due to the severity of environmental pollution by heavy metals as they impose direct toxic effect on human and animal health. Moreover, selective separation of some metals such as silver and gold from other components is of practical interest, either with the aim to separate these metals from natural resources or to treat industrial effluents and waste-water.

The use of 2-hydroxyethyl methacrylate (HEMA) as a grafting monomer onto a range of polymeric substrates with the aim of producing new biomaterials has been increasingly successful. Previous studies showed that the presence of HEMA in copolymers improves the biocompatibility of the materials ***Benson (2002)*** and ***Casimiro et al. (2005 a)***. Fluorinated polymers such as PFA films are not susceptible to surface oxidation by ozone. Also characterized by the unique resistance of fluoropolymers to almost all chemicals has made them suitable for many specialized applications. Despite their chemical stability, fluoropolymers are one of the most sensitive polymers to radiation ***Clough and Gillen (1991)***. Grafted fluoropolymers are also used as charged ultrafiltration membranes ***Yamada et al. (2001)***, waste treatment membranes ***Hegazy et al. (1999)*** and in biomedical applications ***Zou et al. (2002)***. In these applications the principal motivation for the grafting is the modification of the fluoro-polymer surface properties either to enhance the surface hydrophilicity or to promote cell or tissue growth.

Acknowledgment

First of all thanks to GOD for the infinite helps and persistent supply with patience and efforts to accomplish this work successfully.

I would like to express my deep gratitude and thanks to **Prof. Dr. El-Sayed Ahmed Soliman Abd El-Aziz** (prof. of Organic Chemistry - Faculty of Science - Ain Shams University) for his supervision, sponsorship, constructive criticism and deep concern in this work. Deepest thanks and sincere gratitude to **Prof. Dr. Naeem Mohamed El-Sawy** and **Prof. Dr. Hassan Ahmed Abd El-Rehim** (prof. of Radiation Chemistry - Polymer Chemistry department - National Center of Radiation Research and Technology - Atomic Energy Authority) for suggesting the plane point of research, close supervision and cooperation, their interest, valuable discussion and facilities provided during this work.

I am cordially indebted to **Prof. Dr. El-Sayed Abd El-Aziz Hegazy** (Chairman of the National Center for Radiation Research and Technology (NCRRT) - Atomic Energy Authority of Egypt (AEAE). Also, many thanks to **Dr. Eman Abd-Alla Abd El-Hamied Farag** (Lecture in Natural products department - National Center of Radiation Research and Technology- Atomic Energy authority) for her cooperation in the application site. Many thanks to my parents, my wife and all colleagues in hydrogel laboratory and all staff members of Polymer Chemistry Department and groups of irradiation facilities in National Center for Radiation Research and Technology - Atomic Energy Authority of Egypt (AEAE) for their helps and facilities provided throughout this work

Chapter II
Literature Review

This chapter summarizes research progress on the degradation process of naturally occurring polymers and radiation grafting of fluorinated polymers. The literature review is classified into four divisions:

1- Radiation Degradation Process of Naturally Occurring polymers.

2- Thermal and Chemical Degradation Processes of Naturally Occurring polymers.

3- Possible Applications of Degraded Naturally Occurring Polymers.

4- The Radiation-Induced Graft Copolymerization and Their Possible Applications.

II.1- Radiation Degradation Process of Naturally Occurring polymers

Bin et al. (2007) irradiated chitosan samples by ^{60}Co γ -rays in the presence of hydrogen peroxide with radiation dose from 10 to 100 kGy. The degradation was monitored by gel permeation chromatography (GPC), revealing the existence of a synergetic effect on the degradation. Structures of the degraded products were characterized with Fourier-transform infrared spectra (FTIR), ultraviolet visible spectral (UV-Vis) analysis, and X-ray diffraction (XRD). The results showed that the crystallinity of chitosan decreases with degradation and the crystalline state of water-soluble chitosan is entirely different from that of water-insoluble chitosan. An elemental analysis

method was employed to investigate changes in the element content of chitosan after degradation. Mechanism of chitosan radiation degradation with and without hydrogen peroxide was also discussed.

Ling et al. (2007a) focused on the radiation effect of γ -ray on carboxymethylated chitosan (CM-chitosan) in solid state. The changes in molecular weight of CM-chitosan with absorbed dose were monitored by viscosity method. Experimental results indicated that random chain scissions took place under irradiation. Radiation chemical yield (G_d) of CM-chitosan in solid state with N_2 -saturated was 0.49, which showed CM-chitosan has high radiation stability. Biomaterials composed of CM-chitosan can be thought to sterilize with low absorbed dose. FTIR and UV spectra showed that main chain structures of CM-chitosan were retained, carbonyl/carboxyl groups were formed and partial amino groups were eliminated in high absorbed dose. XRD patterns identified that the degradation of CM-chitosan occurred mostly in amorphous region.

Aqueous solutions of carboxymethylated chitosan (CM-chitosan) were radiated with γ -ray in various conditions by *Ling et al. (2007b)*. The degradations of CM-chitosan were faster in the presence of nitrous oxide or hydrogen peroxide, but it was inhibited obviously after adding isopropanol because of the changes of the concentration of hydroxyl radicals in above different conditions. The radiation chemical yields of CM-chitosan degradation were found to decrease at

lower pH in which the polymer chains tend to coiled conformation. Intrinsic viscosity of CM-chitosan decreased faster than that of carboxymethylated chitin, indicating that amino groups could enhance the reactivity. FTIR and UV spectra showed that main chain structures of CM-chitosan were remained and some carbonyl/carboxyl groups were formed during the degradation. The results of EA indicated the contents of C/N were increased which suggested the elimination of partial amino groups during radiation.

Degradation of chitosan and starch by 360-kHz ultrasound was made by *Renata et al. (2005)*. Effects of 360-kHz ultrasound on aqueous solutions of chitosan and starch were studied. This treatment is an efficient procedure for reduction of molecular weight of both polysaccharides. It has been demonstrated that at the applied ultrasound frequency degradation is caused both by $\cdot\text{OH}$ radicals and mechanochemical effects. In Ar-saturated $2 \times 10^{-2} \text{ mol dm}^{-3}$ chitosan solutions pH 3, at an ultrasound dose rate of 170 W kg^{-1} and the average sonochemical chain scission yield in the sonication time range of 0-90 min is ca. $8 \times 10^{-11} \text{ mol J}^{-1}$. This yield has been shown to depend on polymer concentration, ultrasound power and gas used to saturate the solution. Scission is accompanied by side reactions leading to the formation of carbonyl groups. Ultrasound - induced chain scission of starch proceeds with lower yield, one of the reasons being probably the different chain on formation when compared with rod-like chitosan macromolecules.

Irradiation by light is considered to be one of the primary sources of damage exerted upon cellulosic substrates at ambient conditions. *Malesic et al. (2005)* demonstrated that extensive oxidative degradation of cellulose accompanied by formation of hydroxyl radicals, occurs during exposure to light with $\lambda > 340$ nm. The results showed that the rate of degradation, carbonyl formation and brightness decrease may be reduced by addition of magnesium carbonate.

Jaroslawa et al. (2005) studied three degradation methods: ultrasonic, ultraviolet and gamma irradiation were applied to sodium alginate and chitosan in aqueous solutions. The changes in molecular weight were monitored by GPC measurements. It has been found that the most effective method for both polymers is gamma radiation method with a yield of scission $G_s = 0.55 \times 10^{-7}$ mol/J for 1% alginate and $G_s = 3.53 \times 10^{-7}$ mol/J for 1% chitosan. However, considering the reaction time, the ultraviolet method is the most effective, with reaction rate constant $k = 0.52 \text{ h}^{-1}$ for alginate and 1.6 h^{-1} for chitosan. Based on FTIR spectra taken before and after degradation it was revealed that degradation undergoes by the breakage of the glycosidic bonds of polymers. UV spectroscopy showed absorption peak at 265 nm for alginate and two peaks at the range of 250-280 nm for chitosan. UV spectroscopy for ultrasonic is not revealed and any peak suggesting ultrasonic degradation undergoes different mechanism than ultraviolet and gamma degradations, probably mechanical one.

The effect of inorganic salts such as sodium chloride on the hydrolysis of chitosan in a microwave field was investigated ***Ronge et al. (2005)***. While it is known that microwave heating is a convenient way to obtain a wide range of products of different molecular weights only by changing the reaction time and/or the radiation power. The addition of some inorganic salts was shown to effectively accelerate the degradation of chitosan under microwave irradiation. The molecular weight of the degraded chitosan obtained by microwave irradiation was considerably lower than that obtained by traditional heating. Moreover, the molecular weight of degraded chitosan obtained by microwave irradiation assisted under the conditions of added salt was considerably lower than that obtained by microwave irradiation without added salt. Furthermore, the effect of ionic strength of the added salts was not linked with the change of molecular weight. FTIR spectral analyses demonstrated that a significantly shorter time was required to obtain a satisfactory molecular weight by the microwave irradiation-assisted inorganic salt method than by microwave irradiation without inorganic salts and conventional technology.

Shi-Ming et al. (2005) studied the synergetic degradation of chitosan by hydrogen peroxide under irradiation with ultraviolet light. The existence of a synergetic effect on the degradation was demonstrated by means of viscometry. In addition, the optimal conditions of degradation were determined on the basis of orthogonal tests. The structures of the degraded product were characterized by FTIR analysis and

diffuse reflectance spectra (DRS) analysis. The mechanism of the degradation of chitosan was correlated with cleavage of the glycosidic bond.

Relleve et al. (2005) showed that kappa, iota- and lambda-carrageenans were degraded by irradiation with gamma rays in the solid state, gel state or solution with various doses in air at ambient temperature. The molecular weights obtained were in the range of 10.5×10^4 to 0.8×10^4 of narrow molecular weight distribution. The chemical structural changes of carrageenans were accompanied by appearance of UV absorbance peak at 260 nm and a characteristic FT-IR band at 1728 cm^{-1} . Due to radiation-induced desulfation carrageenan oligomer has lower sulfate content. From comparison of radiation degradation yield (G_d), susceptibility to degradation of the three types of carrageenans in aqueous form follows the order of (kappa > iota > lambda) which could have been influenced by their conformational state. The oligomer obtained from k-carrageenan with molecular weight of 1.0×10^4 showed a strong growth promotion effect on potato in tissue culture. Degradation of k-carrageenan solution using vessel-type low energy electron beam accelerator (LEEB) (250 kV, 10 mA) was investigated. LEEB irradiation reduced the molecular weight of carrageenan though the electron beams have a depth penetration range of less than 3 mm in distilled water.

Prolonged exposure of solutions of macromolecules to high-energy ultrasonic waves produces a permanent reduction in viscosity. **Gronroos et al. (2004)** showed that there is an

optimal carboxymethylcellulose (CMC) concentration to the most efficient degradation. Ultrasound degraded preferentially large CMC molecules and cleavage took place roughly at the centre of the CMC molecules. Degradation of CMC did not proceed below a certain molecular mass. During ultrasonic degradation the molecular mass distribution narrowed. For any polymer degradation process to become acceptable to industry, it is important to be able to specify the sonication conditions to produce a particular relative molecular mass distribution.

Abad et al. (2004) investigated the dynamic behavior of irradiated kappa carrageenan (in KCl) as a function of irradiation dose and temperature was done by dynamic light scattering (DLS). The intensity correlation function (ICF) shifted towards shorter relaxation times with increasing radiation dose as a result of radiolysis. The characteristic decay time distribution function, $G(\Gamma)$, indicates the presence of fast and slow mode peaks respectively at around 0.1–10 ms and 100-1000 ms. A peak broadening of the fast mode peak in $G(\Gamma)$ appeared with decreasing temperature, indicating that coil-to-helical conformational transition took place. The conformation transition temperature (CTT) decreased with increasing radiation dose. No transition was observed for k-carrageenan irradiated at 200 kGy. A new faster relaxation mode appeared at around 0.1-1 ms at temperatures below the CTT. This peak is found in k-carrageenan irradiated at doses exclusively between 75 and 175 kGy. The peak height of this mode is largest at 100 kGy which corresponds to the optimum biologic activity of k-carrageenan.

Radoslaw et al. (2004) used the method of pulse radiolysis to study radiation-induced transformations of carboxymethylcellulose (CMC) of various degree of substitution (DS) in aqueous solution. The kinetics of the reactions of intermediate products of water radiolysis with this polymer indicated that hydroxyl radicals react very rapidly with the CMC; the rate constant is about $1 \times 10^9 \text{ dm}^3 \text{ mol}^{-1} \text{ s}^{-1}$ and independent of the DS of the CMC. On the other hand, the hydrated electron can be practically neglected as a precursor for macroradicals formation since its reaction rate constant with CMC is low, i.e. $4.0 - 5.0 \times 10^6 \text{ dm}^3 \text{ mol}^{-1} \text{ s}^{-1}$. As the result of OH radicals attack on the CMC, radicals on the main chain, as well as on side groups (carboxymethyl) are formed. Environmental conditions determine the life-time of macroradicals typically tens of minutes were detected.

Rangrong et al. (2004) focused on the optimal conditions for γ -irradiation to reduce the molecular weight of chitosan but still retain its chemical structure. Chitosan was irradiated under various conditions, i.e. flake solid state, flake dispersed in water, flake dispersed in 0.05, 0.1, 1 and 2% aqueous $\text{K}_2\text{S}_2\text{O}_8$ solution, flake dispersed in 0.5, 1 and 2% aqueous H_2O_2 solution, and chitosan acetic acid solution. Comparative studies were done using three types of chitosans with molecular weights of the order of 10^5 Da with degrees of deacetylation of 0.80, 0.85 and 0.90%. For all conditions, after irradiation, there were two regions of molecular weight reduction. A severe degradation occurred in the first region

with decreases in the molecular weight of 80% for radiation doses up to 50 kGy. In the second region, a slow degradation occurred, which resembled a plateau stage. Since the primary structure of chitosan was changed after the irradiation. The degradation of chitosan by γ -rays was found to be most effective for the amorphous structure..

Radiation depolymerization of chitosan by gamma irradiation in the solid state to prepare oligomers was investigated by ***Le et al. (2003)***. The results showed that the radiation chemical depolymerization yield of chitosan in the solid state, G_d , determined by gel permeation chromatography is 0.9 for chitosan 10B and 1.8 for chitosan 8B. Also low molecular weight chitosan /or oligo-chitosans were separated from a chitosan depolymerized by gamma radiation using mixtures of methanol-water and acetone as the solvents. Due to the differences in solubility revealed upon radiolysis, also it was found that extracts became subdivided into precipitates and soluble fractions. The biological effect of oligo-chitosan in each fraction was evaluated; the preliminary results indicated that the oligo-chitosan with $M_w = 2 \times 10^4$ inhibited the growth of fungi at 100 ppm and that with $M_w = 800$ only enhanced the growth of the same typical fungi.

Chemical damages induced by γ -rays ^{60}Co , proton and oxygen ions in a cellulose nitrate detector (LR115) were quantified by infra-red spectrometry showed by ***Barillon and Yamauchi (2003)***. The linear relationship between chemical damages and parameters like dose, ion influence proves that

similar radiation chemistry occurs for those different exposures and that the chemical damages can not be described with a Poisson law.

The aqueous solution of alginate was irradiated by ^{60}Co γ - rays in the dose range of 10-500 kGy. **Dong et al. (2003)** assessed the effect of irradiation on the degradation of alginate. The irradiation-induced changes in the viscosity, molecular weight, color, monomer composition were measured. The molecular weight of raw alginate was reduced from 300000 to 25000 when irradiated at 100 kGy. The degradation rate decreased and the chain breaks per molecule increased with increasing irradiation dose. The viscosity of irradiated alginate solution reached a near minimum as low as at 10 kGy. No appreciable color changes were observed in the samples irradiated at up to 100 kGy, but intense browning occurred beyond 200 kGy. The ^{13}C - NMR spectra showed that homopolymeric blocks increased and the M/G ratio decreased with irradiation. Considering both the level of degradation and the color change of alginate, the optimum irradiation dose was found to be 100 kGy.

Min and Rong (2003) studied the effect of the degree of deacetylation (DD) of the chitosan used on the degradation rate and rate constant during ultrasonic degradation. Chitin was extracted from red shrimp process waste. Four different DD chitosans were prepared from chitin by alkali deacetylation. Those chitosans were degraded by ultrasonic radiation to different molecular weights. Changes of the

molecular weight were determined by light scattering and data of molecular weight changes were used to calculate the degradation rate and rate constant. The results were as follows: The molecular weight of chitosans decreased with an increasing ultrasonication time. The curves of the molecular weight versus the ultrasonication time were broken at 1h treatment. The degradation rate and rate constant of sonolysis decreased with an increasing ultrasonication time. This may be because the chances of being attacked by the cavitations energy increased with an increasing molecular weight species have shorter relaxation times and, thus, can alleviate the sonication stress easier. However, the degradation rate and rate constant of sonolysis increased with an increasing DD of the chitosan used. This may be because the flexibilities molecules of higher DD chitosans are more susceptible to the shear force of elongation flow generated by the cavitations field or due to the bond energy difference of acetamido and β -1,4-glucoside linkage or hydrogen bonds. Breakage of the β -1,4-glucoside linkage will result in lower molecular weight and an increasing reaction rate and rate constant.

Won-Seok et al. (2002) irradiated chitosans (20 and 100 cp, 2%) in acetic acid solution (2%) with different doses (2-200 kGy) of ^{60}Co gamma rays to investigate the yields of chitosan oligomers. A rapid decrease of viscosity was observed up to 10 kGy and then the viscosity decrease slowed down gradually with increasing irradiation dose. Brown color developed heavily for irradiation dose over 100 kGy. Yields of

chitosan dimer, trimer and tetramer were 3.6, 3.0 and 1.8% respectively, at a dose of 100 kGy in 100 cp chitosan solution.

Gamma ray irradiation of chitosan flakes and introduction of hydrophobic chains onto hydroxyl groups are discussed by **Rangrong et al. (2001)**. At 25 kGy, chain degradation without cross-linking reduces the molecular weight to one-fourth however; structural characterization by FTIR, ^1H NMR, and ^{13}C CP/MAS NMR indicates that the saccharide units are maintained. Introduction of hydrophobic chains is accomplished by introduction of alkylamine groups onto the chitosan carbonyl imidazole precursor. The chitosan coupling reaction is improved and can be done homogeneously as a result of γ -ray irradiation. The optimum conditions for phthalimido group deprotection are studied to generate a unique product with a hydrophobic chain attached mainly at the hydroxyl group (C-6 and/or C-3) while the amino group (C-2) is retained as characterized by FT-IR and ^1H NMR. The final product shows fair solubility in organic solvents such as DMSO, DMAc, DMF and pyridine.

Alginates were irradiated as solids or in aqueous solution with ^{60}Co gamma rays in the dose range of 20 to 500 kGy to investigate the effect of radiation on alginates showed by **Naotsugu et al. (2000)**. Degradation was observed both in the solid state and solution. The degradation in solution was remarkably greater than that in the solid. For example, the molecular weight of alginate in 1% (w/v) solution decreased from 6×10^5 for 0 kGy to 8×10^3 for 20 kGy irradiation while the

equivalent degradation by solid irradiation required 500 kGy. Degradation G-values were 1.9 for solid and 55 for solution, respectively. The free radicals from irradiated water must be responsible for the degradation in solution. The degradation was accompanied by a color change to deep brown for highly degraded alginate. Little color change was observed on irradiation in the presence of oxygen. UV spectra showed a distinct absorption peak at 265 nm for colored alginates, increasing with dose. The fact that discoloration of colored alginate was caused on exposure to ozone suggests a formation of double bond in the pyranose - ring.

Chitosan has potential biomedical applications that may require the final products to be sterilized before use. The γ -irradiation of purified and highly deacetylated chitosan fibers and films at sterilizing doses (up to 25 kGy) caused main chain scissions studied by *Lee-Yong et al. (1998)*. The viscosity average molecular weight of the polymer decreased with increasing irradiation dose, the radiation yields of scission being 1.16 in air and 1.53 in anoxia. Pre-irradiation application of a negative pressure of 100 kPa disrupted the network structure, which may have contributed to the greater radiation yield obtained by chitosan fibers in anoxia. Radiation induced scission of the chitosan chains resulted in a lower glass transition temperature (T_g) indicative of higher segmental mobility. The T_g was below ambient at an irradiation dose of 25 kGy in air. Irradiation in air improved the tensile strength of the chitosan film probably due to changes in chain interaction and rearrangement. Irradiation in anoxia did not

affect film properties significantly, partly because the pre-irradiation application of negative pressure had a negligible effect on the structure of the chitosan film. Polymer network structure and the irradiation conditions are therefore important determinants of the extent of radiation induced reactions in chitosan.

Zhao et al. (1993) studied some chemical changes in chitosan induced by γ -ray irradiation. It was found that the NH- group is more sensitive to irradiation than -NHCOCH₃ group and moreover, the hydroxyl group increases with increasing radiation dose while the -C-O-C- group decreases but no evidence for carbonyl formation was observed.

The Radiation-induced changes in chitosan irradiated in solid state and in aqueous solution were examined by **Ulanski and Rosiak (1992)**. The results indicate that radiation yields of scission in solid state, determined by HPLC/GPC, are $G = 0.9$ in vacuum, $G=1.1$ in air and $G=1.3$ in oxygen; corresponding yields of crosslinking are equal to zero. Increase in absorbance at 247 and 290 nm was observed. Existence of post-effect, i.e. further decrease in molecular weight and increase in absorbance was detected. Also radiation-induced changes in solution were studied by pulse radiolysis. Two time-separated first order processes of chain scission were found ($k_1 = 1.4 \times 10^4 \text{ s}^{-1}$, $k_2 = 0.58 \text{ s}^{-1}$). Time evolution of absorption spectrum of chitosan macroradicals ($\lambda_{\text{max}} = 275 \text{ nm}$) was traced.

Ait and Hadjadj (1990) concerned by the conversion of wheat straw agricultural cellulosic wastes to reducing sugars and glucose has been studied by pretreatments by acid hydrolysis and gamma radiolysis over the dose 0-2 MGy. The pretreatment of cellulosic wastes by gamma radiolysis in the presence of sulfuric acid solution shows that the reducing sugars yield increases with the irradiation dose. The effect of radiation degradation on cellulosic wastes between 0.1MGy and 2 MGy shows the glucose and reducing sugars yields after enzymatic hydrolysis by cellulase vary with the dose. In the relatively low dose range, up to about 0.5 MGy, the reducing sugars yields vary slightly. For an acid hydrolysis followed by radiation at dose range below 0.5 MGy the reducing sugars yields are practically insensitive to radiation. On the other hand, the pretreatment by radiation in higher dose range from 0.5 to 2 MGy followed by enzymatic hydrolysis is effective for the conversion of cellulosic wastes into glucose. The radiation induced degradation of cellulose into glucose depends on the type of acid hydrolysis and on the enzymatic hydrolysis time by cellulase. Pre-irradiation in air is more effective than in acid solution.

The patterns of the radiation-initiated degradation and accumulation of the functional groups (aldehyde, ketone, carboxyl) for cellulose and its derivatives depending on the number of substituted hydroxyl groups in the elementary units of their macromolecules have been studied by *Petryayev et al. (1988)*. It was found that the splitting of the glycoside bond comes about through the reactions of B -fragmentation of the

radicals with free valency localized on the C and (2, atoms accompanied by short chain processes the rate of which is inhibited by the introduction into the elementary polymer unit of a considerable quantity of constituents.

Fast and moderated neutrons emitted from ^{252}Cf as well as low doses of gamma rays from ^{60}Co , produce damaging effects in cellulose nitrate which can be determined viscometrically by calculating the average molecular weight at different doses. Samples were exposed to different doses of gamma rays (1×10^{-4} to 1 Gy) and fission neutron fluences (10^5 - 10^{11} n/cm²) in free space and on a paraffin phantom. The effect of phantom thickness and phantom-to-detector distance on the detector readout has been investigated by *Fadel et al. (1985)*. The results revealed that the predominant bulk effects of radiation on CN are accelerated degradation by random chain scission. Empirical formulae have been given to calculate the absorbed doses of gamma rays and fast neutrons from the measured average molecular weight of the irradiated samples.

Radiation degradation of cellulose was studied by *Leonhardt et al. (1985)*. The results of the degradation of gamma and electron treated wheat straw are reported. Complex methods of treatment (e.g. radiation influence and influence of lyes) are taken into consideration. In vitro-experiments with radiation treated straw show that the digestibility can be increased from 20 % up to about 80 %. A high pressure liquid chromatography method was used to

analyze the hydrolysates. The contents of certain species of carbohydrates in the hydrolysates in dependence on the applied dose are given.

II.2 Thermal and Chemical Degradation Processes of Naturally Occurring polymers

The heterogeneous degradation of chitosan with H_2O_2 was achieved by *Qun et al. (2008)* using phosphotungstate (PTA), an insoluble catalyst synthesized with phosphotungstic acid (PWA) and chitosan in acidic reaction system by electrostatic attraction. The catalyst was characterized by DRS and FTIR spectra. Under the catalysis of PTA, The effect of volume of H_2O_2 , dosage of catalyst, reaction temperature and time on the degradation was discussed by orthogonal tests. The experimental results show that chitosan can be effectively degraded with H_2O_2 under the catalysis of PTA. The catalyst, PTA, may have a promising application in oxidative degradation of polymer.

Dong-Hong et al. (2007) improved the solubility of chitosan at neutral aqueous solution without altering its bioactivity through an alkylation reaction under mild conditions; isobutyl group was introduced to chitosan to form isobutylchitosan which showed a good solubility in neutral aqueous media resulting from the reduced crystallinity of the product. The structure of isobutylchitosan was characterized by IR, 1H NMR spectroscopy, and X-ray diffraction. The results suggested that isobutylchitosan might be one of promising and safe biomaterial with potential applications.

The degradative activities of neutral protease against chitosan samples with different molecular parameters were characterized by *Jin et al. (2007)*. The effects of the degree of deacetylation (DD) and molecular weight (MW) of chitosan on its susceptibility to degradation were investigated. The DD and MW of the chitosans were determined using potentiometric titration and viscometry, respectively. The molecular weight distribution of initial and degraded commercial chitosan was investigated by gel permeation chromatography.

The oxidative degradation of chitosan with H₂O₂ aqueous solution was carried out under the catalysis of phosphotungstic acid in heterogeneous phase *Qun et al. (2007)*. The optimal conditions of degradation were determined by orthogonal tests. The structure of the degraded product was characterized by Fourier-transform infrared spectra (FTIR), diffuse reflectance spectra (DRS) and X-ray diffraction (XRD) analysis. The mechanism of the degradation was correlated with cleavage of the glycosidic bond. The experimental results showed that chitosan can be effectively degraded with H₂O₂ under the catalysis of phosphotungstic acid.

Degradation of chitosan in solution under the action of redox radical initiators was studied by *Fedoseeva et al. (2006)* with the aim to prepare chemically oligomers of natural polysaccharides. The influence of temperature on the rate and extent of the process was examined. The optimal ratios of the

substrate to initiator and of the reductant to oxidant in the initiating system were determined.

Four chitosans with different molecular weights and degrees of deacetylation degree and 28 chitosans derived from these initial chitosans by ultrasonic degradation have been characterized by gel permeation chromatography (GPC), FT-IR spectroscopy, X-ray diffraction and titrimetric analyses. Antimicrobial activities were investigated against *E. coli* and *S. aureus* using an inhibitory rate technique. ***Hui et al. (2006)*** showed that ultrasonic treatment decreased the molecular weight of chitosan, and that chitosan with higher molecular weight and higher DD was more easily degraded. The polydispersity decreased with ultrasonic treatment time, which was in linear relationship with the decrease of molecular weight. Ultrasonic degradation changed the DD of initial chitosan with a lower DD (<90%), but not the DD of the initials chitosan with a higher DD (>90%). The increased crystallinity of ultrasonically treated chitosan indicated that ultrasonic treatment changed the physical structure of chitosan, mainly due to the decrease of molecular weight. Ultrasonic treatment enhanced the antimicrobial activity of chitosan, mainly due to the decrease of molecular weight.

Juan and Pierre (2005) depolymerized chitosan either by HCl hydrolysis or enzymatic degradation with a commercial preparation Pectinex Ultra Spl. The chitooligosaccharides released by both methods were selectively precipitated in methanol solutions and characterized using MALDI-TOF mass

spectrometry. Differences between the two methods were detected and concerned the degrees of polymerization of the fragments produced and their acetylation. The enzymatic method yielded shorter fragments with a higher proportion of fully deacetylated chitooligomers. Conversely, acid hydrolysis of the starting chitosan resulted in fragments with degrees of polymerization up to sixteen and more monoacetylated residues than with the enzymatic procedure.

Tanyarut et al. (2005) controlled alginate gel degradation utilizing partial oxidation and bimodal molecular weight distribution degradability is often a critical property of materials utilized in tissue engineering. Although alginate, a naturally derived polysaccharide, is an attractive material due to its biocompatibility and ability to form hydrogels its slow and uncontrollable degradation can be an undesirable feature. Specifically, alginates were partially oxidized to a theoretical extent of 1% with sodium periodate which created acetal groups susceptible to hydrolysis. The ratio of low MW to high MW alginates used to form gels was also varied while maintaining the gel forming ability of the polymer. The rate of degradation was found to be controlled by both the oxidation and the ratio of high to low MW alginates, as monitored by the reduction of mechanical properties and corresponding number of crosslinks, dry weight loss, and molecular weight decrease.

The influence of high-intensity ultrasonication on the molecular weight and degree of acetylation of chitosan was investigated by *Shari et al. (2005)*. High-molecular weight

shrimp chitosan was purified by alkaline precipitation and dialysis from aqueous solution. A 1% (w/v) chitosan in 1% (v/v) aqueous acetic acid was sonicated for 0, 0.5, 1, 5, 15, and 30 min at 25 °C at power levels of 16.5, 28.0 and 35.2 W cm⁻². Degree of acetylation was determined by high-pressure liquid chromatography with photodiode array at 210 nm, monitoring acetyl groups released after complete hydrolysis and deacetylation of samples. Average molecular weight of ultrasonicated chitosan was determined by measurements of intrinsic viscosity of samples. The degree of acetylation of purified chitosan was 21.5%. Results indicated that neither power level nor sonication time altered the degree of deacetylation of chitosan molecules. Intrinsic viscosity of samples decreased exponentially with increasing sonication time. Rates of intrinsic viscosity decrease increased linearly with ultrasonic intensity. Results were analyzed in terms of molecular weight decreases. The Schmid polymer degradation model was used to analyze the molecular weight decay as a function of sonication time. A first order relationship for the dependence of the reaction rate on the ultrasonic intensity was suggested. Results of this study indicate that high-intensity ultrasonication can be utilized to reduce molecular weight of chitosan while maintaining the degree of acetylation.

Jin et al. (2005) hydrolysed chitosan with 91.7% deacetylation by a commercially available and efficient neutral protease. The degradation was monitored by gel permeation chromatography. Factors affecting the enzymatic hydrolysis of chitosan were studied. The structures of degraded chitosans

were characterised by X-ray diffraction, Fourier transform infrared and MALDI-TOF mass spectrometry.

Chitosan has been extensively used as an absorption enhancer for macromolecules and as gene delivery vehicle. Both properties are molecular weight (MW) dependent. *Shirui et al. (2004)* investigated factors affecting the oxidative depolymerization of chitosan and physicochemical properties of the resulting polymer fractions including their cytotoxicity. The molecular weight of the depolymerized chitosan was influenced by the initial concentration and the source of chitosan. At constant initial concentrations the molecular weight decreased linearly with the chitosan/ NaNO_2 ratio and was a function of logarithm of the reaction time. Chitosan with larger molecular weight was more sensitive to depolymerization.

The mechanism of thermal depolymerization of alginate in the solid state has been investigated by *Hilde et al. (2003)*. Depolymerization at elevated temperatures of two commercial highly purified alginates, one with high content of guluronic acid (G) and another with high content of mannuronic acid (M) was followed by measuring the apparent viscosity and the intrinsic viscosity. The initial rate constants were determined from the intrinsic viscosity data and no significant difference between the G-rich ($F_G = 0.63$) and M-rich ($F_G = 0.43$) alginate was found. The activation energies of the G-rich alginate and the M-rich alginate were determined from the initial rate constants to be 114 ± 6 kJ/mol and 126 ± 12

kJ/mol, respectively. The rate of depolymerization was not affected by the presence of oxygen showing that the oxidative–reductive depolymerization mechanism is not responsible for the thermal depolymerization. The initial rate constants for alginates prepared by freeze-drying of solutions with pH between 3.8 and 9.5 were pH dependent. The depolymerization was found to be catalyzed simultaneously by protons and hydroxide ions. These catalytic effects were negligible between pH 5 and pH 8. The catalytic constants for the OH^- were identical for the M-rich and G rich alginate. However, the catalytic constant for the H^+ was about 2 times greater for the M-rich alginate than for the G-rich alginate. This suggests that the M-rich alginate is more susceptible to acid hydrolysis than the G-rich alginate in the solid state, as also was found for alginate in solution when the mechanism of intramolecular acid catalysis prevailed. ^1H and ^{13}C NMR spectroscopy of the thermally degraded alginates were used to identify new non-reducing ends obtained from the depolymerization. New non-reducing ends from b-elimination caused by alkaline hydrolysis were clearly identified in the spectra obtained from alginates with pH between 4.3 and 9.5, when pH is defined as the pH of 1% (w/w) alginate solution prepared from a given freeze dried sample. The results reported herein indicate that acid hydrolysis and alkaline hydrolysis are the primary mechanisms involved in the thermal depolymerization of highly purified alginate in the solid state.

A thermal dissociation initiator, potassium persulfate (KPS), is added to the chitosan solution at 70 °C immediately,

the solution viscosity and the molecular weight of chitosan decrease in a very short time. Size exclusion chromatography, nuclear magnetic resonance and electron spin resonance were used to study the degradation mechanism by *Shih-Chang et al. (2002)*. A free radical degradation mechanism of chitosan by KPS is then proposed. When KPS is thermally dissociated into anionic radicals, they are attracted to the cationic amino group in the chitosan ring. Subsequently, the anionic radical attacks the C₄ carbon and transfers the radical to the C₄ carbon by subtracting the hydrogen from it. The presence of free radical at C₄ carbon eventually results in the breakage of the glycosidic C-O-C bond in the chitosan main chain. According to this mechanism, the concentrations of KPS, total free radicals and the degraded chitosan chain at different degradation times are all calculated by solving the rate equations. Finally, the calculated average molecular weights of the degraded chitosan chains at different reaction times agree with the experimental values.

The degradation of chitosan by hydrogen peroxide was studied by *Qin et al. (2002)*. The degradation was monitored by gel permeation chromatography (GPC). The molecular weight distribution of partially degraded products from homogeneous reaction displayed a single modal curve whereas that from heterogeneous reaction was bimodal. The molecular weight (Mw) decreased as the temperature, the time and/or hydrogen peroxide concentration increased. The dissolution of chitosan (pH 5.5) in minimum hydrochloride enhanced its degradation, but excessive hydrogen ion potentially inhibited

the degradation. The formation of carboxyl group and deamination in the products indicated that the decrease of Mw was accompanied by structure changes. The degraded chitosans in Mw range from 5.1×10^3 to 1.2×10^3 were characterized by elemental analysis, X-ray diffraction, thermogravimetric analysis (TGA) and differential thermal analysis (DTA), Fourier transform infrared (FT-IR), carbon-13 nuclear magnetic resonance spectroscopy ($^{13}\text{CNMR}$). There was no significant chemical change in the backbone of chitosan with Mw of 5.1×10^3 . But degraded chitosan with Mw of 3.5×10^3 had 1.71 mmol/g carboxyl groups and lost about 15% of amino groups. Further degradation led to more ring-opening oxidation of degraded products, the formation of carboxyl groups and faster deamination. The degraded chitosan with Mw of 1.2×10^3 had 2.86 mmol/g carboxyl groups and lost more than 40% of amino groups.

Pankaj and Lawrence (1999) investigated the influence of reaction temperature, processing time, and mechanical shear on the depolymerization (DP) of chitosans and to evaluate the importance of the sequencing of the deacetylation and DP processes on the resultant macromolecules and their properties. Process sequence did not alter the degree of deacetylation (DD), the intrinsic viscosity, or the molecular weight (MW). Treatment conditions affected the properties of the resultant polymer: the reaction temperature and processing time had a significant impact on the MWs and DDs of the resultant polymer. Mechanical shear, however, did not significantly affect the above properties. Furthermore, polymer

crystallinity was affected by reaction temperature but not by shear or processing time.

Dry chitin was thermally degraded under nitrogen. The main volatile degradation product was acetamide. Chitin and cellulose were depolymerized by thermal degradation in tetraethyleneglycol dimethylether as a high boiling and inert solvent to give water-soluble oligomers with a terminal anhydrosugar unit. In supercritical acetone, cellulose could be degraded to the extent of 98% and chitin to the extent of 85%. Monomeric anhydrosugars were formed with good yields and could be identified and isolated from the degradation syrups *Köll et al. (1991)*.

Chitin and cellulose have been depolymerized by thermal degradation in a high boiling and inert solvent to give water-soluble oligomers with a terminal anhydrosugar unit *Köll et al (1990)*. Pure oligomers have been obtained by preparative gel permeation chromatography, and characterized by ^1H -NMR, ^{13}C -NMR and fast atom bombardment - mass spectrometry.

Information about the thermal degradation of the polysaccharides sodium alginate, carrageenan and carboxymethyl cellulose has been obtained from the time dependence of the viscosity at high temperatures measured using a slit viscometer. The viscosity is related to the molecular weight using relations between the zero shear specific viscosity and the coil overlap parameter in conjunction with the appropriate Mark-Houwink equation.

Bradley et al. (1988) found that alginate is much less stable than carboxymethyl cellulose and carrageenan.

II.3- Possible Applications of Degraded Naturally Occurring Polymers

The method of degradation of natural amino-polysaccharides to obtain a product applicable as biospecimen in protection and stimulation of the plants growth were elaborated by **Chmielewski et al. (2007)**. Depolymerization of chitosan can be carried out by radiation or chemical degradation combined with irradiation method. The efficiency of these methods was verified by viscometric analysis. The chemical-radiation method was much more appropriate from economical point of view. By application of this method it was possible to obtain product with lower crystalline phase content than initial one, what was proved by X-ray diffraction studies. Finally preliminary agricultural tests on spring rape seeds were performed. The results showed that the biggest growth was observed for chitosan (molecular weight 47,000 Da) in concentration of 0.1 g/kg of seeds. The higher concentration did not affect plant's growth. The average growth over-ground plant parts was about 16–22%, diameter of roots was about 11–13%, and mass of roots was about 51–65% higher in comparison to the control.

Low-molecular-weight carboxymethyl chitosans (CMCTSs) were prepared by oxidative degradation method involving hydrogen peroxide (H_2O_2) without or with

microwave radiation *Tao et al. (2007)*. Viscosity determination and end group analysis were applied to measure molecular weights of CMCTSs. Effects of concentration of H_2O_2 and degradation times on molecular weights of CMCTSs were studied. The degradation process of CMCTSs will be accelerated with the aid of microwave radiation and degradation time may be reduced greatly. The superoxide anion scavenging activity of CMCTSs was evaluated by application of flow injection chemiluminescence technology. The 50% inhibition concentrations (IC₅₀s) of CMCTSs A, B, and C (1130, 2430 and 4350 Da) were 10.36, 17.57, and 23.38 mg/mL, respectively. The results showed that CMCTSs with lower molecular weight had better superoxide anion scavenging activity.

Low molecular weight chitosan (LMWC) and chitooligosaccharides (COs), obtained by persulfate-induced depolymerization of chitosan showed scavenging of $OH^{\cdot-}$ and $O_2^{\cdot-}$ radicals and offered protection against calf thymus DNA damage. Over 85% inhibitions of free radicals and DNA protection were observed by *Keelara et al. (2007)*. LMWC (0.05 μ mol) showed a strong inhibitory activity compared to COs (3.6 μ mol). Further, LMWC showed calf thymus DNA condensation reversibly giving stability, as evident from CD, TEM and melting curves (T_m). A fluorescence study suggests the binding of LMWC in the minor groove, forming H-bonds to the backbone phosphates without distorting the double helix structure.

The effect of shrimp and fungal chitosan on the growth and development of orchid plant meristemic tissue in culture was investigated in liquid and on solid medium by ***Khin et al. (2006)***. The growth of meristem explants into protocorm-like bodies in liquid medium was accelerated up to 15 times in the presence of chitosan oligomer, the optimal concentration being 15 ppm. The 1 kDa shrimp oligomer was slightly more effective compared to 10 kDa shrimp chitosan and four times more active compared to high molecular weight 100 kDa shrimp chitosan. The 10 kDa fungal chitosan was more effective compared with 1 kDa oligomer. The development of orchid protocorm into differentiated orchid tissue with primary shoots and roots was studied on solid agar medium. The optimal effect, the generation of 5–7 plantlets in 12 weeks was observed in the presence of 20 ppm using either 10 kDa fungal or 1 kDa oligomer shrimp chitosan. The data are consistent with preliminary results from field experiments and confirm unequivocally that a minor amount of chitosan has a profound effect on the growth and development of orchid plant tissue.

Ajay et al. (2006) developed a protocol for plant regeneration from encapsulated shoot tips collected from in vitro proliferated shoots of *Withania somnifera*. The best gel composition was achieved using 3% sodium alginate and 75 mM $\text{CaCl}_2 \cdot 2\text{H}_2\text{O}$. The maximum percentage response (87%) for conversion of encapsulated shoot tips into plantlets was achieved on MS medium supplemented with 0.5 mg/l IBA after 5 weeks of culture. The conversion of encapsulated shoot tips into plantlets also occurred when calcium alginate beads

having entrapped propagules were directly sown in autoclaved soilrite moistened with 1/4 MS salts.

Chitosan, a natural biopolymer derived by deacetylation of chitin, has been extensively used in biomedical, agricultural and food applications. ***Hong et al. (2006)*** developed various economic/simplified chitosan production processes for particular food applications. Therefore, a set of experiments was designed to evaluate the effect of chitosans prepared under various deproteinization (DP) times (at 0, 5 and 15 min) and demineralization (DM) times (at 0, 10, 20 and 30min) on the growth of soybean sprouts. Chitosan treatment increased the total weight of soybean sprouts by 10.7–13.8% compared with that of the control; the effectiveness of the chitosan treatment was independent of DP and DM times. The increase (12.7%) in the growth of soybean sprouts by chitosan prepared without DP and DM steps was noteworthy. This investigation demonstrates that the elimination of DP and DM steps or a reduction in the reaction time required for optimum DP and DM in the production of chitosan needs further studies before being considered for particular usages.

Czechowska-Biskup et al. (2005) described three physical methods of chitosan degradation: irradiation in dry state, irradiation in aqueous solution and sonication in aqueous solution were tested and compared in the terms of yields and side effects. The influence of average molecular weight of chitosan in its fat-binding ability in vitro has been studied by using a biopharmaceutical model of digestive tract. It was

found that reduction in molecular weight leads to a significant increase in the amount of fat bound by 1 g of chitosan. Thus, radiation- or sonochemical treatment may be useful in improving fat-binding properties of chitosan as an active component of dietary food additives.

Wuling et al. (2005) investigated the mechanisms whereby treatment with chitosan (CHN) is observed to increase the capacity of plants to resist pathogens, CHNs of different molecular weights (MWs) prepared by enzyme hydrolysis were used to treat rice cells in suspension culture and also rice seedlings. The results obtained with cultured cells showed that in this material CHN treatment could trigger a set of defence responses including the production of hydrogen peroxide (H_2O_2), increases in the activities of phenylalanine ammonialyase (PAL; EC 4.3.1.5) and chitinase (CHI; EC 3.2.1.14), increases in transcription of defence-related genes b-1,3-glucanase (glu) and chitinase (chi) and accumulation of pathogen-related protein (PR1). Furthermore, CHNs of different MWs were observed to have different capacities to induce defence responses. CHNs of low MWs were more effective at inducing the described defence responses than those of higher MWs. Enhanced defence against rice blast pathogen *Magnaporthe grisea* 97-23-2D1 was observed in rice seedlings treated with low MW CHNs compared to seedlings treated with higher MW CHNs. In all cases, suppressing the production of H_2O_2 by adding scavengers dimethylthiourea (DMTU), 2,5- dihydroxycinnamic acid methyl ester (DHC), catalase (Cat) or ascorbate (As) blocked the defence responses.

These results indicate that CHNs of low MWs have a greater capacity to induce the production of H₂O₂, thus resulting in stronger defence responses, than those with higher MWs.

Luan et al. (2005) studied the degradation of chitosan, chitosan with an 80% degree of deacetylation and a weight-average molecular mass (Mw) of approx. 48 kDa was irradiated with gamma-rays at doses up to 200 kGy in a 10% (w/v) solution. The Mw of chitosan was reduced from 48 to 9.1 kDa by irradiation. The characteristics of irradiated chitosan were analyzed by using FTIR spectroscopy and an elemental analyzer. The amino group was found to be stable whereas the C-O-C group decreased with increase in the dose. The product of chitosan irradiated at 100 kGy with an Mw of approx. 16 kDa showed the strongest growth promotion effect on plants in vitro. For shoot culture, supplementation with irradiated chitosan increased the fresh biomass of shoot clusters (7.2-17.0%) as well as the shoot multiplication rate (17.9-69.0%) for *Chrysanthemum morifolium* (florist's chrysanthemum), *Limonium latifolium* (limonium or sea-lavender), *Eustoma grandiflorum* (lisianthus, tulip gentian or Texas bluebell) and *Fragaria ananassa* (modern garden strawberry). The optimum concentrations of irradiated chitosan were found to be approx. 70-100 mg/l for chrysanthemum, 50-100 mg/l for lisianthus and 30-100 mg/l for limonium. For the plantlet culture, the optimum concentrations were found to be approx. 100 mg/l for chrysanthemum, 30 mg/l for lisianthus, 40 mg/l for limonium and 50 mg/l for strawberry. Supplementation with optimum

concentrations of irradiated chitosan resulted in a significant increase in the fresh biomass (68.1% for chrysanthemum, 48.5% for lisianthus, 53.6% for limonium and 26.4% for strawberry), shoot height (19.4% for chrysanthemum, 16.5% for lisianthus, 33.9% for limonium and 25.9% for strawberry) and root length (40.6% for chrysanthemum, 66.9% for lisianthus, 23.4% for limonium and 22.6% for strawberry). In addition, treatment with irradiated chitosan enhanced the activity of chitosanase in treated plants and also improved the survival ratio and growth of the transferred plantlets acclimatized for 10-30 days under greenhouse conditions.

Ronge et al. (2004) used microwave radiation to introduce N-sulfo and O-sulfo groups into chitosan with a high degree of substitution and low-molecular weight. The sulfation of chitosan was performed in microwave ovens. It was found that microwave heating is a convenient way to obtain a wide range of products of different degrees of substitution and molecular weight only by changing reaction time or/and radiation power. Moreover, microwave radiation accelerated the degradation of sulfated chitosan and the molecular weight of sulfated chitosan was considerably lower than that obtained by traditional heating. There are no differences in the chemical structure of sulfated chitosan obtained by microwave and by conventional technology. FTIR and ^{13}C -NMR spectral analyses demonstrated that a significantly shorter time is required to obtain a satisfactory degree of substitution and molecular weight by microwave radiation than by conventional technology. Also antioxidant activity of low-

molecular-weight and high-sulfate-content chitosans (LCTS) determined. The results showed LCTS could scavenge superoxide and hydroxyl radical. Its IC_{50} is 0.025 and 1.32mg/mL, respectively. It is a potential antioxidant in vitro.

Alginate with a weight-average molecular mass (M_w) of approx. 9.04×10^5 Da was irradiated at 10-200 kGy in 4% (w/v) aqueous solution. The degraded alginate product was used to study its effectiveness as a growth promoter for plants in tissue culture ***Le et al. (2003)***. Alginate irradiated at 75 kGy with an M_w of approx. 1.43×10^4 Da had the highest positive effect in the growth of flower plants, namely limonium, lisianthus and chrysanthemum. Treatment of plants with irradiated alginate at concentrations of 30-200 mg/l increased the shoot multiplication rate from 17.5 to 40.5% compared with control. In plantlet culture, 100 mg/l irradiated alginate supplementation enhanced shoot height (9.7-23.2%), root length (9.7-39.4%) and fresh biomass (8.1-19.4%) of chrysanthemum, lisianthus and limonium compared with that of the untreated control. The survival ratios of the transferred flower plantlets treated with irradiated alginate were almost the same as the control value under greenhouse conditions. However, better growth was attained for the treated plantlets.

Lian-Ying and Jiang-Feng (2003) used *E. coli* and *Staphylococcus aureus* to study the antimicrobial activity of chitosan of different molecular weights (MW). The effect of the concentration and MW of chitosan were investigated,

respectively, and the antimicrobial mechanism was discussed. For chitosan with MW below 300 kDa, the antimicrobial effect on *S. aureus* was strengthened as the MW increased. In contrast, the effect on *E. coli* was weakened.

Utilization of carbohydrates by radiation processing was introduced by upgrading and utilization of carbohydrates such as chitosan, sodium alginate, carrageenan, cellulose, pectin have been investigated by *Kume et al. (2002)* for recycling these bio-resources and reducing the environmental pollution. These carbohydrates were easily degraded by irradiation and various kinds of biological activities such as anti-microbial activity, promotion of plant growth, suppression of heavy metal stress, phytoalexins induction, etc. were induced. Also some carbohydrate derivatives, carboxymethylcellulose and carboxymethylstarch, could be crosslinked under certain radiation condition and produce the biodegradable hydrogel for medical and agricultural use. Antibacterial activities of six chitosans and six chitosan oligomers with different molecular weights (Mws) were examined by *Hong et al. (2002)* against four gram-negative (*Escherichia coli*, *Pseudomonas fluorescens*, *Salmonella typhimurium*, and *Vibrio parahaemolyticus*) and seven gram-positive bacteria (*Listeria monocytogenes*, *Bacillus megaterium*, *B. cereus*, *Staphylococcus aureus*, *Lactobacillus plantarum*, *L. brevis*, and *L. bulgaricus*). Chitosans showed higher antibacterial activities than chitosan oligomers and markedly inhibited growth of most bacteria tested although inhibitory effects differed with Mws of chitosan and the particular bacterium. Chitosan generally showed stronger bactericidal effects with

gram-positive bacteria than gram-negative bacteria in the presence of 0.1% chitosan. The minimum inhibitory concentration (MIC) of chitosans ranged from 0.05% to > 0.1% depending on the bacteria and Mws of chitosan. As a chitosan solvent, 1% acetic acid was effective in inhibiting the growth of most of the bacteria tested except for lactic acid bacteria that were more effectively suppressed with 1% lactic or formic acids. Antibacterial activity of chitosan was inversely affected by pH (pH 4.5–5.9 range tested) with higher activity at lower pH value. *Le et al. (2001)* studied the effect of radiation-degraded chitosan on plants stressed with vanadium. The toxicity of vanadium (V) and the effect of chitosan have been investigated on soybean, rice, wheat and barley. The results showed that wheat and barley were sensitive to V than rice and soybean but all seedlings of these plants were damaged at 2.5 µg/ ml V (in VCl₃). These damages were reduced by application of radiation-degraded chitosan. The recovery of growth and reduction of V levels in seedlings were obtained by the treatments with 10–100 mg/ml chitosan irradiated at 70–200 kGy of g-rays in 1% solution. The reductions of V and Fe contents in plants were due to the ability of chitosan to form chelate complexes with metals in solution. The result of BAS analysis showed that the absorption and transportation of ⁴⁸V to the leaf from root was suppressed with irradiated chitosan. Therefore, it can be concluded that chitosan irradiated at suitable doses (ca. 100 kGy) is effective as plant growth promoters and heavy metal eliminators in crop production.

Antimicrobial activity of irradiated chitosan was studied by *Matsuhashi and Kume (1997)* against *Escherichia coli* B/r. Irradiation of chitosan at 100 kGy under dry conditions was effective in increasing the activity, and inhibited the growth of *E. coli* completely. The molecular weight of chitosan significantly decreased with the increase in irradiation dose, whereas the relative surface charge of chitosan was decreased only 3% by 100 kGy irradiation. Antimicrobial activity assay of chitosan fractionated according to molecular weight showed that $1 \times 10^5 - 3 \times 10^5$ fraction was most effective in suppressing the growth of *E. coli*. This fraction comprised only 8% of the 100 kGy irradiated chitosan. On the other hand, chitosan whose molecular weight was less than 1×10^5 had no activity. The results show that low dose irradiation, specifically 100 kGy, of chitosan gives enough degradation to increase its antimicrobial activity as a result of a change in molecular weight. **Alginate** has been used as a gelling agent for culture medium in which tobacco and petunia protoplasts were suspended. The gel, formed by cation dependent cross-linkages, supported colony formation with efficiency comparable to agar medium. The **alginate** matrix was liquefied by addition of a chelating agent, making possible the recovery of developing colonies without significantly affecting their continued **growth**. The use of this plating technique offers not only the advantage of suspending **plant** material in semi-solid medium without temperature shock but also potential for subsequent large scale recovery *Adaoha et al. (1982)*.

II.4- Radiation-Induced Graft Copolymerization and Their Possible Applications

The modification of polypropylene (PP) with acrylic acid (AA) by reactive extrusion using pre-irradiated PP (rPP) as initiator was investigated by ***Chuanlun et al. (2008)***. It was found the relatively high graft degree (G_d) and slight degradation of modified PP was obtained when 20wt% rPP was used. This result can be explained in terms of effective concentration of free radicals. Compared with the neat PP, the modified PP showed the high-notched impact strength and improved adhesion of PP to polar substrate. This technique is of potential industrial interest for PP modification.

Binary graft copolymerization of pH sensitive acrylic acid (AAc) and thermosensitive N-isopropylacrylamide (NIPAAm) monomers onto pre-irradiated polypropylene films (PP) was carried out by two individual steps using a ^{60}Co gamma radiation source ***Yessica et al. (2007)***. The influence of preparation conditions, such as pre-irradiation dose and reaction time on grafting yield was studied. The swelling behavior and attenuated total reflection fourier transformation infrared spectroscopy (FTIR-ATR) study for PP films grafted films were investigated.

Polytetrafluoroethylene (PTFE) was grafted with acrylic acid (AAc) by pre-irradiation method using γ -ray to get PTFE-

g-AAc films, then N-isopropylacrylamide (NIPAAm) was grafted onto PTFE-g-AAc films with γ -ray to get (PTFE-g-AAc)-g-NIPAAm. PTFE films were irradiated in air at a dose rate of 3.0 kGy h^{-1} and different radiation dose **Bucio and Burillo (2007)**. The irradiated films were placed in glass ampoules, which contained aqueous solutions with different monomer concentration (AAc) and then they were heated at different temperatures and reaction time. NIPAAm onto PTFE-g-AAc was carried out with the same procedure with monomer concentration of 1 molL^{-1} . The thermosensitivity of the samples was defined and calculated as the ratio of the grafted samples swelling at 28 and 35°C, and pH sensitivity defined as the ratio of the grafted samples swelling at pH 2 and 8.

Graft polymerization of acrylonitrile onto polypropylene (PP) monofilament was carried out by a preirradiation method using a ^{60}Co gamma radiation source by **Bhuvanesh et al. (2006)**. The influence of synthesis conditions such as preirradiation dose, reaction time, monomer concentration, reaction temperature and additives was determined. The grafting was considerably influenced by the instantaneous swelling of the mono filament in the reaction mixture during the course of the grafting process. The order of dependence of the rate of grafting on monomer concentration was found to be 1.04. The nature of the medium of the grafting and the additives had profound influence over the grafting reaction. The accelerative effects of solvent medium on the grafting were higher in methylethyl ketone (MEK) and

dimethylformamide (DMF) as compared to methanol. At the same time, partial replacement of DMF with water led to acceleration in the grafting with peak maxima at 20% solvent composition. The addition of a small amount of sulfuric acid to the reaction mixture also resulted in a significant acceleration of the degree of grafting.

Grafting of phosphate groups has been investigated as a means to render biomedical polymers able to induce the formation of an apatite layer. *Pedro et al. (2006)* regenerated cellulose hydrogels were surface modified by phosphorylation. The in vitro biocompatibility of materials with varying phosphate contents was evaluated in cultured human bone marrow stromal cells (HBMSC) in terms of cytotoxicity, cell attachment, proliferation and immunohistochemistry. Negatively charged cellulose phosphates were neutralized in the form of the calcium salt before contact with cells. Cellulose phosphates were not cytotoxic, independently of the phosphate content. Unmodified regenerated cellulose hydrogels showed good rates of HBMSC attachment and proliferation. On the contrary, negatively charged, highly hydrophilic phosphorylated surfaces showed poor HBMSC attachment and proliferation as well as poor alkaline phosphatase-specific activity and expression of osteocalcin and type I collagen. Differences found are discussed in terms of surface chemical functionality, hydrophilicity and charge.

Jinhua et al. (2006) developed a highly chemically stable polymer electrolyte membrane for application in a direct

methanol fuel cell (DMFC), styrene derivative monomers; m,p-methylstyrene (MeSt), p-tert-butylstyrene (*t*BuSt), divinylbenzene (DVB) and bis(p,p-vinyl phenyl) ethane (BVPE) were graft copolymerized into poly(ethylene-co-tetrafluoroethylene) (ETFE) films followed by sulfonation and hydrolysis. The latter two monomers were used as crosslinkers. The graft copolymerization was carried out by the γ -ray preirradiation method. The influence of the preirradiation dose and the grafting kinetics were investigated in details. Sulfonation of the grafted ETFE films was performed in a chlorosulfonic acid solution by which the sulfonation ratio reached about 90%. By means of the FTIR and TG-DTA measurements, it was evident that the monomers were grafted into the ETFE films and that the sulfonic acid groups were attached to the aromatic rings of the graft chain. Assessing their potential to serve as polymer electrolyte membrane in a DMFC was performed by measurement of the ion exchange capacity, proton conductivity, water uptake, chemical stability and the methanol permeability. The newly obtained membrane possesses significantly higher chemical stability than the traditional styrene/DVB-grafted membrane and six times lower methanol permeability compared to the Nafion 112 membrane. Therefore, it was revealed the possibility of the developed inexpensive four monomers-grafted membranes which could provide an attractive alternative as a substitute for the expensive Nafion membranes for DMFC applications.

The surface properties of low-density polyethylene (LDPE) can be modified by the grafting of 2-

hydroxyethylmethacrylate (HEMA). *Ferreira et al. (2005)* aimed to produce of new materials suitable for bioapplications. Samples with different monomer concentrations were prepared from LDPE particles by gamma irradiation following different irradiation protocols including irradiation in presence and absence of air. The samples were characterized by thermal analysis techniques (DSC and TGA) and by FTIR. The results obtained show a decrease in the crystallinity of the supporting matrix for copolymers with high yields of grafting. However, the new materials prepared maintain good structural order resulting from the protective effect of polyHEMA grafted onto LDPE backbone. These effects can improve the diffusion of other species deeper inside the matrix and increase the material hydrophilicity.

Grafting vinyl acetate (VAc) and maleic anhydride (MAN) comonomer onto high density polyethylene (HDPE) was performed by means of gamma rays. Conditions for the minimum homopolymer formation, maximum grafting yield and alternate copolymer grafts were carried out by *Abd El-Reheim (2005)*. Further chemical treatment with sodium hydroxide, hydrochloric acid, ammonium hydroxide, sulfamic acid and amino pyridine was made on the grafted membranes to increase functionality. The swelling, mechanical, solute permeability and biocompatibility properties of these copolymers were evaluated for possible application as dialysis membranes. The introduction of functional groups on HDPE membranes enhanced their hydration and transport flux. The treated grafted membranes showed improved permeability

towards urea, creatinine and uric acid over the ungrafted HDPE. The permeability rate of the solutes through the membranes depended on the molecular weight and the size of the solutes. The presence of hydrophilic groups on the membranes reduced protein adsorption and enhanced membranes transport. The swelling, solute dialysis permeability and protein low affinity properties of HDPE-g-(VAc-alt-MAn) treated with sulfamic acid or 2-aminopyridine indicate potential use as hemodialysis membranes.

Adem et al. (2005) showed results on radiation grafting of acrylic acid (AAc) and N-isopropylacrylamide (NIPAAm) mixtures onto polytetrafluoroethylene (PTFE) films. The main objective is to use the modified polymer for immobilization of the avidin-streptavidin systems or other bio-compounds. Grafting onto PTFE was carried out by the pre-irradiation oxidative method in air at different dose rates and irradiation doses. The irradiation was produced with the electron beam of a 2 MV Van de Graaf accelerator and gamma-rays from a gamma beam 651 PT. The samples were placed in glass ampoules with the AAc and NIPAAm mixtures in an aqueous solution. Graft polymerization was performed by heating of the polymer-monomer composition in an argon atmosphere at temperature of 50 °C. Surface functionalization was studied by X-ray photoelectron spectroscopy (XPS), morphology of the surface was studied by scanning electron microscopy (SEM) and hydrophylization of the surface by contact angle measurements (static method).

Preparation and characterization of water -soluble maleic anhydride/acrylic acid (MAN/AAC) copolymer and its derivatives were studied by *Abd El-Rehim et al. (2005)* for possible use as antibacterial agents. Preparation conditions that affect the copolymer yield, molecular weight and polymeric chain distribution were studied. As the irradiation dose increases, the copolymer yield as well as molecular weight increases. The higher the MAN content in the comonomer feed solution, the lower the copolymer yield. The derivatives of MAN/AAC copolymers of different functional groups were obtained by treating MAN/AAC copolymer with various organic reagents containing reactive amino groups, such as sulpha drug compounds and amino acid derivatives. Characterization of obtained copolymers using FTIR, ^1H NMR, viscometric, and elemental analysis was carried out. The antibacterial activity of different molecular weight copolymers and their derivatives against gram negative and gram positive bacteria was investigated. The results obtained revealed that such copolymers and the water-soluble derivatives possessed a broad lethal activity against different types of bacteria and could be used as antibacterial agents.

Jianhua et al. (2005) prepared the cation-exchange membranes obtained by pre-irradiation grafting of acrylic acid (AAC) and sodium styrene sulfonate (SSS) onto high-density polyethylene (HDPE) and its properties such as swelling behavior and electric resistance were measured as a function of ion-exchange capacity (IEC). Thermal and chemical stability was also investigated. These properties were found to be

mainly dependent on IEC. The grafted membranes possessed good electrochemical, thermal and chemical properties, and were found to be acceptable for practical use as cation-exchange membranes.

Poly(acrylonitrile -co-N- vinyl -2- pyrrolidone)s (PANCNVP) were synthesized by water-phase precipitation copolymerization (WPPCP) with sodium chlorate–sodium metabisulfite as an oxidant/reducer initiator system *Ling-Shu et al. (2005)*. The copolymers were also synthesized by a solution copolymerization (SCP) initiated with azobis(isobutyronitrile) for comparison. Fourier transform infrared spectroscopy (FT-IR), nuclear magnetic resonance (^1H NMR), and differential scanning calorimetry (DSC) were used to characterize the copolymers. It was found that the copolymerization yield, the molecular weight of the copolymers, and the N-vinyl-2-pyrrolidone (NVP) conversion for WPPCP were much higher than those for SCP. Results indicated that WPPCP was a ‘green’ and effective method to incorporate NVP into polyacrylonitrile. The surface properties of the copolymer dense membranes were studied by water contact angle, protein adsorption, and platelet adhesion measurements. Typical results demonstrated that the introduction of NVP had little influence on the static, advancing and receding contact angles of the dense membrane surface. However, the bovine serum albumin adsorption and the platelet adhesion were remarkably suppressed with the increase in NVP content in the copolymers. When the mole fraction of NVP in the copolymers reached 14.6%, little

platelet adhesion took place. These results revealed that the hemocompatibility of polyacrylonitrile could be greatly improved by the incorporation of NVP.

Zhi-Kang et al. (2005) improved the surface biocompatibility asymmetric membranes fabricated from poly (acrylonitrile-co-maleic acid)s (PANCMA)s synthesized by water-phase precipitation copolymerization were tethered (or immobilized) with poly(ethylene glycol)s (PEGs) by esterification reaction. Chemical changes on the membrane surface were characterized by FTIR and elemental analysis to confirm the immobilization of PEG onto the PANCMA membranes. The hydrophilicity and blood compatibility of the PEG-tethered PANCMA membrane were investigated by water contact angle, water absorption, protein adsorption, plasma platelets adhesion and cell adhesion measurements and the results were compared with the corresponding PANCMA membranes. Also it was found that after the tethering of PEG the hydrophilicity of the membrane can be improved significantly and the protein adsorption, platelets adhesion and macrophage attachments on the membrane surface are obviously suppressed. Furthermore, not only the content of maleic acid in PANCMA, which influences the tethering density of PEG but also the molecular weight of PEG has great effect on the surface modification of PANCMA membranes for biocompatibility.

As a polysaccharide of natural origin, chitosan has the inherent properties of being biocompatible, biodegradable, and

non-toxic. These properties make chitosan an ideal candidate for based backbone in copolymeric matrices for use in biomedical applications. Poly(hydroxyethylmethacrylate) is a synthetic hydrogel which possesses a high mechanical strength. The conjunction of these two components results in a new matrix that combines the useful properties of the synthetic pHEMA and natural chitosan. *Casimiro et al. (2005b)* obtained chitosan/pHEMA membranes by γ -irradiated under nitrogen atmosphere. The effect of various synthesis conditions on the chemical, physical and biological properties was evaluated. The chitosan/pHEMA membranes were characterized using FTIR spectroscopy, scanning electron microscopy SEM and thermal analysis techniques. Its hydration capacity and its antimicrobial properties were also determined. The obtained results showed that the hydration capacity decreases in the irradiated membranes. It was also found that chitosan/pHEMA membranes present good barrier properties against microbes.

Poly(vinyl chloride) (PVC) was aminated by treating the resin with a concentrated aqueous solution of ethylenediamine. The aminated PVC was then reacted with hexamethylene diisocyanate to incorporate the isocyanate group onto the polymer backbone. The isocyanated PVC was further reacted with poly (ethylene glycol) (PEG) of molecular weight 600 Da. The modified polymer was characterized using infrared and X-ray photoelectron spectroscopy (XPS) and thermal analysis. Infrared and XPS spectra showed the incorporation of PEG onto PVC. The thermal stability of the modified polymer

was found to be lowered by the incorporation of PEG. Contact angle measurements on the surface of polymer films cast from a tetrahydrofuran solution of the polymer demonstrated that the modified polymer gave rise to a significantly hydrophilic surface compared to unmodified PVC. The solid/water interfacial free energy of the modified surface was 3.9 ergs/cm² as opposed to 18.4 ergs/cm² for bare PVC surface. Static platelet adhesion studies using platelet-rich plasma showed significantly reduced platelet adhesion on the surface of the modified polymer compared to control PVC. The surface hydrophilicity of the films was remarkably retained even in the presence of up to 30wt% concentration of the plasticizer di-(2-ethylhexyl phthalate). The results showed that bulk modification of PVC with PEG using appropriate chemistry can give rise to a polymer that possesses the anti-fouling property of PEG and such bulk modifications are less cumbersome compared to surface modifications on the finished product to impart anti-fouling properties to the PVC surface *Biji et al. (2005)*.

Shailesh and Ashok (2005) studied the grafting of vinyl benzyl trimethyl ammonium chloride (VBTAC) onto polyethylene (PE) film by simultaneous irradiation technique by ⁶⁰Co γ -radiation in the presence of 2-hydroxyethyl methacrylate (HEMA) and air. The effect of solvents, monomer concentration, total dose and dose rate on grafting was studied. All the above parameters affect the grafting of VBTAC. It was also observed that the presence of HEMA is essential to initiate the grafting and low dose rate to facilitate

the grafting rate. Properties such as grafting amount, ion exchange capacity and water uptake of the grafted PE film were determined. The ion exchange capacity was found to increase with increasing percentage of grafting, which in turn was found to be dose dependent. The grafting was confirmed by Fourier transform infrared (FTIR) and thermogravimetric analysis (TGA).

Abd El-Rehim and El-Arnaouty (2004) introduced N-vinyl pyrrolidone/sodium acrylate (NVP/Na-AAc) binary monomers onto polypropylene (PP) films by a radiation grafting method. The effect of solvent and comonomer composition on the degree of grafting was determined. Studies of the mechanical properties and water content of such graft copolymers showed that as the grafting yield increases the elongation percent decreases. However, the water content increases with increasing grafting yield. The blood compatibility of the original PP and PP-g-NVP/Na-AAc films was evaluated by determination of the extent of platelet adsorption and thrombus formation. The blood compatibility of PP-g-NVP/Na-AAc seems to be better than that of original PP.

The preparation of various types of ion exchange membranes by radiation-induced graft copolymerization of polar and functional monomers onto non-polar polymeric films and fibers is reviewed by *Nasef and Hegazy (2004)*. The general mechanisms by which graft copolymerization reactions proceed under various irradiation conditions are described. The

effects of reaction parameters on the degree of grafting in the copolymer membranes are thoroughly discussed. The performance of the membranes and its relation with the polymer structure developing during membrane preparation are also considered. A number of potential applications of the radiation grafted membranes in different fields of industrial interest are highlighted and reviewed.

Poly(ethylene oxide) (PEO) could be grafted on the surface of polyaniline (PANI) films by chlorosulfonating the films with chlorosulfonic acid followed by reacting the modified films with PEO in a pyridine solution. The modified PANI films were examined by X-ray photoelectron spectroscopy and water droplet contact angles. The surface of the PEO grafted to hydrophobic PANI films became hydrophilic and the amounts of bovine serum albumin and human blood plasma platelet adsorbed onto it were decreased by more than 80%. For comparison purposes and because the water wetting angle can be used as a measure of biocompatibility and wetting angle experiments have been also carried out for Pluronic triblock copolymer grafted to PANI and PEO or Pluronic molecules entrapped on the surfaces of PANI films. PANI was selected as substrate because one can easily change its surface properties by PEO grafting and because being conductive can be used as a sensor *Li and Ruckenstein (2004)*.

Methylmethacrylate/maleic anhydride (MMA/MAn) copolymers were synthesized using gamma rays. Preparation

conditions such as irradiation dose, comonomer composition and type of diluent affecting the degree of comonomer conversion were investigated by *Abd El-Rehim et al. (2004)*. The suitable diluent for obtaining reasonable MMA/MAN copolymer yield was acetone. The higher copolymer yield was achieved when the amount of methyl methacrylate in comonomer feed solutions as well as irradiation dose increased. The effect of ZnCl_2 on the MMA/MAN copolymer yield and structure was studied. Characterization of the prepared MMA/MAN copolymers was performed using FTIR, and thermogravimetric and viscometric analysis. The derivatives of MMA/MAN copolymers were obtained by treating them with different reagents such as sulpha-drugs, hydroxylamine hydrochloride and 4-amino sodium salicylate. The antimicrobial activity of MMA/MAN copolymers and their derivatives was examined. The activity of such copolymers against *Staphylococcus aureus* and *Escherichia coli* increased by increasing MAN content in the copolymer. The MMA/MAN copolymers treated with sulpha-drugs exhibited particularly high biological activity against different microorganisms. The results revealed that the prepared MMA/MAN copolymer and its derivatives have a broad antimicrobial activity.

Graft copolymer systems have frequently been suggested for biomedical applications. Since the properties of polymers are altered by the grafting process thorough characterization is critical particularly for the surface region of these copolymers. *Buddy (2004)* discussed the grafting process and then described characterization procedures for graft copolymers. Gravimetric characterization, thermodynamic measurements,

surface chemistry analysis and surface topographical analysis are considered in detail. Also the relevance of materials characterization for predicting and understanding the biocompatibility response is discussed. Most of the analytical techniques described are applicable to all biomaterials and should be considered for the routine characterization of materials which will be interfaced with biological systems

Chun et al. (2004) improved the blood compatibility of polyethylene (PE) film. O-Butyrylchitosan (OBCS) was grafted to PE film by using a radiation grafting technique. The grafted sample films were verified by ATR-FTIR), electron spectroscopy for chemical analysis (ESCA) and the water contact angle measurements. The blood compatibility of the OBCS-grafted PE films was evaluated by platelet-rich plasma (PRP) contacting experiments and protein adsorption experiments that the results were described. The blood compatibility of OBCS-grafted PE film is better than that of blank PE film. These results suggest that the photocrosslinkable chitosan developed here has the potential of serving in blood-contacting applications in medical use.

Mao et al. (2004) improved the blood compatibility of artificial biomaterials through immobilization of the anticoagulative or antithrombogenic biomolecule. A novel immobilization reaction scheme was utilized to incorporate O-butyrylchitosan (OBCS) onto the activated glass surface with an aim to develop an anticoagulative substrate. Activation of the glass surface was carried out by silanization and then

OBCS was grafted to the silanized surface via a radiation grafting technique. The OBCS-grafted glass surfaces were characterized by electron spectroscopy for chemical analysis (ESCA) and atomic force microscopy (AFM). The blood compatibility of the OBCS-grafted glass was evaluated by platelet rich plasma (PRP) contacting experiments and protein adsorption experiments in vitro. The results have demonstrated that the surface with immobilized OBCS shows much less platelet adhesive and fibrinogen adsorption compared to the control surface. Therefore, the novel reaction scheme proposed here is very promising for future development of an anticoagulative glass substrate.

Young and Oh (2003) improved surface blood compatibility on cellulose film for hemodialysis. Acrylic acid, 2-hydroxyethyl methacrylate and three kinds of polyethylene glycol methacrylates were grafted onto the cellulose film surface by radiation grafting technique. Heparin was introduced onto the grafted cellulose film surfaces. The grafting and heparinization were confirmed by FTIR-ATR spectroscopy and electron spectroscopy for chemical analysis. The blood compatibility of the modified cellulose film was examined by the determination of platelet adhesion and thrombus formation.

Chelating poly (vinylpyrrolidone/acrylic acid) (PVP/AAc) copolymer hydrogels were prepared by radiation-induced copolymerization. The effects of preparation parameters such as PVP content in the hydrogel and irradiation dose on the

swelling behavior of the hydrogel were studied by *El-Hag et al. (2003)*. The pH dependent swelling was investigated. The thermal stability of the prepared hydrogel and the metal chelated ones was characterized by TGA. The removal of Fe(III), Cu(II) and Mn(II) from aqueous solution by the prepared PVP/AAC chelating hydrogel was examined by batch equilibration technique. The influence of treatment time, pH and the initial feed concentration on the amount of the metal ions removed was studied. The results show that the removal of the metal ion followed the following order: Fe(III) > Cu(II) > Mn(II). The amounts of the removed metal ions increased with treatment time and pH of the medium. To re-use the hydrogel the metal ions were stripped by using 2 N HCl.

El-sawy and Al Sagheer (2002) prepared ET-g-pAAC membranes by radiation grafting of acrylic acid onto Poly(tetrafluoroethylene - ethylene) copolymer films using a mutual technique. The ion selectivity of the grafted membranes was determined towards K^+ , Ag^+ , Hg^{2+} , Co^{2+} and Cu^{2+} in a mixed aqueous solution. The ion - exchange capacity of the grafted membranes was measured by back titration and atomic absorption spectroscopy. The Hg^{2+} ion content of the membrane was more than that of either K^+ or Ag^+ ions. The presence of metal ions in the membranes was studied by infrared and energy dispersive spectroscopy measurements. Scanning electron microscopy SEM of the grafted and metal-treated grafted membranes showed modification of the morphology of the surface due to the absorption of K^+ and Ag^+ ions. No changes were observed for the surface of the

membrane that was treated with Hg^{2+} ions. The thermal stability of different membranes was improved more with Ag^+ and Hg^{2+} ions than with K^+ ions. It was found that the modified grafted membranes possessed good hydrophilicity which may make them promising candidates for practical applications such as for cation-exchange membranes in the recovery of metals from an aqueous solution.

Young et al. (2002) studied the grafting of 2,3-epoxypropylmethacrylate (EPMA) to polypropylene (PP) film by using a radiation grafting technique. The phosphoric acid group was introduced to the EPMA-grafted PP films with different grafting yields. The blood compatibility of the phosphoric acid group-introduced PP films was evaluated by the determination of platelet adsorption and thrombus formation. The EPMA grafting extent was found to be dependent on the absorbed dose, reaction time and temperature. The grafting and phosphonation reactions were confirmed by FTIR-ATR and electron spectroscopy for chemical analysis. The amount of thrombus and adherent platelet on modified PP film was evaluated by an in vitro method and scanning electron microscope respectively. The phosphoric acid group-introduced PP film was found to have good blood compatibility which increased with the content of the introduced phosphoric acid group.

The radiation - induced grafting of acrylic acid onto poly (tetrafluoroethylene - perfluorovinylether) copolymer film (PFA-g-pAAc) was carried out by *El-sawy and Al Sagheer*

(2001) to synthesize graft copolymer membranes of complexing ability with some selected transition metal ions such as Cr^{III} , Mn^{II} , Cu^{II} , Ag^{I} and Cd^{II} . The complex formation of these graft copolymer metal complexes was studied by atomic absorption spectroscopy, X-ray fluorescence, IR, UV and electron spin resonance spectrometry (ESR). The overall results suggest octahedral geometry for both Cr^{III} and Mn^{II} but square planar for Cu^{II} . The results revealed the high stability of the obtained ligand metal complexes. The biological activity of the grafted film and its complexes with various metal ions was investigated under the same conditions. Silver (I) complexed membrane had a strong biocidal effect for all tested bacteria. The biological activity for Cr^{III} complex has been affected on *E. coli* and *S. aureus*, whereas the Cd^{II} complex has its effect on *E. coli*, *B. anthrax* and *B. cereus*. The Cu^{II} complex has only antifungal activity.

Selective removal and recovery of metals from industrial eluent is an environmental problem and economic concern. There are a number of heavy metals that are candidates for removal prior to having waste solutions coming in contact with the environment. Therefore, **Hegazy et al. (2000)** prepared hydrophilic membranes having both anionic and cationic exchangers. To achieve such properties in the required membranes a trial has been made on the radiation graft copolymerization of binary monomers possessing anionic and cationic exchangers such as acrylic acid/2- and 4-vinyl pyridine (AAc/2-VP) (AAc/4-VP) onto available commercial polymeric substrate such as low-density polyethylene (LDPE).

The preparation conditions at which the grafting process proceeds homogeneously are determined. Characterization and some selected properties of the prepared grafted membranes were studied and accordingly the possibility of its practicable use in waste water treatment from heavy and toxic metals such as Pb, Zn, Cd, Fe was investigated. The metal uptake by such prepared membranes was determined by using atomic absorption technique. The membrane efficiency and durability was investigated. The maximum uptake for a given metal was higher for the LDPE-g-p(AAc/2VP) membranes than that for the LDPE-g-p(AAc/4VP). The chelated metal ions were easily desorbed by treating the membrane with 0.1 N HCl for 2 h at room temperature. A mixture of two or three metals in the same feed solution was used to determine the selectivity of the membrane towards different metals. The results obtained for the prepared membranes showed a great promise for their applicability in the removal of heavy metals from wastewater.

Radiation graft copolymerization of styrene /maleic anhydride (Sty/MAn) comonomer onto low density polyethylene (LDPE) membrane was investigated by *Abd El-Rehim et al. (2000)*. The prepared grafted membranes were treated with different reagents containing various functional groups and studied as a matrix for the purpose of water purification from heavy metals. The metal ion uptake by the functional groups of membranes was determined by the use of X-ray fluorescence (XRF) and atomic absorption (AA). The effect of pH of the metal feed solution and immersion period needed for maximum capacity was investigated. The

selectivity of different prepared membranes towards some selected metal ions such as Fe, Cu, Pb,... etc. which commonly exist in waste water was determined. The affinity of the treated grafted films to recover Fe(III), Cu(II) or Pb(II) from their aqueous solutions containing other metal ions such as Cd(II), Ni(II) or Hg(II) was studied. Also the selectivity of treated grafted membranes towards Cu(II), Cr(III) and Fe(III) in a mixture was investigated at room temperature and 70 °C. It was found that the thiosemicarbazide-, hydroxylamine- HCl- and NaOH-treated grafted films showed high selectivity towards Cu(II), Cr(III) and Fe(III), respectively, at 70°C. However, the selectivity of such treated grafted membranes was remarkable towards Fe(III) at room temperature. The results obtained suggested that the treated grafted membrane possessed good chelating properties towards different metal ions. This suggests that such membranes could be accepted for practical uses.

El-sawy (2000) prepared membranes by the direct radiation grafting of acrylonitrile onto low-density polyethylene films (LDPE-g-PAN) these grafted membranes were amidoximated using hydroxylamine hydrochloride in basic medium. The influence of monomer concentration and swelling behaviour of grafted membrane, amidoximated grafted membrane, and its sodium salt were also studied. Amidoximated grafted membrane and their copolymer – metal complexes of Cu^{II} or Cr^{III} were prepared. These membranes were characterized using different analysis techniques such as IR, UV and ESR spectrometry. The results showed that the UV and ESR analysis revealed that the geometry structure for Cu^{II}

is square planar, while for Cr^{III} is octahedral. Also the amidoxime ligand was used for separating metal ions from aqueous solutions by a complexation process. The thermal stability of different membranes was investigated through TG analysis. it was found that amidoximate - grafted membranes possess good hydrophilic properties that may make them promising for some practical applications such as the recovery of metals from their aqueous systems.

Preparation of synthetic membranes using simultaneous radiation grafting of acrylic acid (AAc) and styrene (Sty) as individually and in binary monomer mixture onto low density polyethylene (LDPE) has been carried out by *Hegazy et al. (1999)*. The effect of preparation conditions such as irradiation dose, monomer concentration, comonomer composition and solvent on the grafting yield was investigated. Characterization and some properties of the prepared membranes using different analytical techniques are studied accordingly the possibility of its practical use in industrial waste treatment is determined. The swelling behavior, electrical conductivity, thermal stability, and mechanical properties of the membranes were investigated as a function of the grafting degree. The prepared cation-exchange membranes possessed good electrical and mechanical properties, high thermal stability and possess good characteristics for separation processes. These membranes have also good affinity toward the adsorption or chelation with Fe^{3+} and Pb^{2+} ions either in mixture containing other metals or if exists alone in the waste solution.

The preparation and characterization of supported hydrogels obtained by radiation-induced graft copolymerization of styrene/maleic anhydride (Sty/MAn) binary monomers system onto low density polyethylene films were investigated by *Hegazy et al. (1999)*. Attention was focused on the selection of the reaction parameters suitable for the commercial production of such hydrogels. The factors which affect the preparation process and grafting yield are type of solvent, dose rate, total dose, comonomer composition and their concentrations in the diluents. The structure and composition of the grafted chains were also determined. The change in tensile strength and percent elongation at break with degree of grafting was determined for the untreated LDPE-g-p(Sty/MAn) membranes. It was found that the tensile strength improved by grafting but the percent elongation decreased. The change in thermal parameters was measured using differential scanning calorimeter (DSC). The grafted p(Sty/MAn) chains are amorphous in nature and a slight effect on the crystallinity of PE structure was observed. The possibility of the practical uses of such modified membranes was suggested.

Abd EL-Rehim et al. (1999) modified water-soluble poly(vinyl alcohol) (PVA) by grafting acrylic acid and styrene (AAc/Sty) comonomers using gamma rays as an initiator. The factors that affect the preparation process and grafting yield were studied and more economical grafts under the most favorable reaction conditions were obtained. It was found that the high degree of grafting in such systems was obtained in the presence of an ethanol–water mixture in which water plays a significant role in enhancing the graft copolymerization. The

critical amount of water to afford the maximum grafting yield was evaluated. The effect of the comonomer composition on the grafting yield was also investigated and it was observed that using a mixture of AAc/Sty monomers influences the extent of grafting of each monomer onto the PVA substrate and the phenomenon of synergism occurs during such a reaction. Also, the degree of grafting increases as the content of the solvent decreases in the reaction medium. However, the grafting yield increased as the total dose increased. The graft copolymer was characterized by IR and UV spectroscopic methods. The permeation of heavy metals such as Ni and Co through the grafted membranes was investigated and the efficiency of the separation process was also determined.

Radiation induced graft polymerization of acrylic acid onto poly (tetrafluoroethylene–perfluorovinylether) copolymer films has been prepared using γ -irradiation by the mutual method was made by *El-sawy (1998)*. The grafted copolymer membranes rapidly complexed with rhodium ions through the carboxylic groups. The complexation process was followed by measuring the variation of the pH of aqueous RhCl_3 solution of several concentrations as a function of time. Spectroscopic, electrical, thermal and diffraction measurements have been investigated. The results revealed high stability of the ligand - metal complex formed. Thus, a practical application of the grafted copolymer in the field of rare metal waste treatment is implied.

El-Sawy and Al Sagheer (1998) studied the graft copolymers obtained by radiation induced grafting of acrylic acid onto poly(tetrafluoroethylene-ethylene) (ET) films. The

conversion of the graft copolymers (60 wt%) into metal acrylate copolymer complexes was carried out by treatment with various concentrations of aqueous CuCl_2 . These graft copolymer-metal complexes were studied by IR, UV spectrometry, X-ray diffraction (XDR), and electron spin resonance (ESR). The effect of temperature on the trunk, untreated grafted and treated grafted copolymer films was investigated by IR and thermogravimetric (TG) analysis. The influence of metal complexes of Cu^{2+} ions on the thermal properties and electrical conductivity was determined. It is assumed that such materials may be of great interest in the field of semiconducting materials, in addition to their resistance to degradation under high temperature, up to 300°C .

Investigations were carried out on different ionic membranes, which were prepared by radiation-induced graft copolymerization. Cationic (low density polyethylene (LPDE)-g-poly(acrylic acid) (PAAc)) and cationic/anionic (LDPE-g-P(AAc/4-vinyl pyridine (4VP) membranes) were used to elucidate the possibility of their practical use by *Hegazy et al. (1997)*. The metal uptake via their functional groups was determined by using atomic absorption and X-ray fluorescence. The amount of metal uptake by the prepared membranes increased significantly as the pH of the metal feed solution increased (pH 5.3) and the chelated metal ions were easily desorbed by treating the membrane with 0.1 M HCl for 2 h at room temperature. The maximum uptake for a given metal was higher for the cationic/ anionic membranes than for the cationic ones. The selectivity of the cationic/anionic membranes towards different metals was investigated using mixtures of two or three metals in the same feed solution. The

membranes showed high selectivity towards Fe(III) ions. Characterization of the graft copolymers containing metals was determined by thermogravimetric analysis (TGA) and X-ray diffraction (XRD). TGA results showed that the decomposition of the graft copolymer in the presence of chelated metal ion occurred at temperatures above 300°C. The XRD of LDPE-g-P(AAc/4VP) treated with Fe(III) at various concentrations showed that the crystallinity decreased to a certain limiting value. The complexed copolymers could be recycled several times and showed high selectivity to the Fe(III) ion in the presence of the other metal ions investigated. This may make such grafted membranes acceptable for practical use in waste water treatment

The radiation graft copolymerization of hydrophilic monomers onto polyphosphazenes carried out by ***Carenza et al. (1996)***. Kinetics of grafting by the mutual irradiation method at room temperature of monomer-solvent mixtures were followed. Hydrophilicity, structure, mechanical properties, biocompatibility and anticoagulating properties of the modified samples were reported. Some experiments on the grafted polymer to which heparin were ionically bonded with a high yield were also carried out.

Hegazy et al. (1992) Prepared a good hydrogel supported on a fluorinated polymer film has been achieved by means of simultaneous radiation-induced grafting of N-vinyl-2-pyrrolidone (NVP) onto (tetrafluoroethylene - perfluorovinyl ether) copolymer (PFA). The conditions at which the graft polymerization proceeded with a suitable yield were determined. Ammonium ferrous sulphate (Mohr's salt), as an

inhibitor, failed to inhibit the homopolymerization of NVP during the radiation grafting process. In contrast, the addition of Cu_2Cl_2 (0.5 wt%) effectively inhibited the homopolymerization process and smooth grafted films with suitable grafting yield were obtained. The grafting onto PFA films, which scarcely swell in any solvent or monomer, was critically controlled by the diffusivity of reactants through the grafted layers initially formed near the film surface. The addition of ZnCl_2 (3 wt %) to the monomer solution slightly enhanced the grafting and much smoother grafted films were obtained. The dependence of initial rate of grafting on NVP concentration was of the order 0.54. The graft copolymer possessed good mechanical properties and high thermal and chemical stability. Such non-ionic supported hydrogel on fluorinated polymer may be of interest for some practical use in which high electrical conductivity is not required, as in biomaterials.

Fang and Shi (1988) prepared polypropylene dialysis membranes by direct grafting by means of cobalt-60 gamma radiation of 2-hydroxyethyl methacrylate onto polypropylene membranes. The influence of dose, dose rate, and concentration of monomer on the degree of grafting was investigated. The structure and the morphology of both the grafted membrane and the polypropylene membrane were observed by scanning electron microscopy and IR spectroscopy, respectively. The mechanical properties of the membranes were also determined. The permeability of the grafted membranes and polypropylene membranes toward urea and uric acid was studied in a dialyzer. In all cases, the grafted membranes showed improved permeability toward

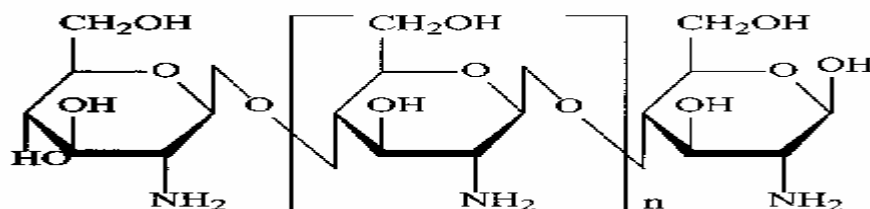
those solutes in comparison with the polypropylene membranes. The permeation coefficients of urea and uric acid through the grafted membranes were about 4.6 and 19 times larger than that of polypropylene membranes.

Chapter III

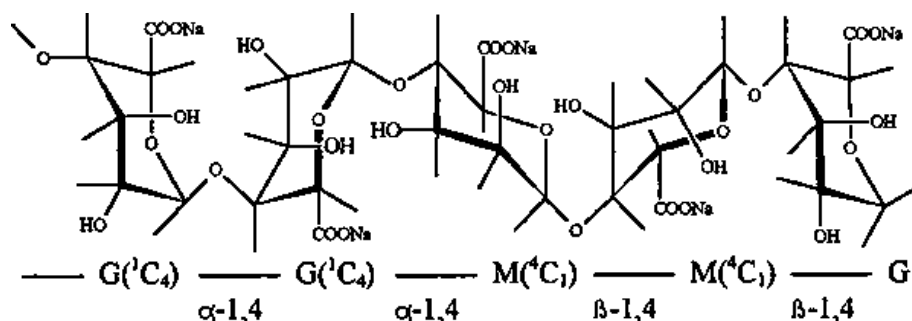
Experimental

III.1-Materials

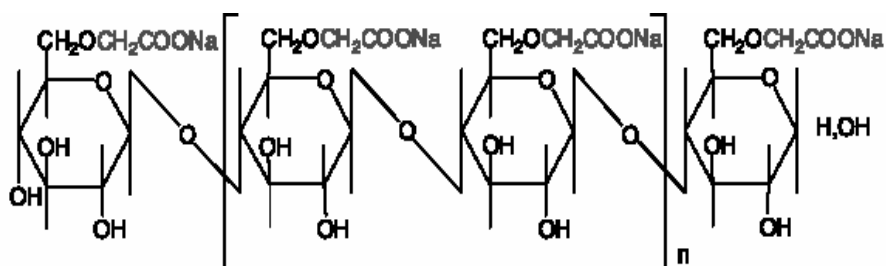
1- Chitosan, high molecular weight, Aldrich.



2- Sodium alginate, Aldrich



3- Commercial carboxymethylcellulose sodium salt (CMC-Na), high molecular weight and degree of substitution not less than 0.4 (El Nasr Co.).



- 4- Hydrogen peroxide (H_2O_2) 30% Loba chemie
- 5- Maize and faba bean seeds, Elwady company for production of seeds and agricultural crops.
- 6- Poly(tetrafluoroethylene-perfluorovinyl ether) copolymer films (PFA) of thickness 100 μm were supplied by Hoechst, Germany. $[\text{CF}_2\text{-CF}_2\text{-CF(OR)}]_m$
- 7- Vinyl acetate (VAc) $\text{CH}_3\text{COO-CH=CH}_2$, 99% Merck-Schuchardt, Germany, $d = 0.931$.
- 8- 2-Hydroxyethylmethacrylate (HEMA)
 $\text{CH}_2=\text{C}(\text{CH}_3)\text{-COO-CH}_2\text{-CH}_2\text{OH}$, 97%, Aldrich Chemie, GmbH, Germany, $d = 1.073$.
- 9- Glacial acetic acid and sodium acetate.
- 10- Glutaraldehyde
- 11- Copper nitrate $\text{Cu}(\text{NO}_3)_2$ and Chromium nitrate $\text{Cr}(\text{NO}_3)_3 \cdot 9\text{H}_2\text{O}$, Hopkin and Williams Ltd., England.
- 12- Different inorganic salts like ammonium per-sulphate, potassium per-sulphate, ammonium phosphate, potassium phosphate and ferric chloride. The other chemicals such as solvents and other reagents were reagents grade and used without further purifications. (El Nasr Co.).

III.2. Apparatus and Methods

III.2.1-Gamma Radiation Source

The samples were irradiated with the ^{60}Co candian irradiation facility gamma rays at a dose rate ranging from 6.5 to 7 kGy/h. The irradiation facility was constructed by the National Center for Radiation Research and Technology (NCRRT), Atomic Energy Authority of Egypt (AEA) Cairo.

III.2.2- Preparation of Low Molecular Weights of Naturally Occurring Polymers

III.2.2.1- Gamma Irradiation Method

Chitosan, sodium alginate and CMC (solid form) were mixed well with different amounts of H₂O₂ (v/w) or KPS wt% or APS wt%. The mixtures were packaged in polyethylene bags and subjected to gamma irradiation ⁶⁰Co- source with various doses ranged from 20 to 200 kGy.

III.2.2.2- Chemical and Thermal Treatment Method

Chitosan, sodium alginate and CMC (solid form) were mixed well with different amounts of H₂O₂ (v/w) or KPS wt% or APS wt%. The mixtures were packaged in polyethylene bags and subjected to 70°C in a water bath. Samples were taken after 10, 20, 30, 40, 50 and 60 minute to determine their intrinsic viscosity (η).

III.2.3- Determination the Intrinsic Viscosity of Degraded Naturally Occurring Polymers

The Ubbelohde viscometer was used to measure the viscosity of the degraded samples. To investigate the viscosity behavior of polymer solution in extremely dilute concentrations. The following experimental procedures were performed using *Haiyang et al (2001)* method.

1- Filling the viscometer with pure solvent to a given level, and then measuring the drain time for the pure solvent, η_0 .

2- Filling the viscometer with the same solvent with a dilute concentration of dissolved polymer and measuring the drain time again, η it will take longer because of the increase in viscosity:

The relative viscosity (η_{rel}) of the polymer was calculated as follow:

$$(\eta_{rel}) = (t) / (t_0) \quad \text{----- (1)}$$

and the inherent viscosity (η_{inh}) of the polymer was calculated as follow:

$$(\eta_{inh}) = [\text{Ln} (\eta_{rel}) / C] \quad \text{----- (2)}$$

where C is the concentration of the prepared polymer solution.

Also, the specific viscosity of the polymer was calculated as follow:

$$(\eta_{sp}) = (\eta_{rel}) - 1 \quad \text{----- (3)}$$

and the reduced viscosity (η_{red}) of the polymer was calculated as follow:

$$(\eta_{red}) = (\eta_{sp}) / C \quad \text{----- (4)}$$

To determine the intrinsic viscosity (η) of the polymer solution in extremely diluted concentrations, a plot between the inherent viscosity (η_{inh}) and the reduced viscosity (η_{red}) on the y- axis and the concentration of the prepared polymer solution (C) on the x- axis was made. On extrapolating to zero concentration the intrinsic viscosity (η) ml/g can be obtained

III.2.4- Determination the Molecular Weight of Degradable Naturally Occurring Polymers

The weight-average molecular weights of the degraded polymers were determined by two methods:

III.2.4.1- The Vicometric Method

The weight-average molecular weights of the polymers were determined on the basis of the Mark - Houwink equation

$$[\eta] = K M^{\alpha}$$

where $[\eta]$ is the intrinsic viscosity of the polymers, K and α are constants and M is the weight-average molecular weight.

The molecular weight of sodium alginate and CMC can be determined by measuring the intrinsic viscosity of polymer solution in 0.01 M NaCl solution taking $K = 8.1 \times 10^{-3}$ ml/g and $\alpha = 0.92$ *Pengfei et al. (2002)* also the molecular weight of chitosan can be determined by measuring the intrinsic viscosity in 0.3 M acetic acid - 0.2 M sodium acetate solution taking $K = 0.076$ ml/g and $\alpha = 0.76$ *Rinaudo et al. (1993)*.

III.2.4.2- Gel Permeation Chromatography (GPC) Method

Gel permeation chromatography (GPC) of irradiated samples was performed using 1100 Agilent instrument equipped with organic and aqueous GPC-SEC start up kits with a flow rate of 2 ml/min, maximum pressure 150 bar, minimum pressure 5 bar, injection volume 50 μ L and column temperature thermostat 25°C. The eluent was monitored by a refractive index detector of optical unit temperature 25°C and

peak width 0.1 min. polymer concentration was 0.1 (w/%). The molecular weights were determined from a calibration curve using polystyrene and polyethylene oxide standards for organic and aqueous systems, respectively.

III.2.5. Separation of Water Soluble Chitosan

The chitosan mixed with 10 wt% APS and irradiated at different irradiation doses from 40 to 200 kGy is heated in distilled water at 70°C in a water bath for 2h and then filtrated. Few drops of methanol were added to precipitate the soluble chitosan. The precipitate was collected and left for 1h in an oven at 50°C.

III.2.6- Plantation

To investigate the effect of degraded chitosan or sodium alginate on maize plants, the concentration of 100 ppm was used. The field can be divided into 8 separate lines. After plantation of ages 30, 60 and 90 days, each line of plants are sprayed by 100 ppm solution of (a) Untreated polymer (chitosan or sodium alginate), (b) Irradiated polymer at 200 kGy, (c) Polymer treated by APS at 40 kGy, (d) Polymer treated by APS at 80 kGy, (e) Polymer treated by APS at 120 kGy, (f) Polymer treated by APS at 160 kGy and (g) Polymer treated by APS at 200 kGy. The growth rate of the plants by these treatments is compared with control (untreated plant). The same method can be applied for faba bean plants.

III.2.7- Radiation-Induced Graft Copolymerization of VAc / HEMA Binary Monomers onto PFA Films

The graft copolymers films were prepared by a simultaneous technique. Strips of PFA films were immersed in VAc / HEMA (50/50 wt%) in glass ampoules. Ferric chloride (0.1wt %) was added to the reaction medium to minimize the homopolymerization of VAc / HEMA during the radiation grafting process. The reactant mixtures in the glass ampoules were deaerated by bubbling nitrogen gas for 3-5 min, sealed and then subjected to γ -radiation from ^{60}Co at 30 kGy and a dose rate of 1.85 Gy/s. The PFA-g-p(VAc/HEMA) membrane were removed and washed thoroughly with methanol and benzene to eliminate the residual monomer and homopolymer occluded in the films. The films were then dried in a vacuum oven for 24 h at 50°C and weighed. The degree of grafting was calculated as follows:

$$\text{Degree of grafting (\%)} = [(W_g - W_o) / W_o] \times 100$$

where W_o and W_g are the weights of initial and grafted films, respectively.

III.2.8- Synthesis of Metal-doped Graft Copolymer

The different graft copolymer metal complexes of PFA (5.3, 21.2, 31.5 and 42 %) were prepared by immerising the films in 3 wt% NaOH for 30 min at 70°C then washed by distilled water and refluxing in 1wt% of aqueous metal salts of $\text{Cu}(\text{NO}_3)_2$ and $\text{Cr}(\text{NO}_3)_3 \cdot 9\text{H}_2\text{O}$ for 24h at 100°C. The treated films were washed with distilled water and then dried at 50°C.

III.2.9- Platelet Adhesion Assesment

Human blood was collected with a polypropylene syringes containing 3.8% sodium citrate solution. Platelet-rich plasma were obtained by centrifuging human blood at 1000 for 20 min for platelet adhesion. PFA and PFA-g-p(VAc/HEMA) films were hydrated by placing them in phosphate-buffered solution (pH 7.4) for 10 min. Each hydrated film was transferred to platelet-rich plasma at body temperature for 30 min. After incubation at 37°C, the samples were washed carefully with phosphate-buffered solution to remove weakly adhered platelets. The platelets adherent to the films were fixed with 2.5% glutaraldehyde in phosphate-buffered solution for 10 min at body temperature. Each film was washed with phosphate-buffered solution the dehydrated in an ethanol-water mixture (60, 70, 80, 90 and 99%) for 10 min and allowed to dry at room temperature. The platelets attached to the PFA films were exained with the use of a JEOL JSM-5400 (Japan) scanning electron microscopy (SEM) after gold deposition in vacuum for 3 min *Abd El-Rehim and El-Arnaouty (2004)* and *Nho et al. (2002)*.

III.2.10- pH Measurements

The pH values of buffer solutions was determined by using Jenway 3310 pH Meter.

III.2.11- Infra - red Spectroscopy (IR)

Analysis by infra - red spectrophotometer was carried out in the form of KBr pellets by using Matton 1000, Unicam, Cambridge, England in the range of 400 - 4000 cm^{-1} .

III.2.12- Ultra Violet Spectroscopy (UV-Vis)

Analysis by a UV-spectrophotometer was carried by using Jasco V-560, Japan, in the range from 190 to 900 nm.

III.2.13- X-ray Fluorescence Measurements

The XRF (hnu, PC TEFA, Tube Excited Fluorescence Analyzer System, USA) was used to confirm the existence of doped metal which may be formed in the graft copolymer.

III.2.14- Mechanical Measurements

Tensile strength and elongation at break were examined from stress – strain curves measured by using a tension meter carried out with use of (H10KS Hounsfield Co. UK), tension speed was 25 mm/min, load rang 1000 N and extension range 1500 N. Samples in a dumbbel shape of 50 mm long and 4 mm neck width of different degrees of grafting were used for mechanical testing.

III.2.15- Differential Scanning Calorimetry (DSC)

Thermal parameters of the samples, melting temperature (T_m), heat of melting and recrystallization (ΔH_m and ΔH_{rc}) were determined by Differential Scanning Calorimeter (DSC), Perkin Elmar equipped with a DSC-7 data station, specimen (≈ 5 mg) of the sample is used for DSC measurements. The measurements were carried out in N_2 atmosphere at a heating rate of $10^\circ C \text{ min}^{-1}$.

III.2.16- Thermal Gravimetric Analysis (TGA)

Perkin Elmar TGA system under Nitrogen atmosphere of 10 ml/min was used. The temperature range was from ambient temperature to 600 at flow rate ≈ 10 ml/min.

III.2.17- X-Ray Diffraction (XRD)

X-Ray Diffraction patterns were obtained with a XRD-DI series, Shimadzu apparatus using Ni-filter and Cu-Ka target.

III.2.18- Scanning Electron Microscopy (SEM)

The surface topology of the grafted membranes was measured with JEOL JSM-5400 (Japan). Scanning Electron Microscopy (SEM). The surfaces of the grafted membranes were sputter-coated with gold for 3 min.

III 2.19- Electron Spin Resonance (ESR)

ESR signals were recorded at room temperature by using a Bruker EMX spectrometer (X-band) of Bruker, Germany.

The polymer films were cut in strips and placed in the sample tubes. The stretching direction of the films was either parallel or perpendicular to the axis of the magnetic field.

III.2.20- Electrical Conductivity Measurement

Electrical resistance measurements were carried out using a Mega Ohm type MOM (WTW Co., Germany). The specific electrical conductivity was calculated as follows:

$$\sigma = L / R \alpha \text{ (}\Omega^{-1}\text{cm}^{-1}\text{)}$$

where L is the thickness of the sample (cm), α is the surface area of the sample (cm²), and R is the ohmic resistance (Ω).

Chapter IV
Results and Discussion

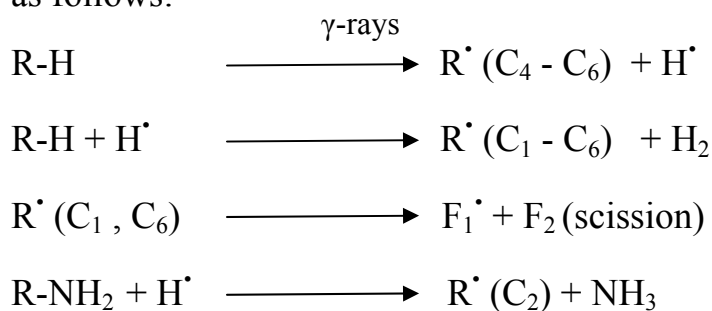
IV.I- Controlling the Radiation Degradation Process of Some Naturally Occurring Polymers

IV.I.1- Effect of Gamma Irradiation on Polymeric Materials

Radiation-induced effects onto polymers can occur through the molecular changes resulting from radiation-induced chemical reactions and may be classified as: (i) Chain cross-linking causing an increase in the molecular weight and forming a microscopic network structure. (ii) Chain scission causing a decrease in the molecular weight and substantially changing the polymer material properties. (iii) Small molecule products, resulting from main chain scission followed by either abstraction or combination reaction or both of them. (iv) Structural changes in the polymer accompanying the formation of small molecule products. The extent of each one of these reactions depends on the chemical nature of the polymer and irradiation conditions i.e., irradiation dose and dose rate ***Reichmanis et al. (1993).***

Figure (1) shows the changes in the viscosity average molecular weights of chitosan, sodium alginate and CMC when exposed to various gamma irradiation doses in the solid form. The chitosan, sodium alginate and CMC molecules undergo degradation reactions resulting in the reduction of its viscosity average molecular weights. Meanwhile, as the irradiation dose increases, the viscosity average molecular weight of chitosan, sodium alginate and CMC molecules decreases. The decrease in the molecular weight is very fast up to 80 kGy. Thereafter, the degradation rate was very low.

Ershov et al. (1987) proposed a scheme for the degradation mechanism of chitosan irradiated in the solid state, as follows:



where R-H and R-NH₂ are chitosan macromolecules, R[•] (C_n) is a chitosan macro-radical localized on C_n carbon atom and F₁[•], F₂ are fragments of the main chain after scission.

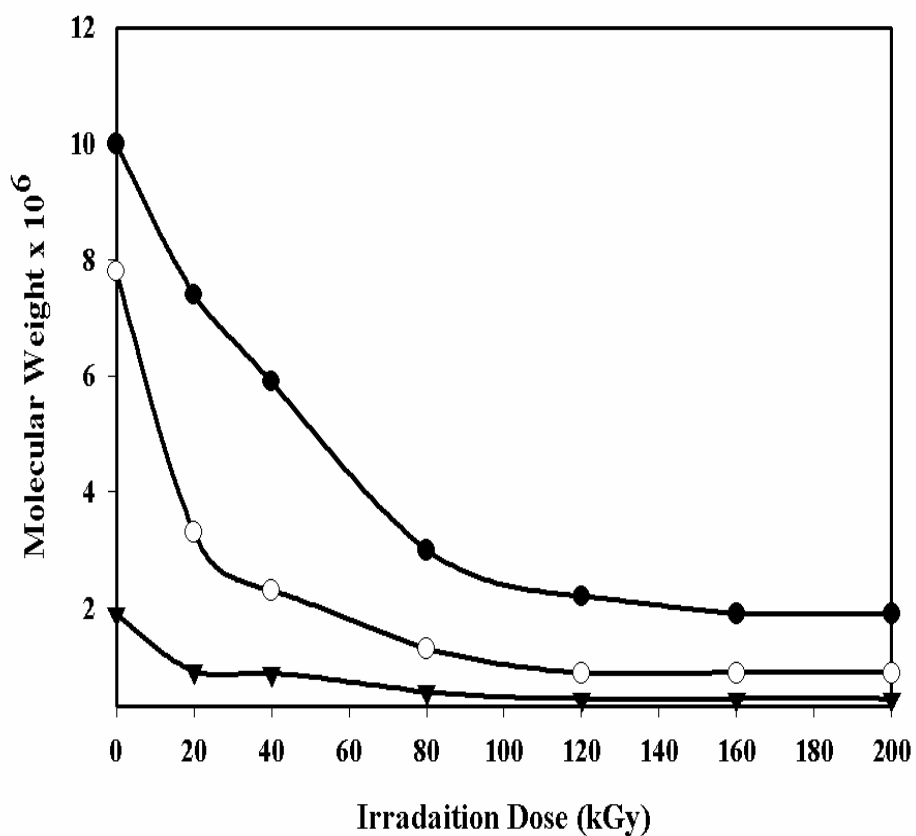


Figure (1): Changes in the viscosity average molecular weights of (●) chitosan, (○) CMC and (▼) sodium alginate (solid form) when exposed to gamma irradiation, (the dose rate 6.7 kGy/h).

IV.I.2- Effect of Gamma Irradiation on the Degradation process of Some Natural Polymers in the Presence of Some Initiators

Natural polymers are typical degradable materials under ionizing radiation based on the reduction of molecular weight without adding any chemical additives at ambient temperature. The dose needed to degrade natural polymers is very much lower for gel state than for solid polysaccharides. This is expected due to the indirect effect of radiation brought about by the water molecules. Degradation and cross-linking of polymers are affected by the atmosphere of irradiation.

In fact, from the economic point of view these doses are not accepted; the cost is high. Therefore, trials have been made to reduce the cost of degradation process of solid polysaccharides by using some additives during irradiation processes by reducing the dose of irradiation.

Figures (2, 3 and 4) show the effect of gamma irradiation at 80 kGy or thermal heating at 70°C on degradation of sodium alginate, chitosan and CMC, respectively in the presence of some initiators as a function of molecular weight changes. Sodium alginate was mixed with different additives (w/w)

such as, hydrogen-peroxide or potassium per-sulfate or ammonium per-sulfate (i.e. chemical-radiation degradation reaction) and subjected to gamma irradiation at 80 kGy irradiation dose. It is observed that the addition of ammonium per-sulfate or potassium per-sulfate or hydrogen peroxide to sodium alginate during the irradiation or thermal heating processes accelerate the degradation process. The rate of radiation degradation of sodium alginate in the presence of such additives is much higher if compared with the thermal degradation rate of such natural polymer.

The same behavior was obtained for degradation of chitosan and CMC as shown in Figure (3) and (4), respectively.

The presence of hydrogen peroxide or potassium per-sulfate or ammonium per-sulfate beside gamma irradiation increases the formation of free radicals and enhances the degradation process of sodium alginate or chitosan or CMC resulting in reduction the irradiation dose required for degradation and reduce the degradation cost.

Also, Figures (2, 3 and 4) showed that the ammonium per-sulfate is the most effective imitator for degradation of sodium alginate, chitosan and CMC. The molecular weights of 9.2×10^4 , 1.3×10^4 and 3.7×10^5 for sodium alginate, chitosan and CMC were obtained at 80 kGy irradiation dose in the presence of APS, respectively. However, the molecular weights of

gamma irradiated samples at 80 kGy were 5.5×10^5 , 3×10^6 and 1.3×10^6 , respectively.

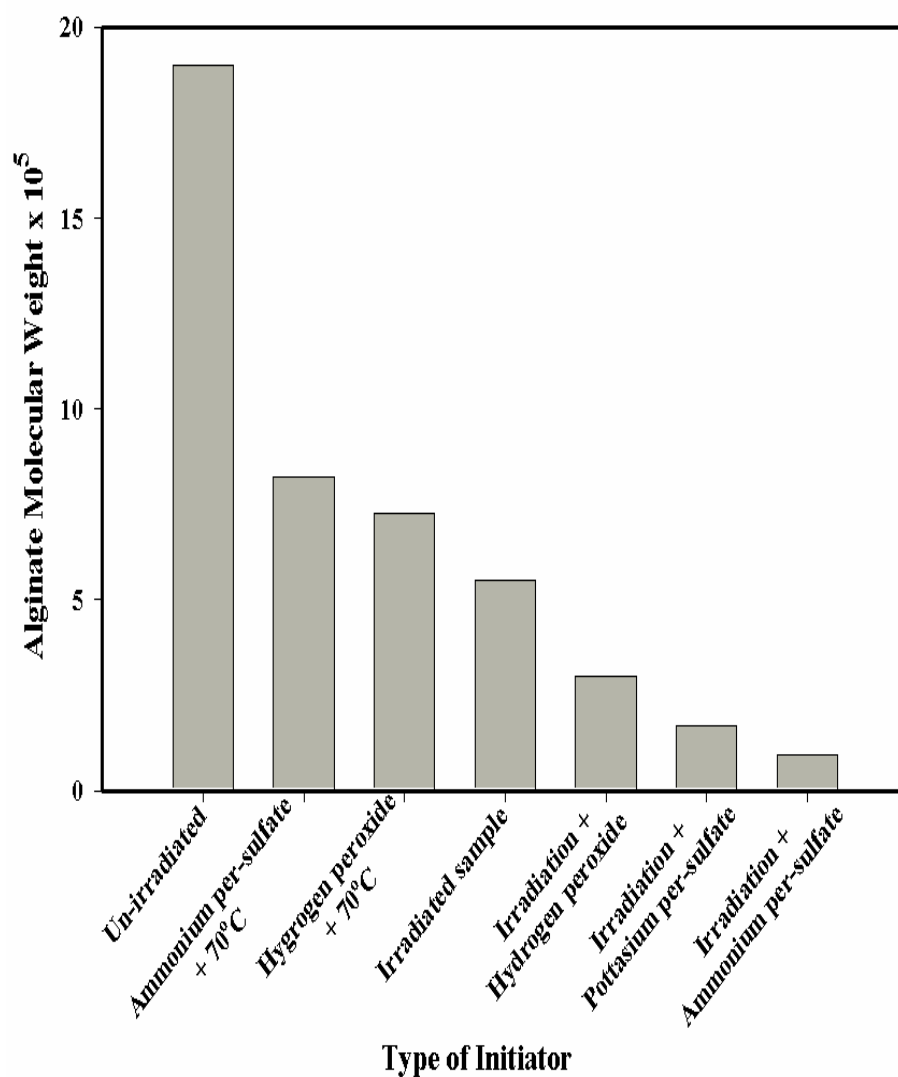


Figure (2): The effect of some initiators on degradation process of sodium alginate induced by gamma irradiation at 80 kGy or thermal heating at 70°C. (The dose rate 6.7 kGy/h).

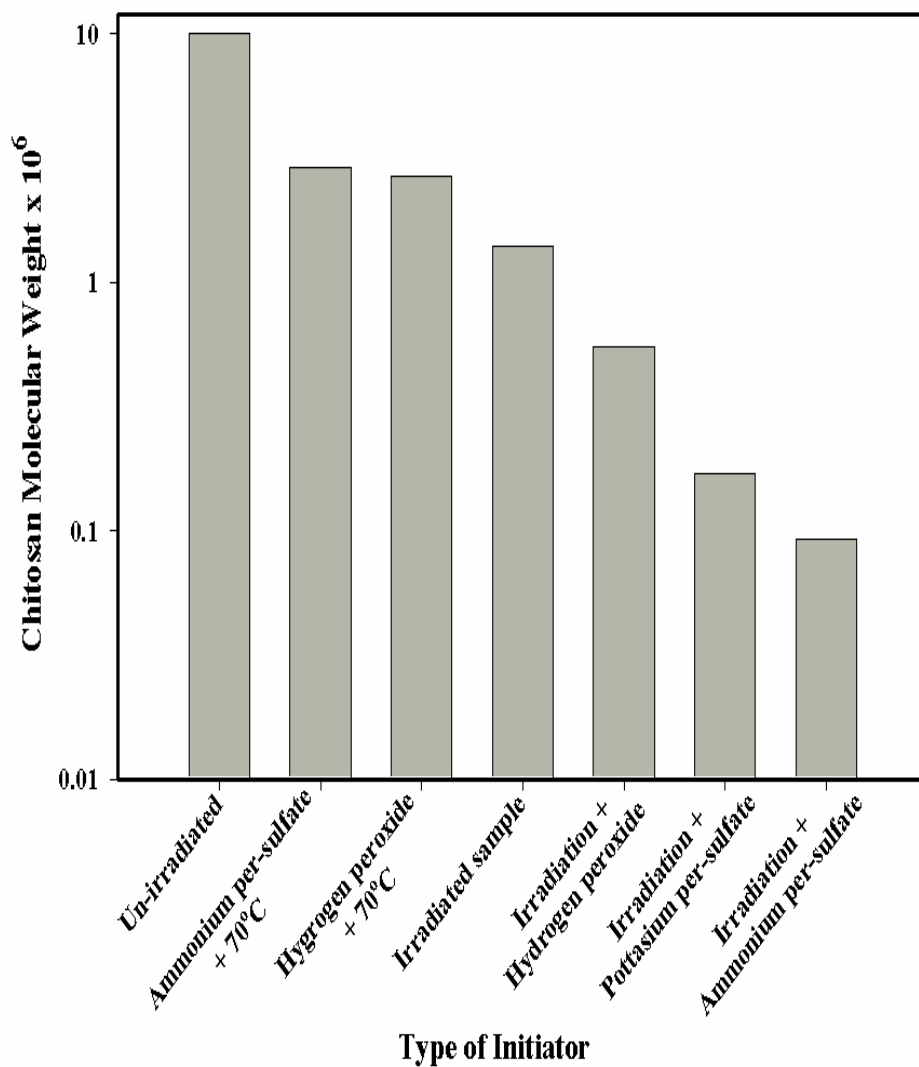


Figure (3): The effect of some initiators on degradation process of chitosan induced by gamma irradiation at 80 kGy or thermal heating at 70°C. (The dose rate 6.7 kGy/h).

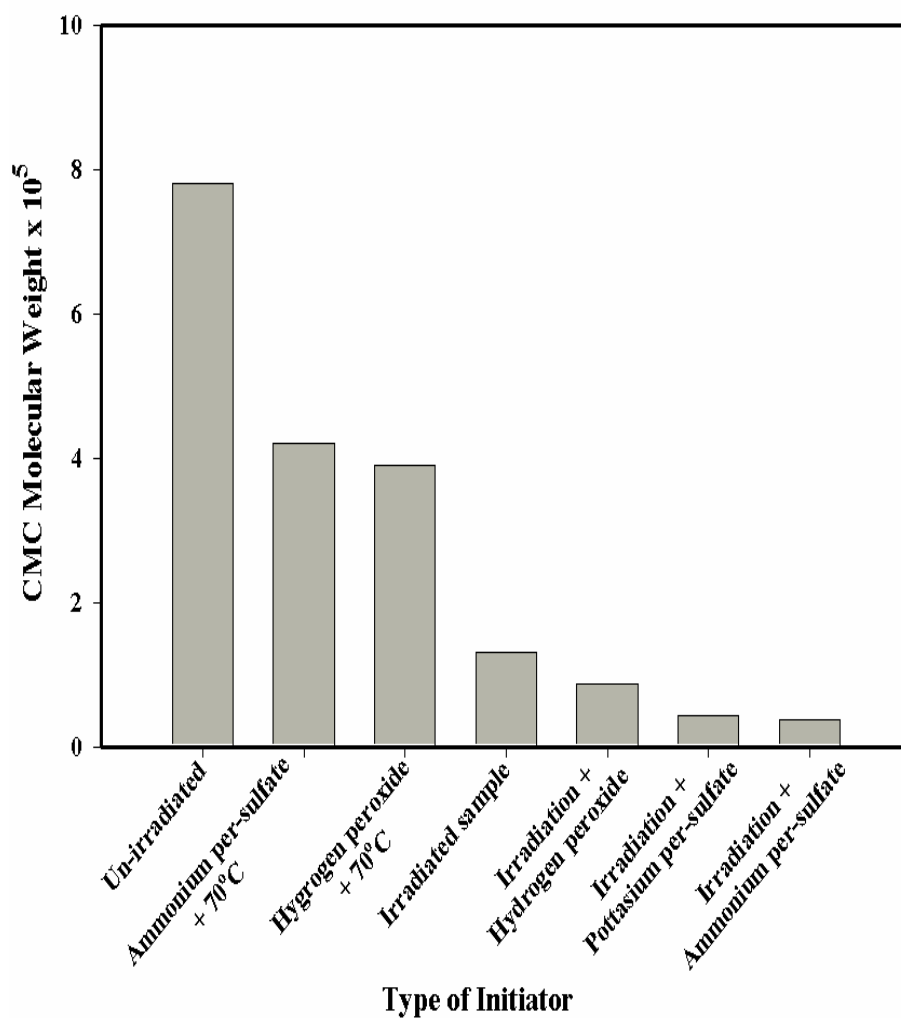
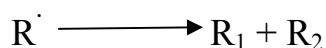
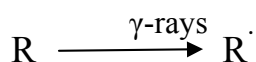


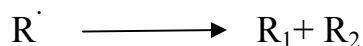
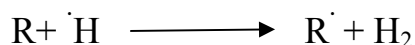
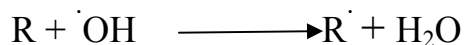
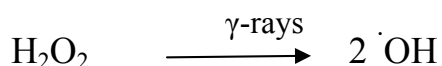
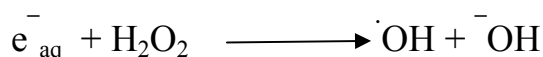
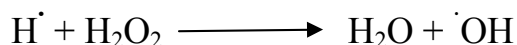
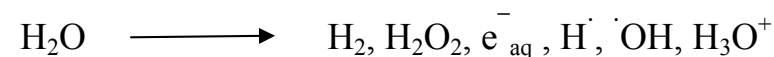
Figure (4): The effect of some initiators on degradation process of CMC induced by gamma irradiation at 80 kGy or thermal heating at 70°C (The dose rate 6.7 kGy/ h).

Oxidative degradation is based on the formation of reactive radicals by the disassociation of initiators or gamma

rays. These reactive radicals which are powerful oxidizing species can attack the β -1-4 glycosidic linkages, resulting in the degradation of sodium alginate. **Woods and Pikaev (1994)** suggested that under gamma irradiation the following reactions may be ascribed to the direct action of radiation on the chitosan chains:



and in the presence of H_2O_2 besides radiation degradation reactions, the primary reactions might occur as follows:



thus, the formation of $\cdot OH$ radical is enhanced through the radiolysis of H_2O_2 or water. Hydroxyl radicals, as powerful oxidizing species, can attack the β -1-4 glycosidic bonds of chitosan. Hence, the radiation treatment on chitosan in the presence of hydrogen peroxide could reduce its molecular weight very effectively.

IV.1.3- Effect of Initiator Concentration on Degradation of Natural Polymers Induced by Gamma Irradiation

Figures (5, 6 and 7) show the effect of ammonium per-sulfate concentration on degradation of sodium alginate, chitosan and CMC, respectively. For sodium alginate, it was found that with increasing the concentration of ammonium per-sulfate, the degradation rate sharply increases and the change in molecular weight degradation is enhanced from 5.5×10^5 at 80 kGy to 9.2×10^4 in case of treatment by 10 (wt%) APS at the same dose. Meanwhile, in case of chitosan and CMC, the high degradation rate is noticed at 5 and 2.5 (wt%) concentration of APS, respectively. The same behavior is obtained as reported by *Shih-Chang (2002)* who suggested a free radical degradation mechanism of chitosan by KPS. When KPS was thermally dissociated into anionic radicals, they were very likely to be attracted to the cationic amino groups (NH_3^+) at the C-2 carbon of the chitosan ring because of the electrostatic attraction. Subsequently, the anionic radical would attack the C-4 carbon and transferred the radical to the C-4 carbon by subtracting the hydrogen from it. The presence of a free radical at the C-4 carbon would have weakened and homolytically broken the next C-O bond at the C-1 carbon and transfer the free radical to the C-1 carbon. Consequently, the chitosan chain was degraded into two shorter chains. One had a free radical on the C-1 carbon at the end and the other had a carbonyl group at the C-4 carbon in the terminal ring.

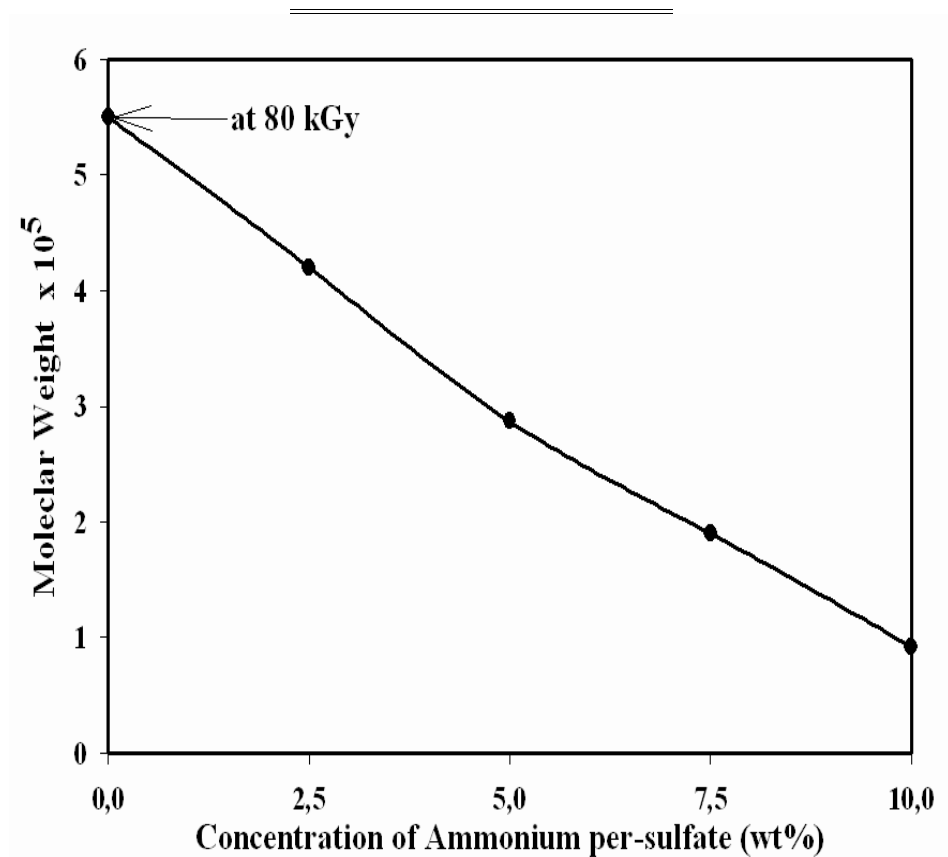


Figure (5): The effect of ammonium per-sulfate concentration on degradation of sodium alginate (paste) induced by gamma irradiation at 80 kGy as a function of the change in viscosity average molecular weight, (the dose rate 6.7 kGy/h).

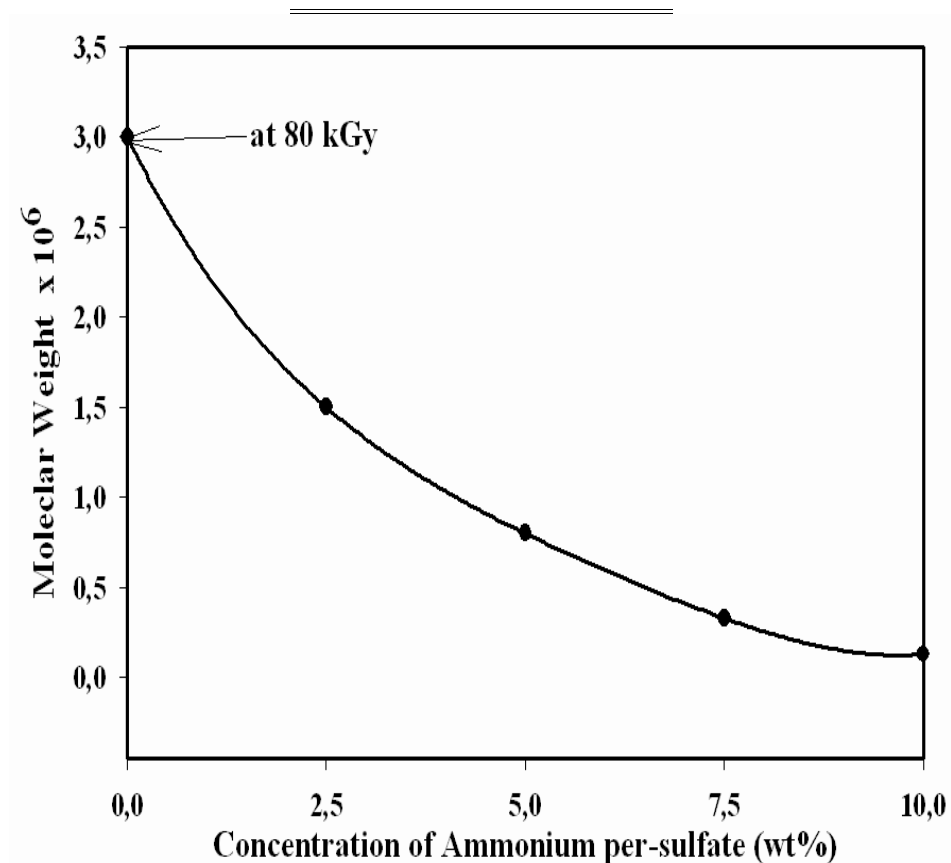


Figure (6): The effect of ammonium per-sulfate concentration on degradation process of chitosan (paste) induced by gamma irradiation at 80 kGy as a function of the change in viscosity average molecular weight, (the dose rate 6.7 kGy/h).

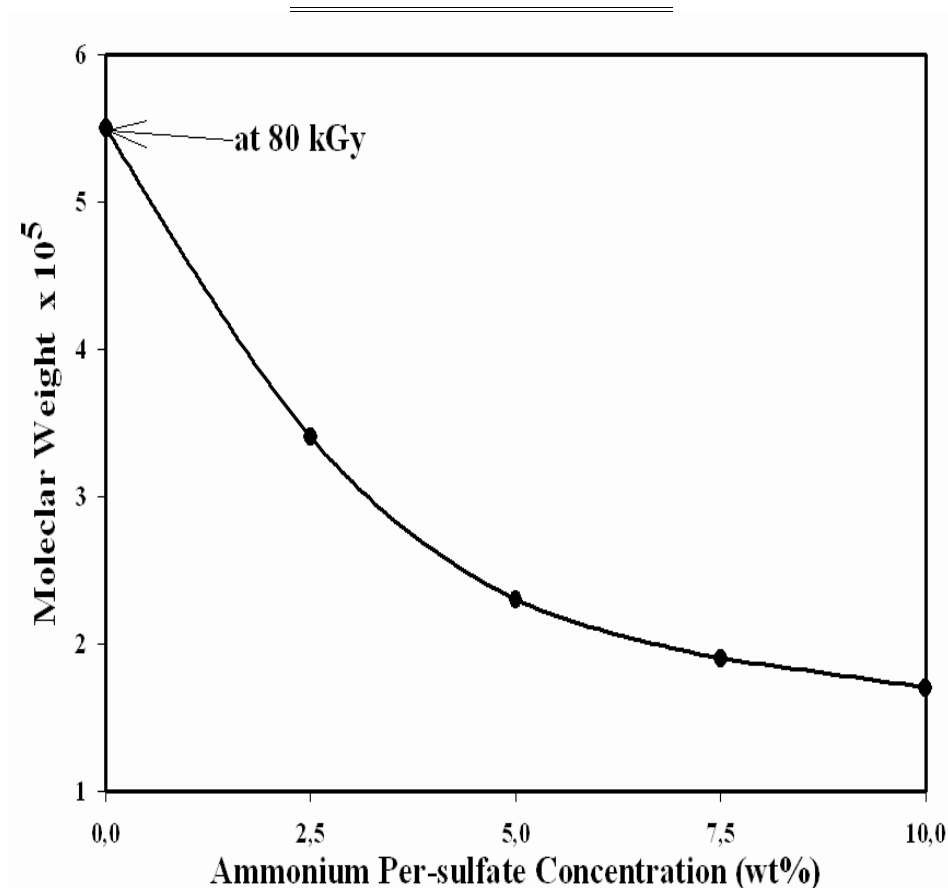


Figure (7) The effect of ammonium per-sulfate concentration on degradation process of CMC (paste) induced by gamma irradiation at 80 kGy as a function of the change in viscosity average molecular weight, (the dose rate 6.7 kGy/ h).

IV.I.4- Degradation of Chitosan, Sodium Alginate and CMC by Gamma Irradiation in Comparison with Thermal Treatments Using Initiators

Figures (8, 9 and 10) show the effect of treatment time (min) on the degradation of chitosan, sodium alginate and CMC, respectively as a function of the change in its viscosity average molecular weights in presence and absence of initiators as H_2O_2 and APS using gamma irradiation and thermal heating at 70°C .

It is clear that the presence of initiators accelerates the rate of degradation for these polymers by heating or gamma irradiation as well. However, the rate of degradation for both polymers during gamma irradiation, at a given additives is higher than that for thermal degradation at 70°C . This indicates the synergistic effect on the degradation rate of such natural polymers when gamma irradiation is used in the presence of APS or H_2O_2 than that of thermal treatment which tapers off at the early stages nearly 60 min. This explained the preference and the advantages of radiation processing of polysaccharides over other chemical alternatives where the degradation process can be performed at room temperature, the simplicity of controlling the whole process, the possibility to obtain various molecular weights fragments of these polymers in the solid state and large scale applications.

Shih-Chang (2002) used the thermal dissociation initiator of potassium per-sulfate (KPS) in the chitosan solution at 70 °C immediately the solution viscosity and the molecular weight of chitosan decrease in a very short time.

Naotsugu et al. (2000) showed that the molecular weight for alginate aqueous solution degraded at 20 kGy for 1% (w/v) or at 50 kGy for 4% (w/v) was equivalent to that of alginate irradiated in solid format 500 kGy. Hence, the irradiation dose needed to get the same molecular weight of alginate in 1% (w/v) aqueous solution is equivalent to ca. one twentieth of the dose needed for solid phase irradiation. This may be mainly due to the suppression of recombination of main chains because of high mobility of alginate chains in aqueous solution. The H[•] and [•]OH radicals formed by radiolysis during irradiation of water accelerated the molecular chain scission of sodium alginate. Reaction between the above free radicals and alginate molecules leads to rapid degradation of alginate in aqueous solution.

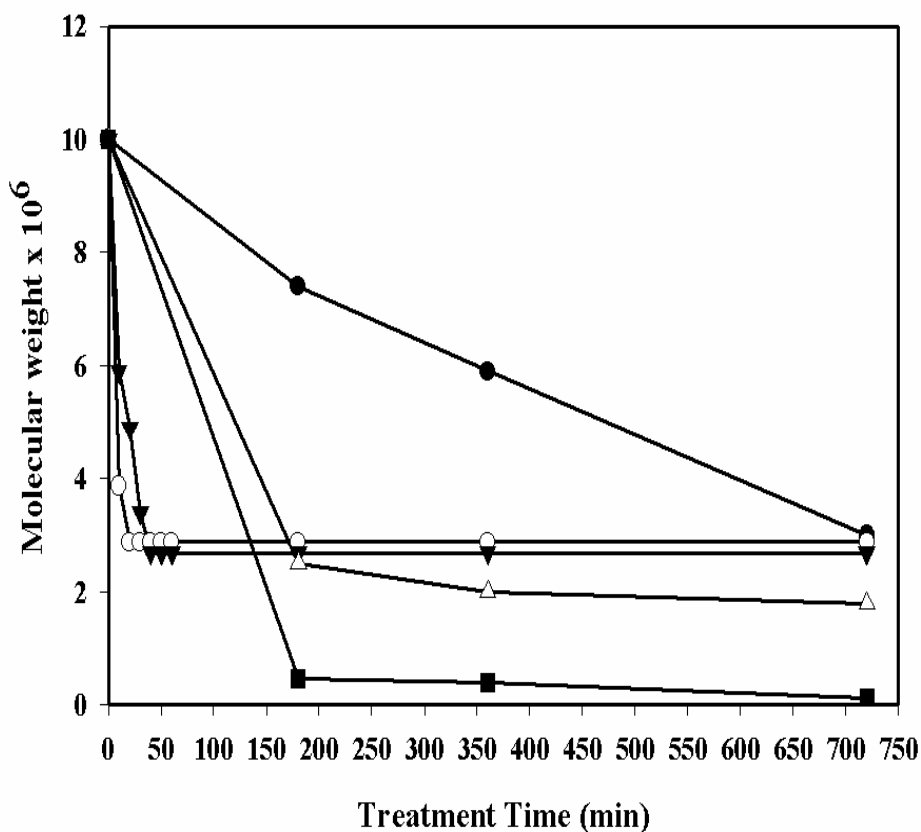


Figure (8): Effect of treatment time on the degradation of chitosan (paste) as a function of the changes in its viscosity average molecular weight in the presence of initiators using gamma irradiation or thermal heating at 70°C. (●) γ -irradiation only (○) 10% H_2O_2 (v/w) at 70 °C (▼) 10% APS (w/w) at 70 °C, (Δ) 10% H_2O_2 (v/w) γ -irradiation and (■) 10% APS (w/w) γ -irradiation, (the dose rate 6.7 kGy/h).

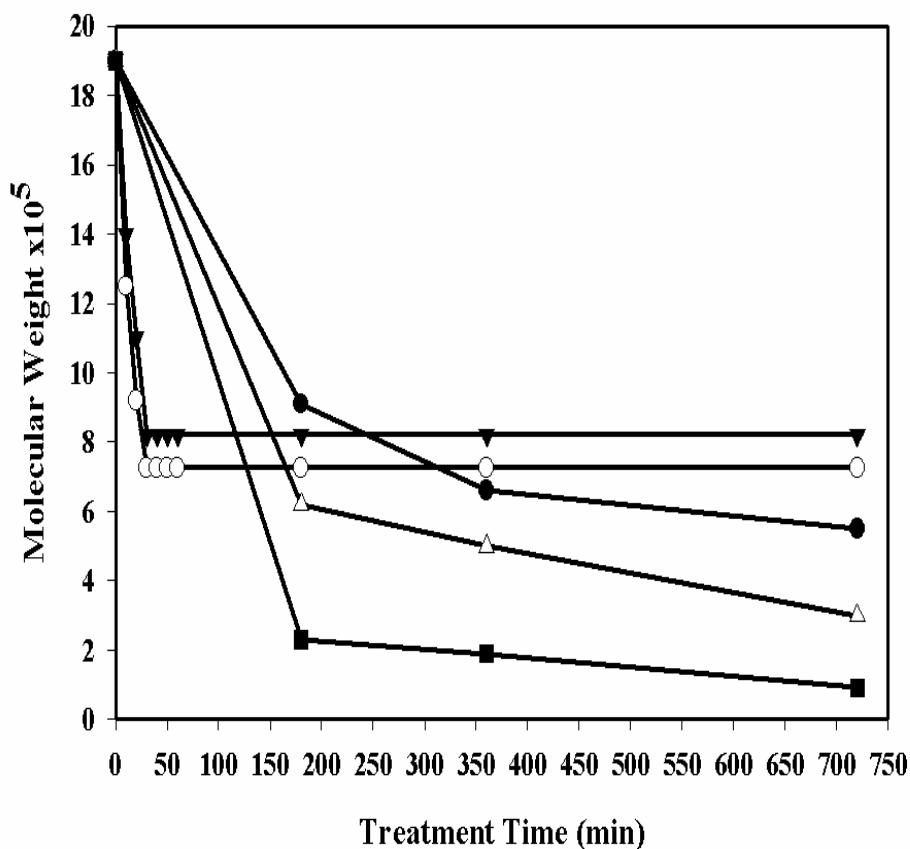


Figure (9): Effect of treatment time on the degradation of sodium alginate (paste like condition) as a function of the change in its viscosity average molecular weight in presence of initiators using gamma irradiation or thermal heating at 70°C. (●) γ -irradiation only (○) 10% H_2O_2 (v/w) at 70 °C (▼) 10% APS (w/w) at 70 °C, (△) 10% H_2O_2 (v/w) γ -irradiation and (■) 10% APS (w/w) γ -irradiation, (the dose rate 6.7 kGy/h).

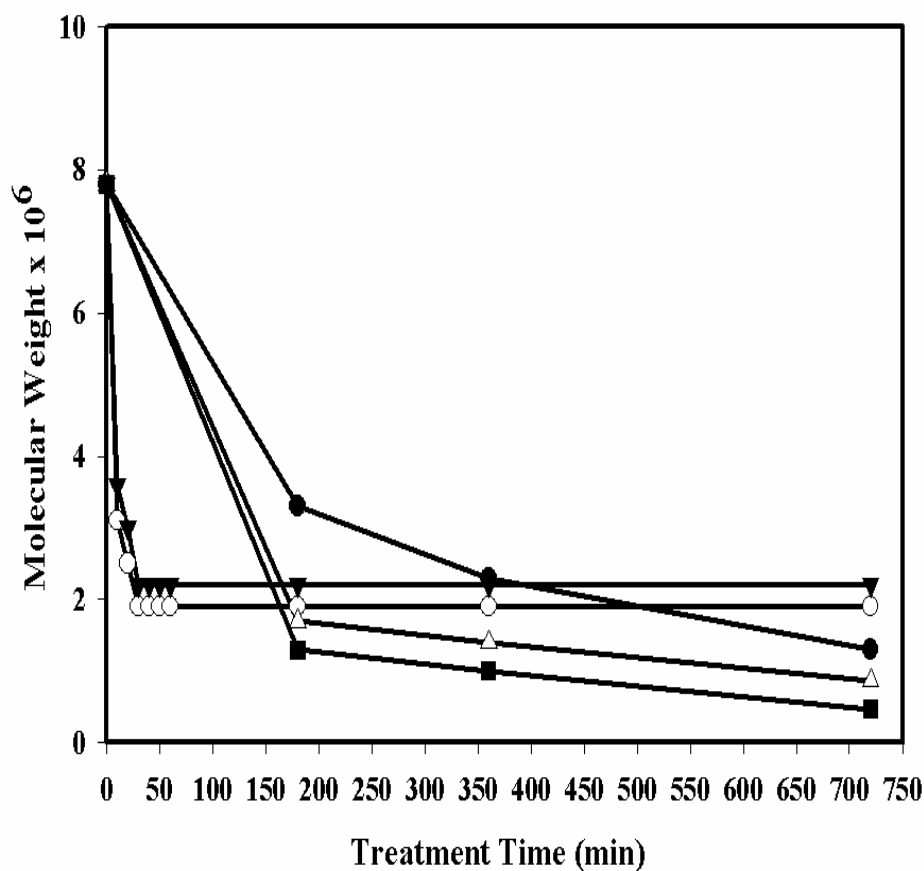


Figure (10): Effect of treatment time on the degradation of CMC (paste) as a function of the change in its viscosity average molecular weight in presence of initiators using gamma irradiation or thermal heating at 70°C. (●) γ -irradiation only (○) 10% H_2O_2 (v/w) at 70 °C (▼) 10% APS (w/w) at 70 °C, (△) 10% H_2O_2 (v/w) γ -irradiation and (■) 10% APS (w/w) γ -irradiation, (the dose rate 6.7 kGy/h).

IV.I.5- Effect of Irradiation Dose on Degradation of Natural Polymers: Determination the Molecular Weight and the Synergetic Effect

It was found that the degradation process of chitosan, sodium alginate and CMC increased by increasing the irradiation dose. The reduction in the molecular weights and the synergetic effect of these polymers can be evaluated by determine the molecular weight through two methods as follows:

IV.I.5.1- Viscometric Method

Alla et al. (1999), Shih-Chang et al. (2002), Lee-Yong et al. (1998) and Ulanski and Rosiak (1992) measured the intrinsic viscosity $[\eta]$ of chitosan samples with an ubbelohde viscometer and used the Mark-Hownique equation to determining the viscosity average molecular weight.

Figures (11, 12 and 13) show the changes in the viscosity average molecular weights measured by viscometric method as a function of the irradiation dose for pure chitosan, sodium alginate and CMC, respectively and those mixed with (w/w) 10% H₂O₂, 20% H₂O₂, 10% KPS or 10% APS.

It is observed that the addition of initiators to the polysaccharides during the irradiation process accelerates the degradation process. Meanwhile, in all treatment conditions with increasing the irradiation dose, the decrease in the

viscosity average molecular weight of chitosan, sodium alginate and CMC as well as the increase in the rate of degradation process were observed. The degradation rate depends on the type of initiators used. However, gamma radiation in combined with H_2O_2 or APS accelerates the degradation rate of polymers and reduces the dose required for polymer degradation.

The highest degradation rate is obtained when APS used in combining with gamma irradiation and the lower one is observed when pure chitosan, sodium alginate and CMC subjected to gamma irradiation. The rate of degradation is increased and felling order as followed APS > KPS > 20% H_2O_2 > 10% H_2O_2 > gamma irradiation alone. At 20 kGy the reductions rates in the viscosity average molecular weights of chitosan, sodium alginate and CMC and the treatment by H_2O_2 , KPS and APS is higher in comparison with the gamma irradiation alone. The synergetic reductions in the viscosity average molecular weights increased with increasing the irradiation dose and level off at 120 kGy and so a wide variety of lower molecular weights and shorter chain polymers or oligomers could be produced depending on the treatment conditions used. From the results obtained it can be concluded that the chitosan, sodium alginate and CMC molecules were depolymerized resulting in the reduction of their molecular weights. The degradation of the backbone occurs in a random fashion.

Table (1, 2 and 3) show the different viscosity average molecular weights of pure chitosan, sodium alginate and CMC, respectively and those mixed with H₂O₂, KPS and APS on exposure to gamma irradiation. As seen from tables results that the rate of degradation reactions and the reduction in the molecular weight is higher in presence of ammonium persulfate and hydrogen peroxide if combined with the molecular weight irradiated alone but the rate of degradation is leveling off at 120 kGy.

Using 80 KGy irradiation dose reduces the average molecular weight of chitosan, sodium alginate and CMC molecules from 1×10^7 to 3×10^6 , 1.9×10^6 to 5.5×10^5 and 7.8×10^6 to 1.3×10^6 , respectively but the irradiation of chitosan, sodium alginate and CMC molecules at 40 kGy in the presence of APS is enough to reduce the average molecular weight of chitosan, sodium alginate and CMC molecules from 1×10^7 to 1.3×10^5 , 1.9×10^6 to 9.2×10^4 and 7.8×10^6 to 3.7×10^5 , respectively.

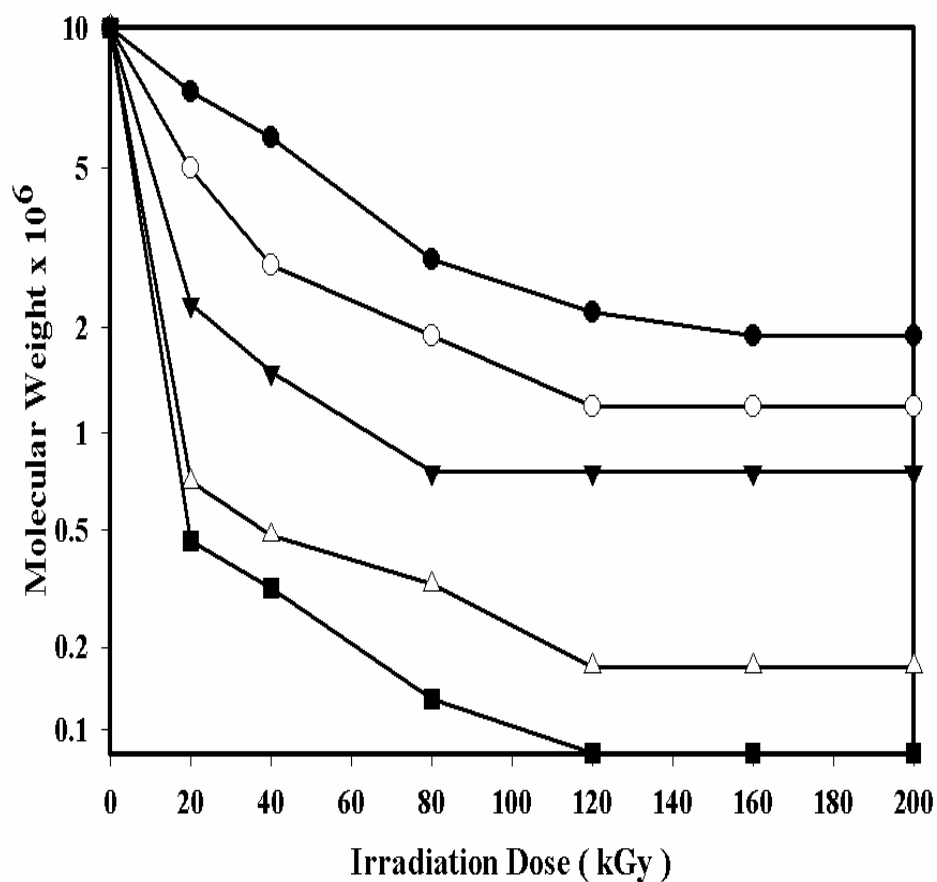


Figure (11): The changes in the viscosity average molecular weight of pure chitosan when exposed to gamma irradiation: (●) γ -irradiation only and that mixed with (○) 10% H₂O₂ (v/w) (▼) 20% H₂O₂ (△) 10% KPS and (■) 10% APS (w/w), (paste), (the dose rate 6.7 kGy/h).

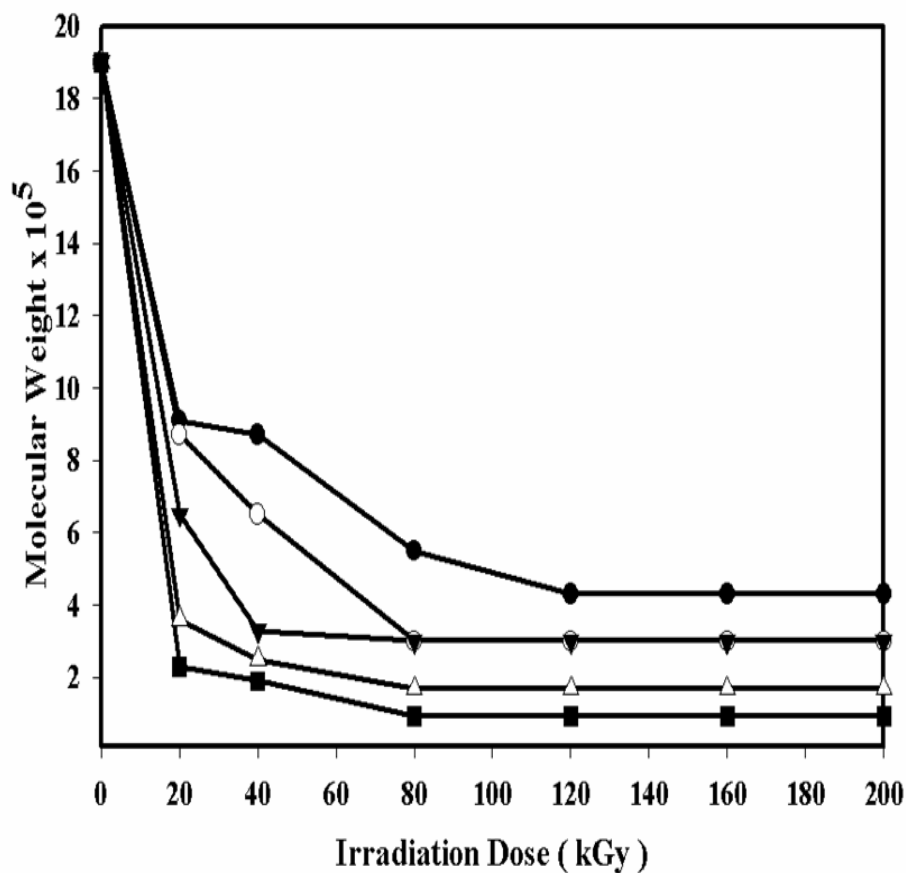


Figure (12): The changes in the viscosity average molecular weight of pure sodium alginate on exposure to gamma irradiation (●) γ -irradiation only and that mixed with (○) 10% H_2O_2 (v/w) (▼) 20% H_2O_2 , (Δ) 10% KPS and (■) 10% APS (w/w), (paste), (the dose rate 6.7 kGy/h).

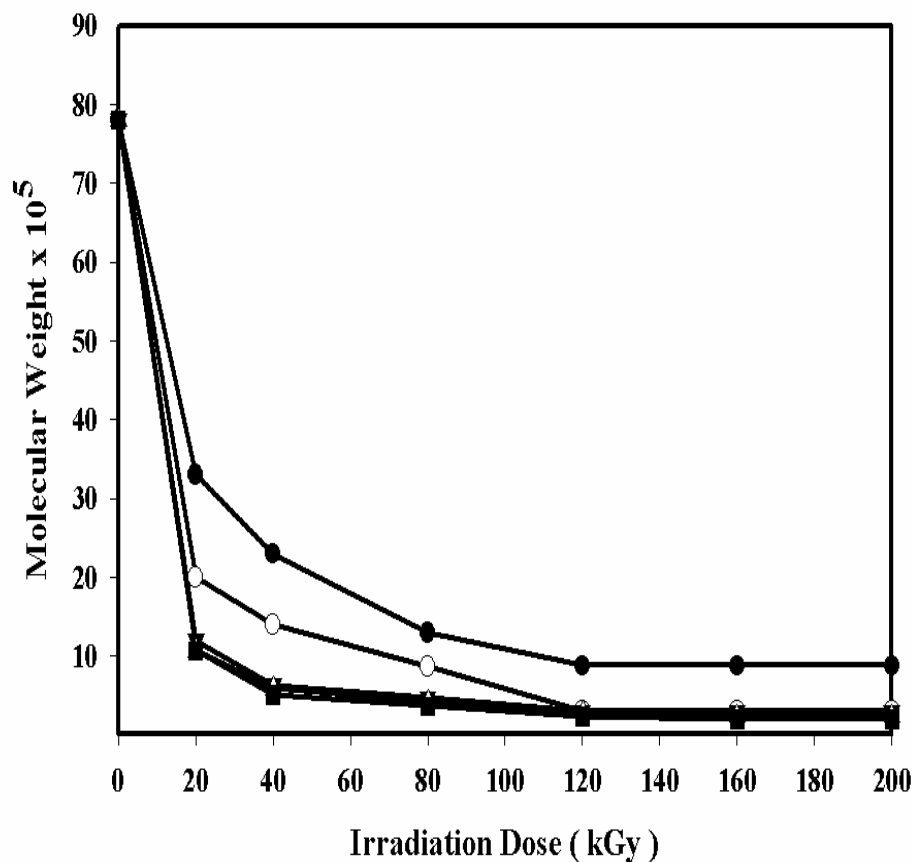


Figure (13): The changes in the viscosity average molecular weight of pure CMC on exposure to gamma irradiation (●) γ -irradiation only and that mixed with (○) 10% H₂O₂ (v/w) (▼) 20% H₂O₂, (Δ) 10% KPS and (■) 10% APS (w/w), (paste), (the dose rate 6.7 kGy/h).

Table (1): Viscosity average molecular weights of chitosan when exposed to different irradiation doses and in presence of initiators measured by viscometric method.

Irradiation Dose(kGy)	(Blank)	with 10 % H ₂ O ₂ (v/w)	With 20 % H ₂ O ₂ (v/w)	with 10 (wt%) kPS	with 10 (wt%) APS
0	1×10^7	1×10^7	1×10^7	1×10^7	1×10^7
20	7.4×10^6	5×10^6	2.3×10^6	1.2×10^6	4.6×10^5
40	5.9×10^6	2.9×10^6	1.5×10^6	7.1×10^5	4×10^5
80	3×10^6	1.8×10^6	7.6×10^5	3.3×10^5	1.3×10^5
120	2.2×10^6	1.2×10^6	7.6×10^5	1.7×10^5	8.1×10^4
160	1.9×10^6	1.2×10^6	7.6×10^5	1.7×10^5	8.1×10^4
200	1.9×10^6	1.2×10^6	7.6×10^5	1.7×10^5	8.1×10^4

Table (2): Viscosity average molecular weights of sodium alginate when exposed to different irradiation doses and in presence of initiators measured by viscometric method.

Irradiation Dose(kGy)	(Blank)	with 10 % H ₂ O ₂ (v/w)	With 20 % H ₂ O ₂ (v/w)	with 10 (wt%) kPS	with 10 (wt%) APS
0	1.9×10^6	1.9×10^6	1.9×10^6	1.9×10^6	1.9×10^6
20	9.1×10^5	8.7×10^5	6.5×10^5	1.2×10^6	2.5×10^5
40	8.7×10^5	6.5×10^5	3×10^5	2.5×10^5	1.9×10^5
80	5.5×10^5	3×10^5	3×10^5	1.7×10^5	9.2×10^4
120	4.3×10^5	3×10^5	3×10^5	1.7×10^5	9.2×10^4
160	4.3×10^5	3×10^5	3×10^5	1.7×10^5	9.2×10^4
200	4.3×10^5	3×10^5	3×10^5	1.7×10^5	9.2×10^4

Table (3): Viscosity average molecular weights of CMC when exposed to different irradiation doses and in presence of initiators measured by viscometric method.

Irradiation Dose(kGy)	(Blank)	with 10 % H ₂ O ₂ (v/w)	With 20 % H ₂ O ₂ (v/w)	with 10 (wt%) kPS	with 10 (wt%) APS
0	7.8×10^6	7.8×10^6	7.8×10^6	7.8×10^6	7.8×10^6
20	3.3×10^6	2×10^6	6.5×10^5	1.7×10^5	1.2×10^6
40	2.3×10^6	1.4×10^6	3×10^5	5.9×10^5	5.1×10^5
80	1.3×10^6	8.7×10^5	3×10^5	4.3×10^5	3.7×10^5
120	8.8×10^5	3.1×10^5	3×10^5	2.9×10^5	2.4×10^5
160	8.8×10^5	3.1×10^5	3×10^5	2.4×10^5	2×10^5
200	8.8×10^5	3.1×10^5	3×10^5	2.4×10^5	2×10^5

IV.I.5.2- Gel Permeation Chromatography (GPC) Method

Jin et al. (2007), Hui et al. (2006), Jaroslaw et al. (2005), Qin et al. (2002) and Naotsugu et al. (2000) measured the number average molecular weight and weight average molecular weights by gel permeation chromatography (GPC).

Figure (14) shows the GPC elution curves of pure, irradiated sodium alginates at 120 kGy and those mixed with 10% H₂O₂ or 10% APS irradiated at 120 kGy as a function of retention time (min). According to the principles of GPC apparatus, the large molecular weight molecules of large size appears with low retention time and the lower molecular weight molecules of small size at high retention time. The retention time of low molecular weight molecules is high.

Figures (15, 16 and 17) show the changes in the number-average molecular weights measured by GPC measurements as a function of increasing the irradiation doses for pure chitosan, sodium alginate and CMC, respectively when exposed to gamma irradiation and storing for 2 months of gamma irradiated, untreated and treated sodium alginate with 10% H₂O₂ or 10% APS or 10% H₂O₂.

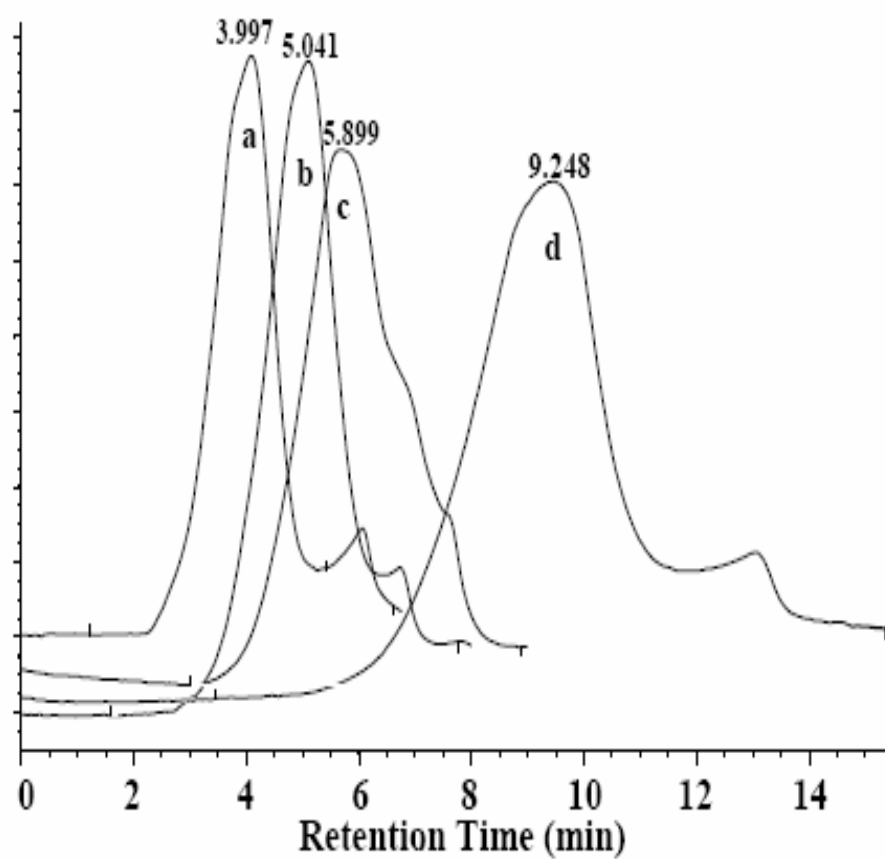


Figure (14): GPC elution curves of sodium alginates as a function of retention time (a) pure, (b) irradiated at 120 kGy, (c) treated by 10% APS at 120 kGy and (d) treated by 10% H_2O_2 at 120 kGy, (paste), (the dose rate 6.7 kGy/h).

A steep reduction in the number-average molecular weights of chitosan, sodium alginate and CMC was observed up to 20 kGy in presence of ammonium per-sulfate and hydrogen peroxide which gradually increased as the irradiation dose increased as seen in Figures (15, 16 and 17).

The storing effect on the molecular weight of irradiated chitosan, sodium alginate and CMC mixed with 10% H₂O₂ and 10% APS was interesting. Tables (4, 5 and 6) show the different number-average molecular weights of pure chitosan, sodium alginate and CMC, respectively when exposed to gamma irradiation and those mixed with different initiators measured by GPC. The reduction in the number-average molecular weights is higher in case of hydrogen peroxide in combined with gamma irradiation after storage for 2 months.

The degradation reactions of these polymers depend on the amount of free radicals formed during the irradiation process and the direct dissociation of APS and H₂O₂. The possibility of recombination of free radicals formed from the dissociation of APS is much higher than that in dissociation of H₂O₂, which lead to terminate the degradation reaction after irradiation in case of APS only to give stable fragments or oligomers with shorter chains and molecular weights can be applicable. The free radicals formed in the presence of H₂O₂ is very low decay and therefore, the degradation process is in continuous.

Water soluble chitosan fragments can be obtained by heating in water at 70 °C, filtration and precipitation with methanol occurred after treatment of chitosan with gamma irradiation and ammonium per-sulfate to obtain molecular weights of 8.5×10^4 , 2.7×10^4 , 1.44×10^4 , 6.8×10^3 and 4.17×10^3 at 40, 80, 120, 160 and 200 kGy, respectively. The amount of water soluble chitosan obtained increased with increasing the irradiation dose.

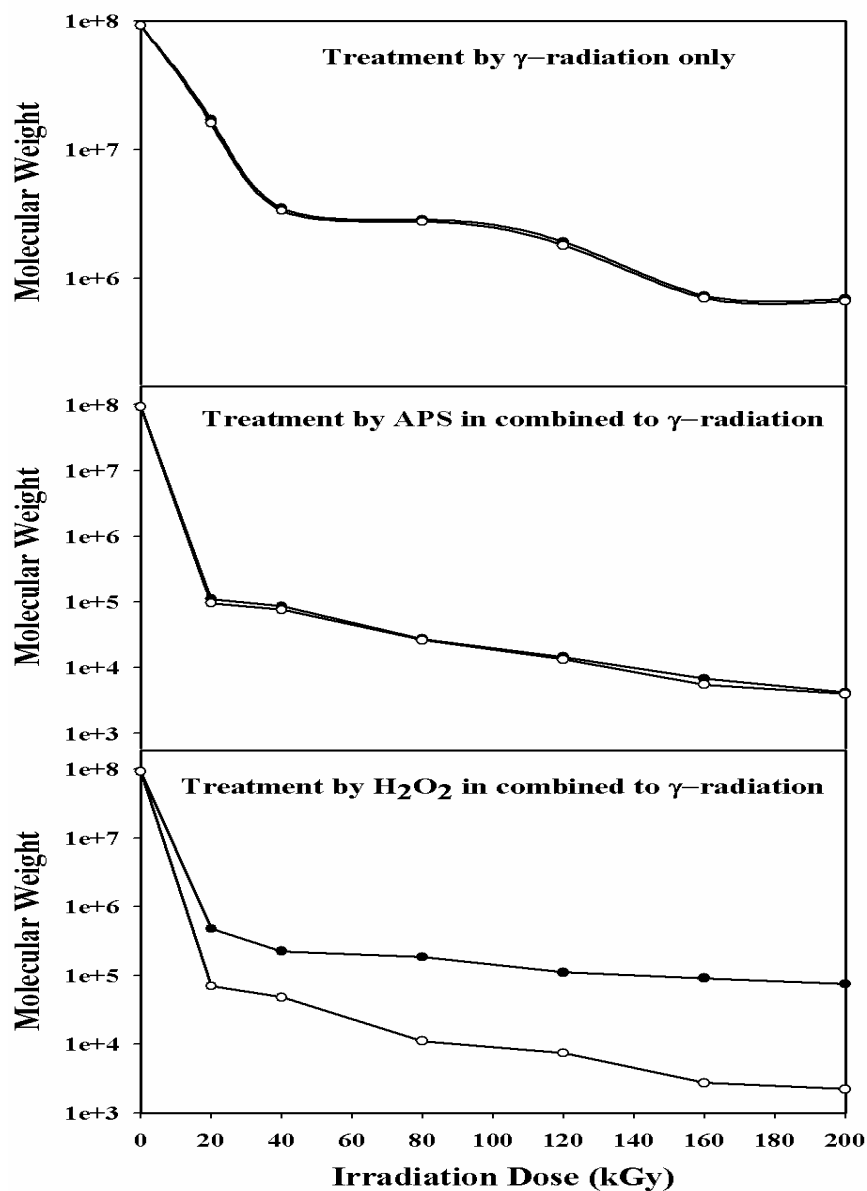


Figure (15): The changes in the number average molecular weight of chitosan measured by GPC when exposed to gamma irradiation and that mixed with 10% H_2O_2 (v/w) or 10% APS (w/w) beside gamma irradiation (●) after irradiation and (○) after storing for 2 months.

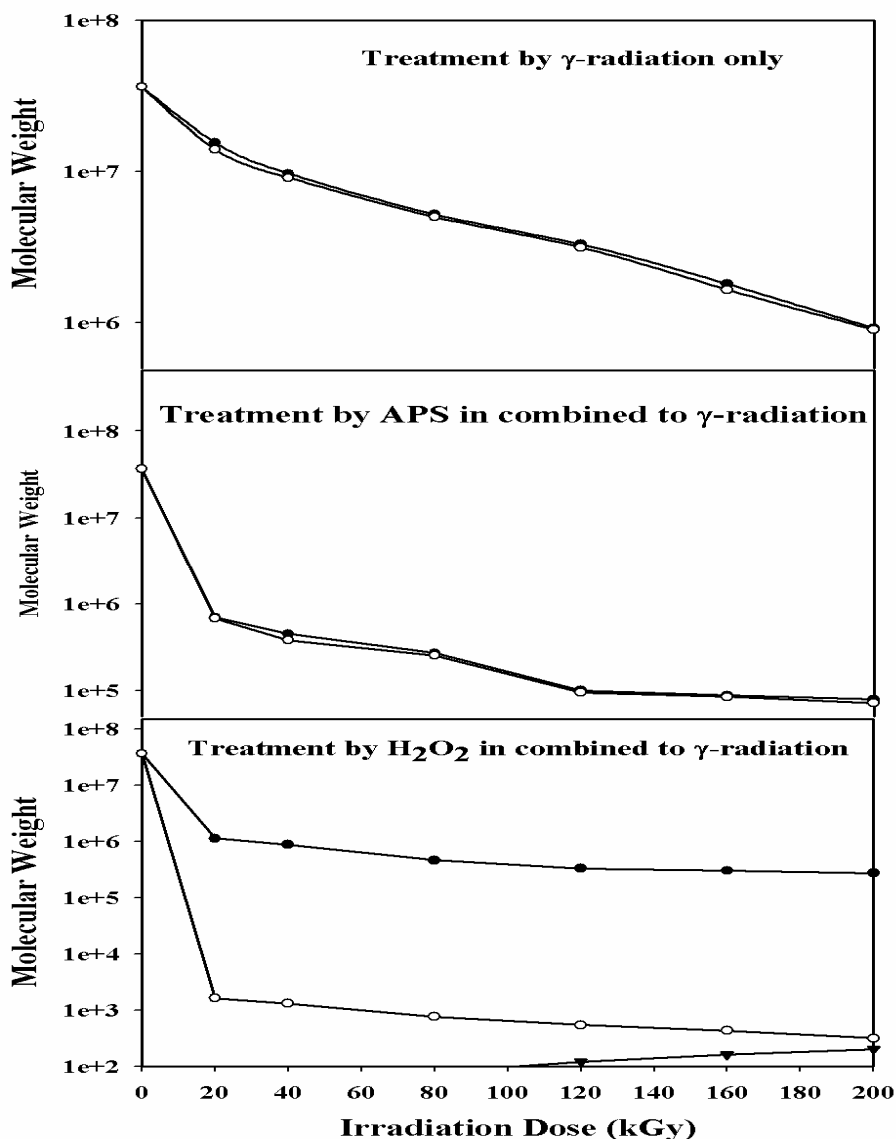


Figure (16): The changes in the number average molecular weight of sodium alginate measured by GPC when exposed to gamma irradiation and that mixed with 10% H_2O_2 (v/w) or 10% APS (w/w) beside gamma irradiation (●) after irradiation and (○) after storing for 2 months.

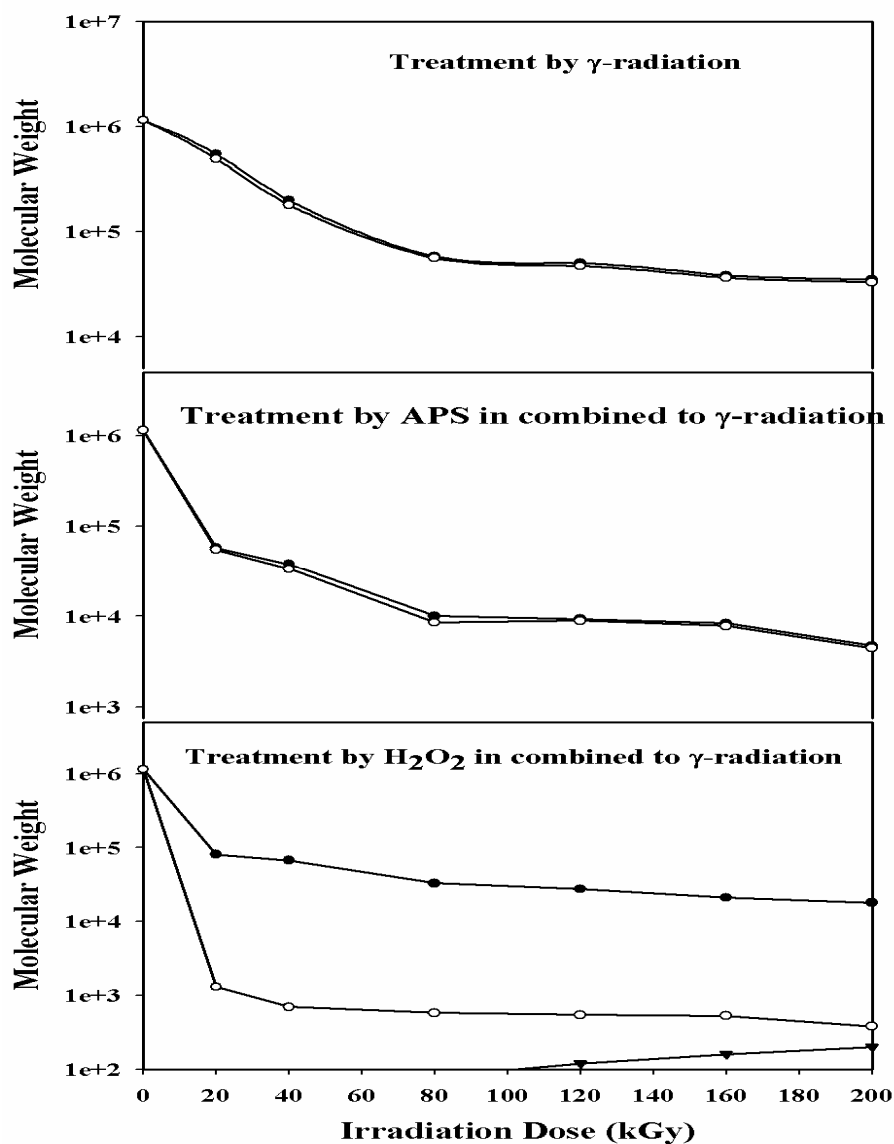


Figure (17): The changes in the number average molecular weight of CMC measured by GPC when exposed to gamma irradiation and that mixed with 10% H_2O_2 (v/w) or 10% APS (w/w) beside gamma irradiation (●) after irradiation and (○) after storing for 2 months.

Table (4): Number-average molecular weights of chitosan on exposure to gamma irradiation and that mixed with different initiators measured by GPC.

Radiation Dose (kGy)	Irradiated chitosan		Irradiated chitosan + APS		Irradiated chitosan + H ₂ O ₂	
	After irradiation	After storing	After irradiation	After storing	After irradiation	After storing
0	9.2×10^7	9.2×10^7	9.2×10^7	9.2×10^7	9.2×10^7	9.2×10^7
20	1.7×10^7	1.58×10^7	1.1×10^5	9.8×10^4	4.77×10^5	7×10^4
40	3.5×10^6	3.34×10^6	8.5×10^4	7.35×10^4	2.23×10^5	4.73×10^4
80	2.85×10^6	2.73×10^6	2.7×10^4	2.54×10^4	1.85×10^5	1×10^4
120	1.91×10^6	1.8×10^6	1.44×10^4	1.32×10^4	1.1×10^5	7.4×10^3
160	7.3×10^5	9.09×10^4	6.8×10^3	5.5×10^3	9.09×10^4	2.7×10^3
200	6.9×10^5	7.5×10^4	4.17×10^3	3.97×10^3	7.5×10^4	2.2×10^3

Table (5): Number-average molecular weights of sodium alginate on exposure to gamma irradiation and that mixed with different initiators measured by GPC.

Radiation Dose (kGy)	Irradiated alginate		Irradiated alginate + APS		Irradiated alginate + H ₂ O ₂	
	After irradiation	After storing	After irradiation	After storing	After irradiation	After storing
0	3.64×10^7	3.64×10^7	3.64×10^7	3.64×10^7	3.64×10^7	3.64×10^7
20	1.55×10^7	1.39×10^7	7×10^5	6.8×10^5	11.2×10^5	1.63×10^3
40	9.7×10^6	9.1×10^6	4.5×10^5	3.8×10^5	8.7×10^5	1.3×10^3
80	5.2×10^6	5.0×10^6	2.9×10^5	2.55×10^5	4.6×10^5	7.6×10^2
120	3.3×10^6	3.15×10^6	1×10^5	9.5×10^4	3.3×10^5	5.3×10^2
160	1.8×10^6	1.65×10^6	8.8×10^4	8.5×10^4	3×10^5	4.2×10^2
200	9.2×10^5	8.12×10^5	7.9×10^4	7.2×10^4	2.7×10^5	3.13×10^2

Table (6): Number-average molecular weights of CMC on exposure to gamma irradiation and that mixed with different initiators measured by GPC.

Radiation Dose (kGy)	Irradiated CMC		Irradiated CMC + APS		Irradiated CMC + H ₂ O ₂	
	After irradiation	After storing	After irradiation	After storing	After irradiation	After storing
0	1.15×10^6	1.15×10^6	1.15×10^6	1.15×10^6	1.15×10^6	1.15×10^6
20	5.5×10^5	4.95×10^5	5.8×10^4	5.5×10^4	1.15×10^6	1.3×10^3
40	2×10^5	1.8×10^5	3.8×10^4	3.35×10^4	8.05×10^4	7×10^2
80	5.8×10^4	5.6×10^4	1×10^4	8.9×10^3	6.7×10^4	5.8×10^2
120	5×10^4	4.7×10^4	9.3×10^3	8.5×10^3	3.3×10^4	5.5×10^2
160	3.8×10^4	3.63×10^4	8.3×10^3	7.8×10^3	2.75×10^4	5.2×10^2
200	3.5×10^4	3.3×10^4	4.7×10^3	7.2×10^4	2.1×10^4	3.8×10^2

IV.I.6- Characterization of Degraded Naturally Occurring Polymers

IV.I.6.1- UV-Vis Spectroscopy

UV-Vis spectroscopy of the original polymers and degraded ones were carried out to investigate the structural changes formed during the degradation of natural polymers

Figure (18) shows the UV-Vis spectra of pure chitosan, and that treated with 10 (wt%) ammonium per-sulfate and irradiated at different doses of 40, 80, 120, 160 and 200 kGy. For original chitosan a strong absorption band was absorbed around 280 nm which was caused by the $n \rightarrow \delta^*$ transition for the amino groups of chitosan. A spectral absorption band could be seen at 300 nm which is assigned to the $n \rightarrow \pi^*$ transition for the carbonyl or carboxyl groups. It might be the new side group of degraded chitosan. Also in Figure (18) a new absorption band between 250 nm and 280 nm was observed and the peak intensity increased with increasing the irradiation dose. This peak can be ascribed to carbon-oxygen double bonds (carbonyl groups) formed after the main chain scission of chitosan and hydrogen abstraction reaction followed by the ring opening *Ulanski and Rosiak (1992)*.

Figures (19 and 20) show the UV-Vis spectra of pure sodium alginate and CMC and those treated with 10 (wt%) ammonium per-sulfate and irradiated at different doses of 40, 80, 120, 160 and 200 kGy, respectively. The color of the aqueous solution of sodium alginate and CMC changed to a more intense brown with increasing irradiation dose. There are a new absorption band between 265 and 280 nm and the peak intensity increases with increasing the irradiation dose. This can be assigned to double bonds of sodium alginate formed after main chain scission and/or hydrogen abstraction reaction occurred during irradiation *Nagasawa et al (2000)*.

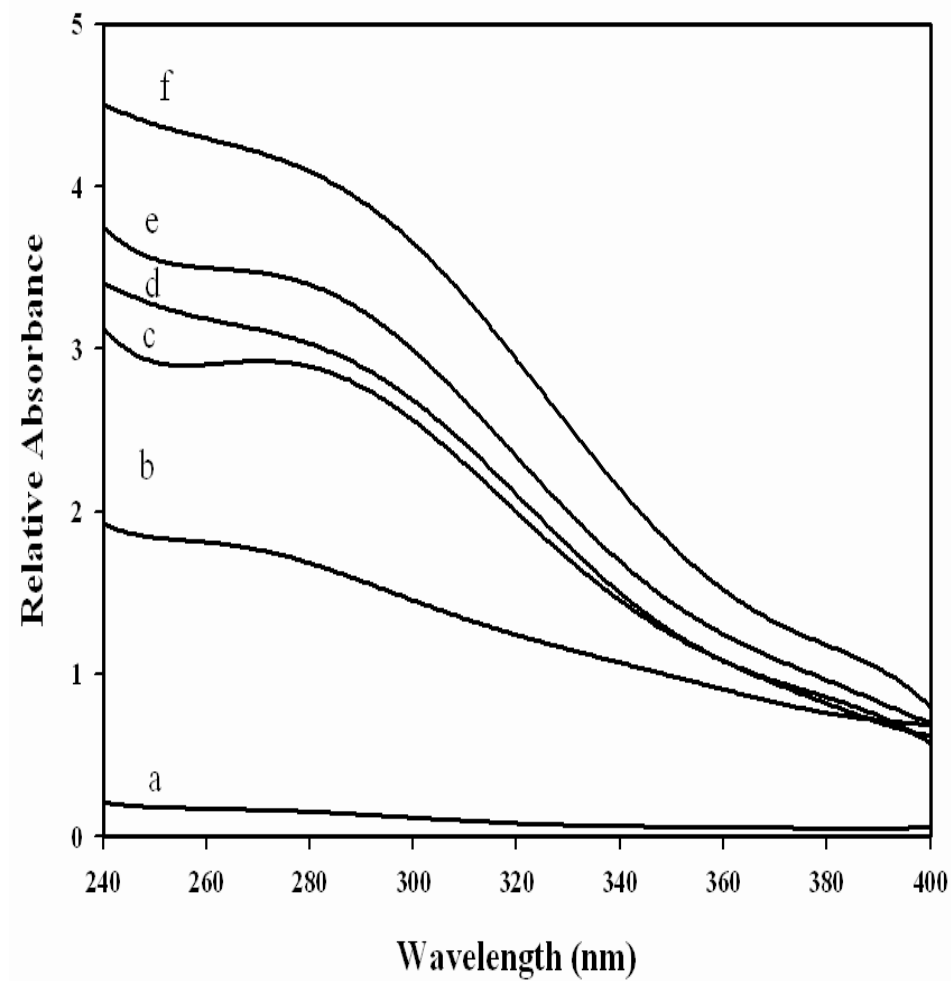


Figure (18): UV-Vis spectra of (a) pure chitosan and that mixed with 10 (wt%) ammonium per-sulfate at different irradiation doses of (b) 40 kGy, (c) 80 kGy, (d) 120 kGy, (e) 160 kGy and (f) 200 kGy. (the dose rate is 6.7 kGy/h).

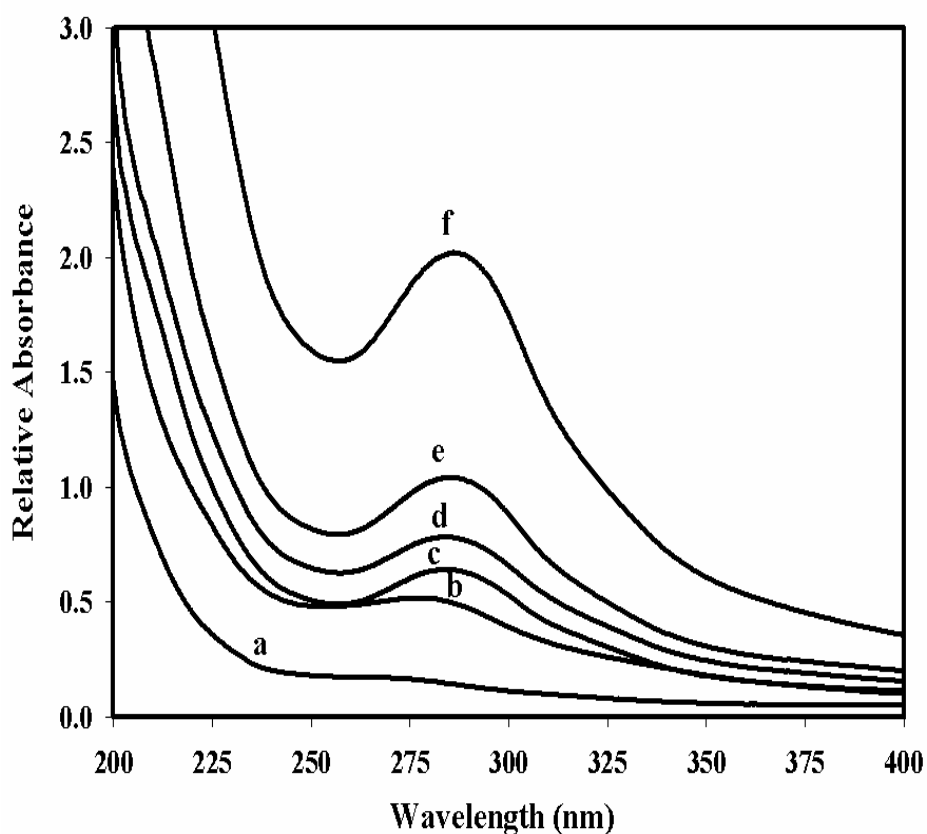


Figure (19): UV-Vis spectra of (a) pure sodium alginate and that mixed with 10 (wt%) APS at different irradiation doses of (b) 40 kGy, (c) 80 kGy, (d) 120 kGy, (e) 160 kGy and (f) 200 kGy. (the dose rate is 6.7 kGy/h).

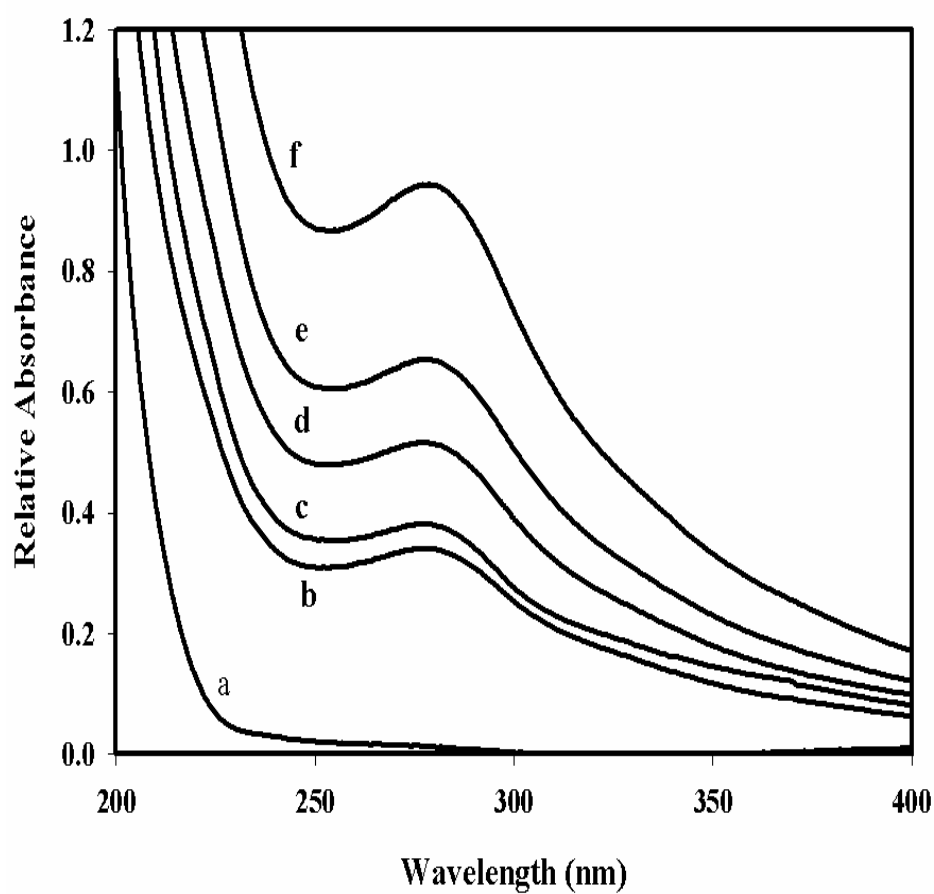


Figure (20): UV-Vis spectra of (a) pure CMC and that mixed with 10 (wt%) APS at different irradiation doses of (b) 40 kGy, (c) 80 kGy, (d) 120 kGy, (e) 160 kGy and (f) 200 kGy, (the dose rate is 6.7 kGy/h).

IV.I.6.2- XRD Analysis

Figures (21, 22 and 23) show X-ray diffraction patterns of pure chitosan, sodium alginate and CMC and those treated with 10 (wt%) ammonium per-sulfate and irradiated at doses of 40, 120 and 200 kGy, respectively.

As seen in Figure (21), original chitosan and chitosan after irradiation exhibited two characteristic peaks at $2\theta = 10.4^\circ$ and $2\theta = 19.8^\circ$ which coincided with the pattern of the L-2 polymorph of shrimp chitosan as reported by *Satio and Tabeta (1987)* and *Hasegawa et al. (1992)*. There is change in the intensity of the peaks with increasing the irradiation dose. Radiation degradation did not destroy crystal structure of chitosan up to 200 kGy. For chitosan after chemical-radiation degradation the first peak at $2\theta = 19.8^\circ$ is much less intensive and the peaks at $2\theta = 10.4^\circ$ may be disappeared due to the destruction of hydrogen bonding between amino groups and hydroxyl groups in chitosan *Kim and Lee (1993)*. The results show that chemical-radiation degradation of chitosan by ammonium per-sulfate caused reduction of the crystal structure. The water-soluble fraction became amorphous. Thus, it was assumed that the degradation first occurred preferentially in the amorphous region and then proceeded very moderately from the edge to the inside of the crystalline.

Also, as seen in Figures (22 and 23), original sodium alginate and CMC after irradiation exhibited a characteristic peaks at $2\theta = 21$ and 19.8° , respectively. There is change in intensity of the peak with increasing the irradiation dose. Radiation degradation destroyed the crystal structure of sodium alginate up to 200 kGy in presence of 10 (wt%) APS. The results show that chemical-radiation degradation of sodium alginate by APS caused destruction of the crystal structure. Thus, it was assumed that the degradation first took place preferentially in the amorphous region and then proceeded very moderately from the edge to the inside of the crystalline.

It is known that radiation-induced degradation of polymers in amorphous regions is faster than that in crystalline regions *Mitomo et al. (1994)*. In the present case, the degradation occurring in the earlier stage is mainly assigned to that occurring in amorphous regions and slow degradation at higher doses is assigned to that in occurring crystalline regions. Also the degradation was probably due to the direct effect of radiation and the indirect effect due to oxidation process.

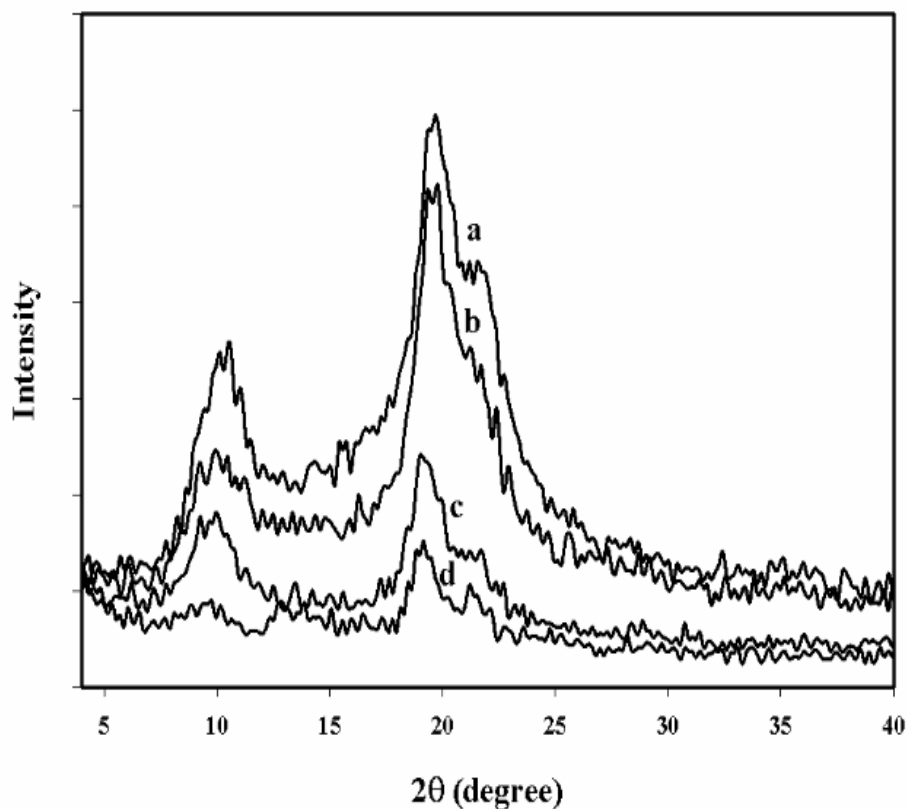


Figure (21): XRD spectra of (a) pure chitosan and that mixed with 10 (wt%) ammonium per-sulfate at different irradiation doses of (b) 40 kGy, (c) 120 kGy and (d) 200 kGy, (the dose rate is 6.7 kGy/h).

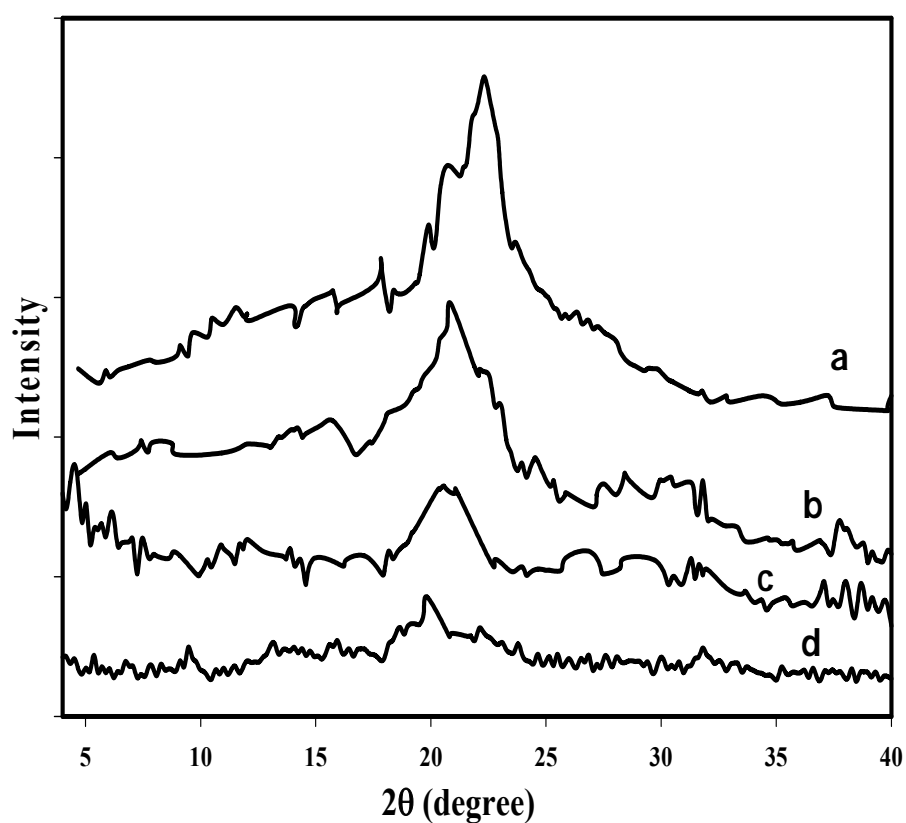


Figure (22): XRD spectra of (a) pure sodium alginate and that mixed with 10 (wt%) ammonium per-sulfate at different irradiation doses of (b) 40 kGy, (c) 120 kGy and (d) 200 kGy, (the dose rate is 6.7 kGy/h).

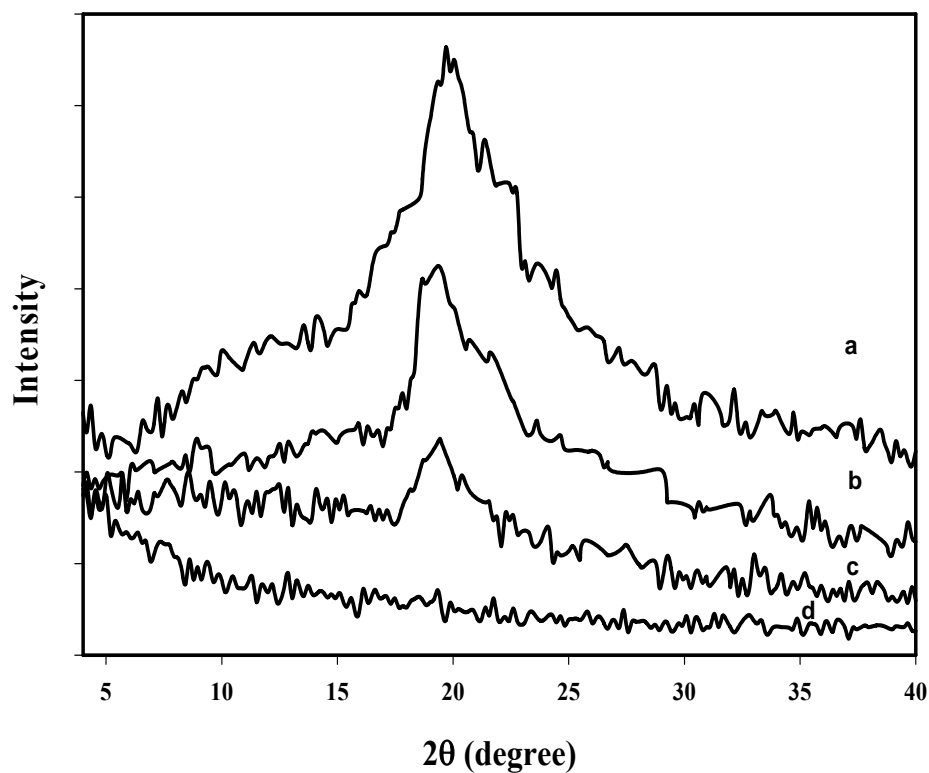


Figure (23): XRD spectra of (a) pure CMC and that mixed with 10 (wt%) ammonium per-sulfate at different irradiation doses of (b) 40 kGy, (c) 120 kGy and (d) 200 kGy, (the dose rate is 6.7 kGy/h).

IV.I.6.3- TGA Analysis

Thermo-gravimetry is a technique that can yield information about humidity and ash contents in a simple and fast way. Figures (24, 25 and 26) show the effect of radiation doses in the presence of APS on the thermal stability of chitosan, sodium alginate and CMC, respectively.

As seen from the Figure (24), for chitosan the weight loss took place in two stages. The first one starts below 150°C and is assigned to loss of water. Since a considerable amount of water is released at temperatures below 150°C. It can be concluded that, at low water contents, the water molecules should be predominantly bound to the amine groups. Consequently, it might be thought that, in the case of pure chitosan, water molecules bound to amine groups could be more easily removed (at lower temperature) than those molecules bound to hydroxyl groups.

The second stage starts at 240 °C and reaches a maximum at 350 °C corresponds to the main chain decomposition (thermal and oxidative) of chitosan, vaporization and elimination of volatile products *Nieto et al. (1991)* and *Tirkistani (1998)*.

Figures (25 and 26) represented the TGA of for sodium alginate and CMC, respectively there are three stages of decomposition, firstly the salt decomposition by dehydration from 50 to 150 °C followed by, secondly, degradation to Na₂CO₃ from 200-260 and from 200 to 300 °C for sodium

alginate and CMC, respectively. The Na_2CO_3 decomposition is dependent on the sample holder and atmosphere used. Thirdly, degrade to carbonized material that decomposes slowly from 300 - 600 °C.

Table (7, 8 and 9) show the weight loss percent for pure chitosan, sodium alginate and CMC, respectively and those treated with 10 wt% ammonium per-sulfate at different irradiation doses of 40, 120 and 200 kGy. It is obvious that the thermal stability of pure chitosan, sodium alginate and CMC is higher than those treated with ammonium per-sulfate. Also there is no difference between the thermal stability and weight loss percent for those mixed by ammonium per-sulfate in comparison with each other at different irradiation doses.

According to *Nieto et al. (1991)*, pyrolysis of polysaccharides starts by a random split of the glycosidic bonds, followed by a further decomposition forming acetic and butyric acids and a series of lower fatty acids, where C_2 , C_3 and C_6 predominate.

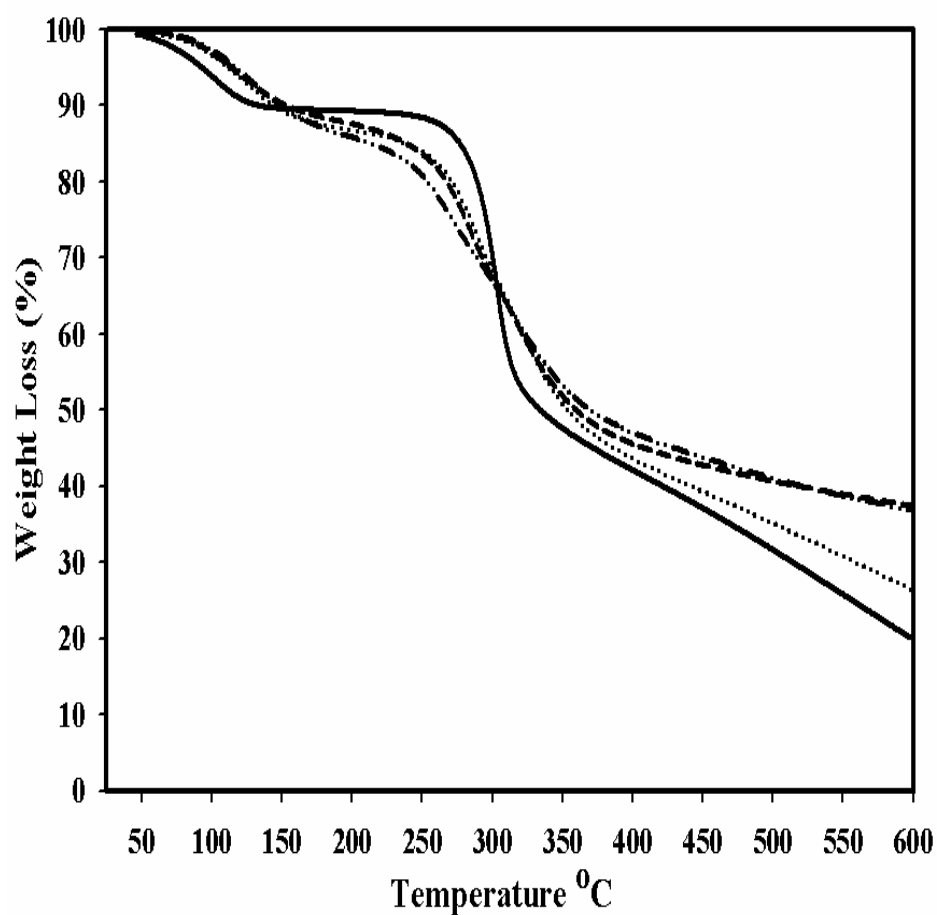


Figure (24): TGA diagram of (—) pure chitosan and that mixed with 10 wt% ammonium per-sulfate at different irradiation doses of (····) 40 kGy, (---) 120 kGy and (·-·-·-·) 200 kGy, (the dose rate is 6.7 kGy/h).

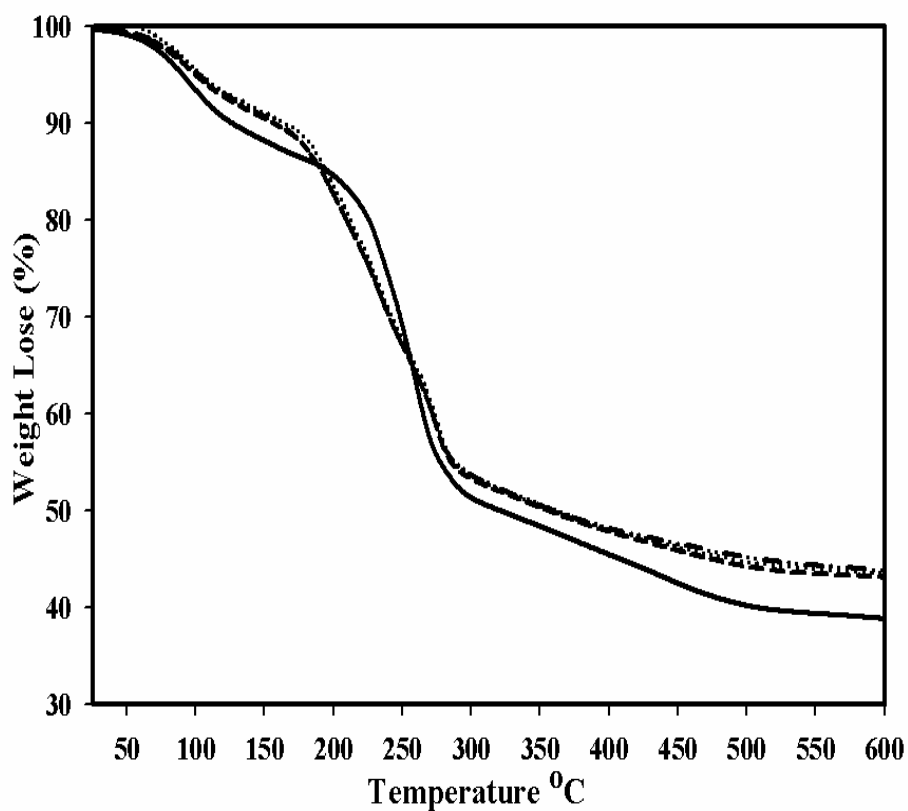


Figure (25): TGA diagram of (—) pure sodium alginate and that mixed with 10 (wt%) ammonium persulfate at different irradiation doses of (····) 40 kGy, (---) 120 kGy and (·-·-·) 200 kGy, (the dose rate is 6.7 kGy/h).

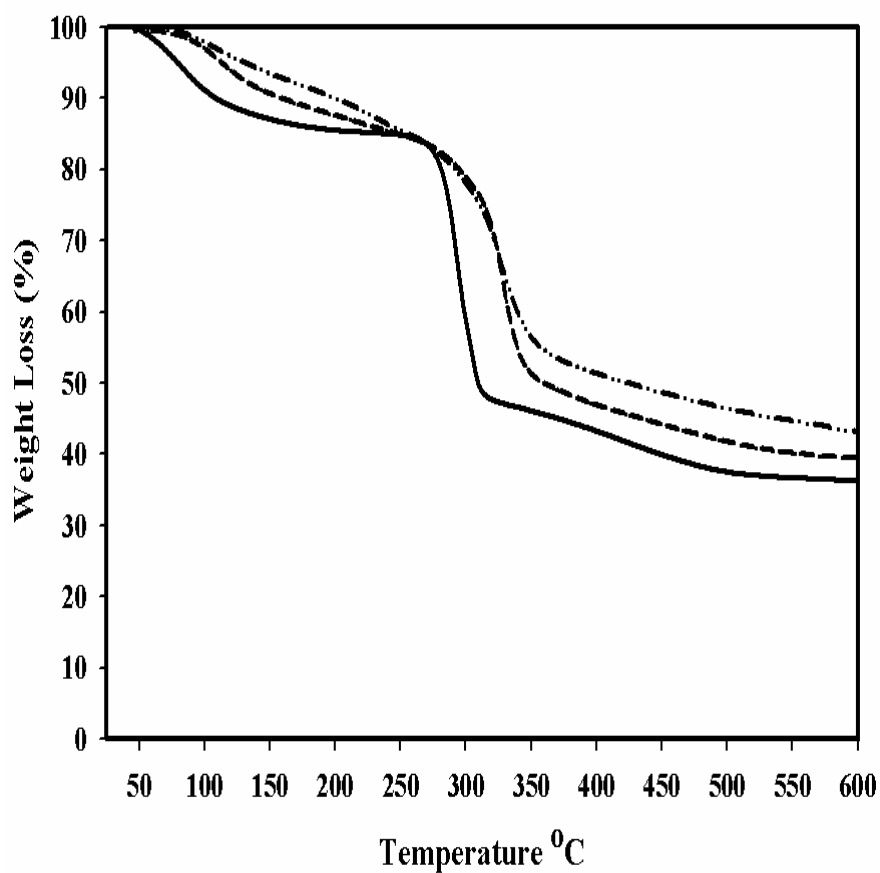


Figure (26): TGA diagram of (—) pure CMC and that mixed with 10 (wt%) ammonium per-sulfate at different irradiation doses of (.....) 40 kGy, (---) 120 kGy and (·-·-·-·) 200 kGy, (the dose rate is 6.7 kGy/h).

Table (7): The weight loss percent for pure chitosan and that mixed with 10 (wt%) ammonium per-sulfate at different irradiation doses of 40, 120 and 200 kGy.

Sample	Weight loss (%)				
	25-100 °C	100-200 °C	200-250 °C	250-300 °C	300-350 °C
Pure chitosan	6.2	10.8	11.7	29.5	52.5
Chitosan+APS at 40 kGy	6.5	12.51	13.4	30.3	50.2
Chitosan+APS at 120 kGy	5.9	13.6	21.5	41	51.8
Chitosan+APS at 200 kGy	6.1	16	26.1	40.8	50.5

Table (8): The weight loss percent for pure sodium alginate and that mixed with 10 (wt%) ammonium per-sulfate at different irradiation doses of 40, 120 and 200 kGy.

Sample	Weight loss (%)				
	25-100 °C	100-200 °C	200-250 °C	250-300 °C	300-350 °C
Pure Alginate	6.4	15.5	30.8	48.8	51.8
Alginate +APS at 40 kGy	4.5	16.5	32.2	46.4	49.5
Alginate +APS at 120 kGy	5.1	17.5	33.1	46.8	49.8
Alginate+APS at 200 kGy	5	17.8	33.4	46.5	49.5

Table (9): The weight loss percent for pure CMC and that mixed with 10 (wt%) ammonium per-sulfate at different irradiation doses of 40, 120 and 200 kGy.

Sample	Weight loss (%)				
	25-100 °C	100-200 °C	200-250 °C	250-300 °C	300-350 °C
Pure chitosan	6.9	14.4	15.1	30	53.6
CMC+APS at 40 kGy	6.5	13.7	16.7	31.4	52.3
CMC+APS at 120 kGy	5.9	13.6	16.9	32.3	51.8
CMC+APS at 200 kGy	4.2	12.1	17	32.7	48.1

IV.I.6.4- ESR Analysis

Figures (27, 28 and 29) show the ESR spectra of irradiated chitosan, sodium alginate and CMC, respectively in the presence and absence of 10 (wt%) ammonium per-sulfate (APS) or 10% H_2O_2 (v/w) after storing for 1, 8 and 15 day.

From the ESR data after storing for 1 day, it is obvious that, the intensity of free radicals formed for irradiated chitosan, sodium alginate and CMC, and those irradiated in the presence of with 10 (wt %) APS and 10% H_2O_2 (v/w) are the same.

After storing for 8 and 15 days of irradiation, the intensity of free radicals for these natural polymers irradiated in the presence of hydrogen peroxide still present with lower intensity if compared with that formed after 1day. The free radical intensity is higher than that for irradiated natural polymer in absence or presence of ammonium per-sulfate at the same dose. The intensity of free radicals for irradiated natural polymer in absence or presence of ammonium per-sulfate decreased and disappeared after storage for 8 days. This indicate that the radicals formed in the presence of hydrogen peroxide is successive and continuously. Again ESR studies for the irradiated samples revealed that the decay rate of the radicals formed during irradiation for the samples irradiated in the presence of hydrogen peroxide is much lower than that for samples irradiated in the presence of Ammonium per-sulfate.

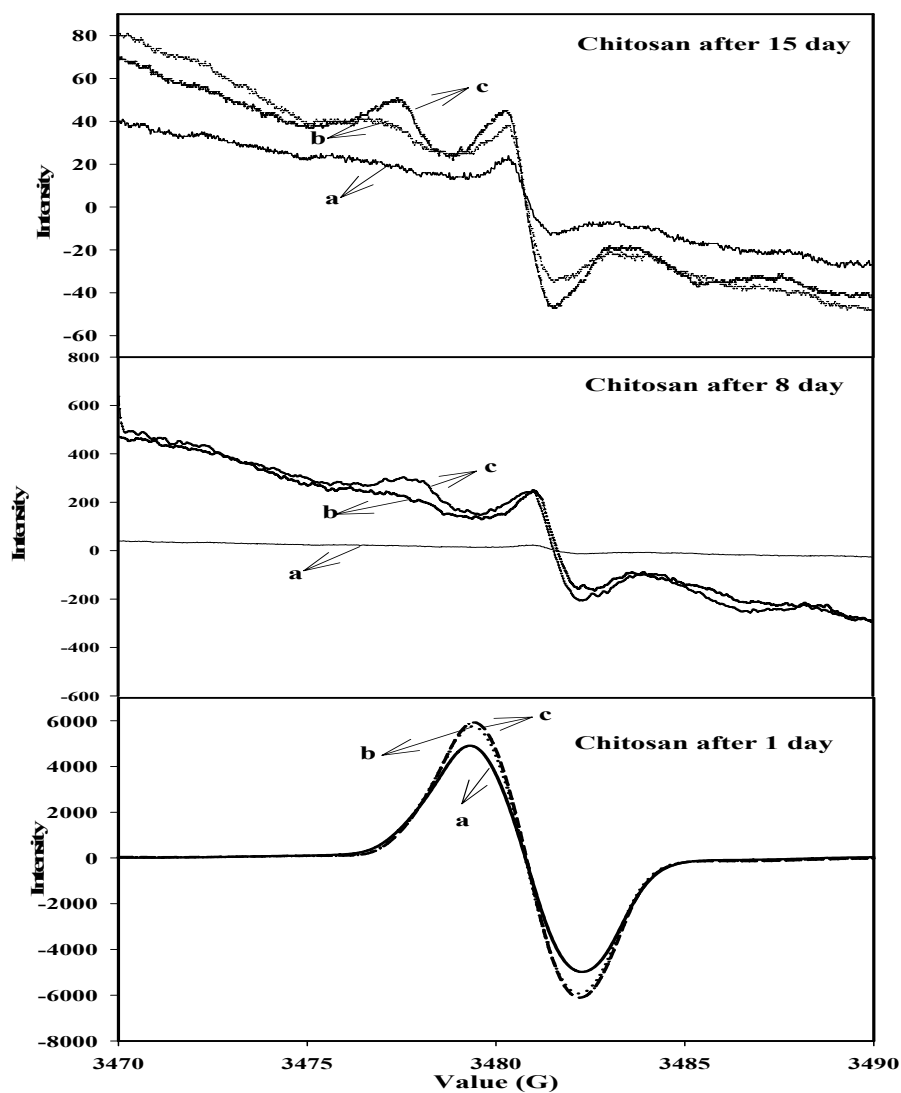


Figure (27): ESR spectrum of (a) pure chitosan irradiated at dose of 120 kGy and that mixed with (b) 10 (wt%) APS and (c) 10% H₂O₂ (v/w) at the same dose were measured after 1, 8 and 15 day, dose rate 6.7 kGy/h.

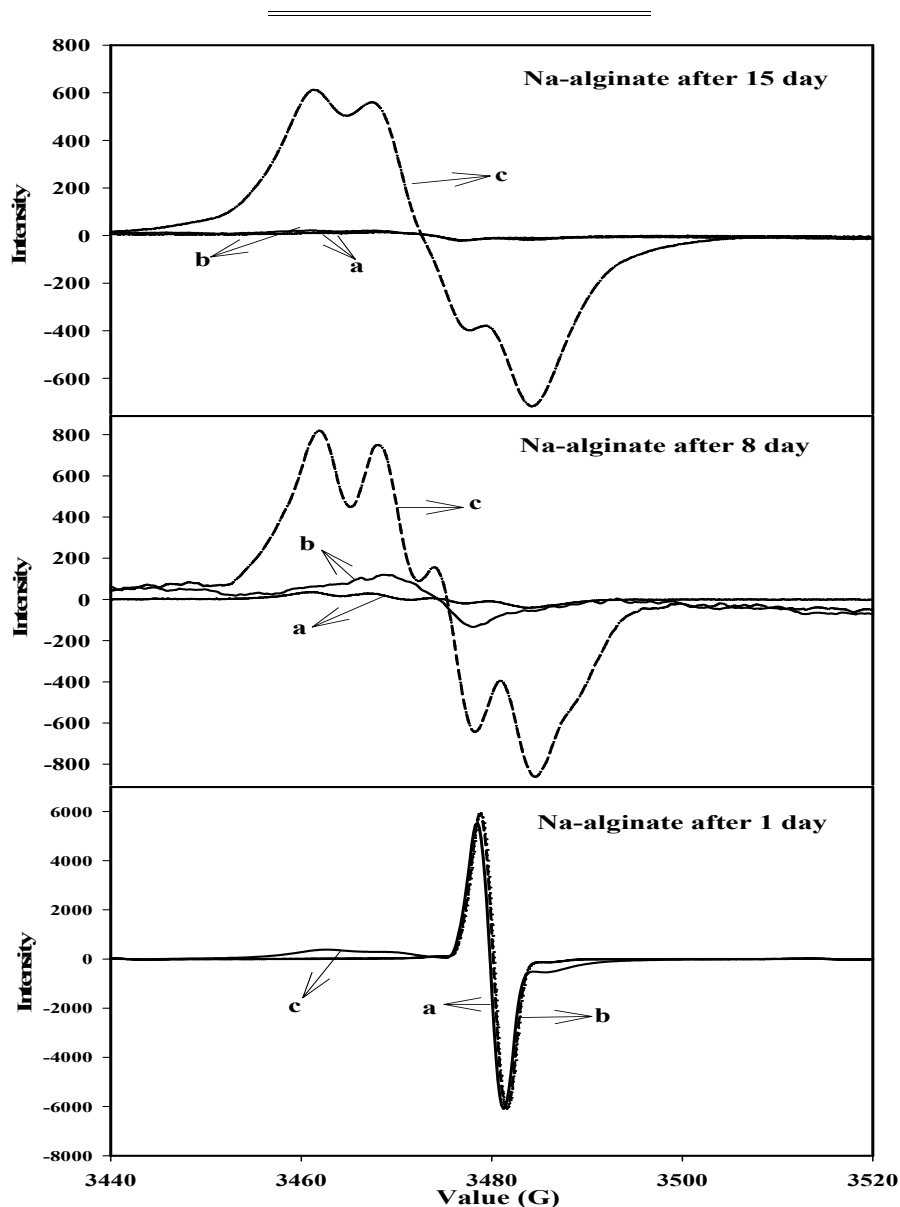


Figure (28): ESR spectrum of (a) pure sodium alginate irradiated at dose of 120 kGy and that mixed with (b) 10 (wt%) APS and (c) 10% H₂O₂ (v/w) at the same dose were measured after 1, 8 and 15 day, dose rate 6.7 kGy/h.

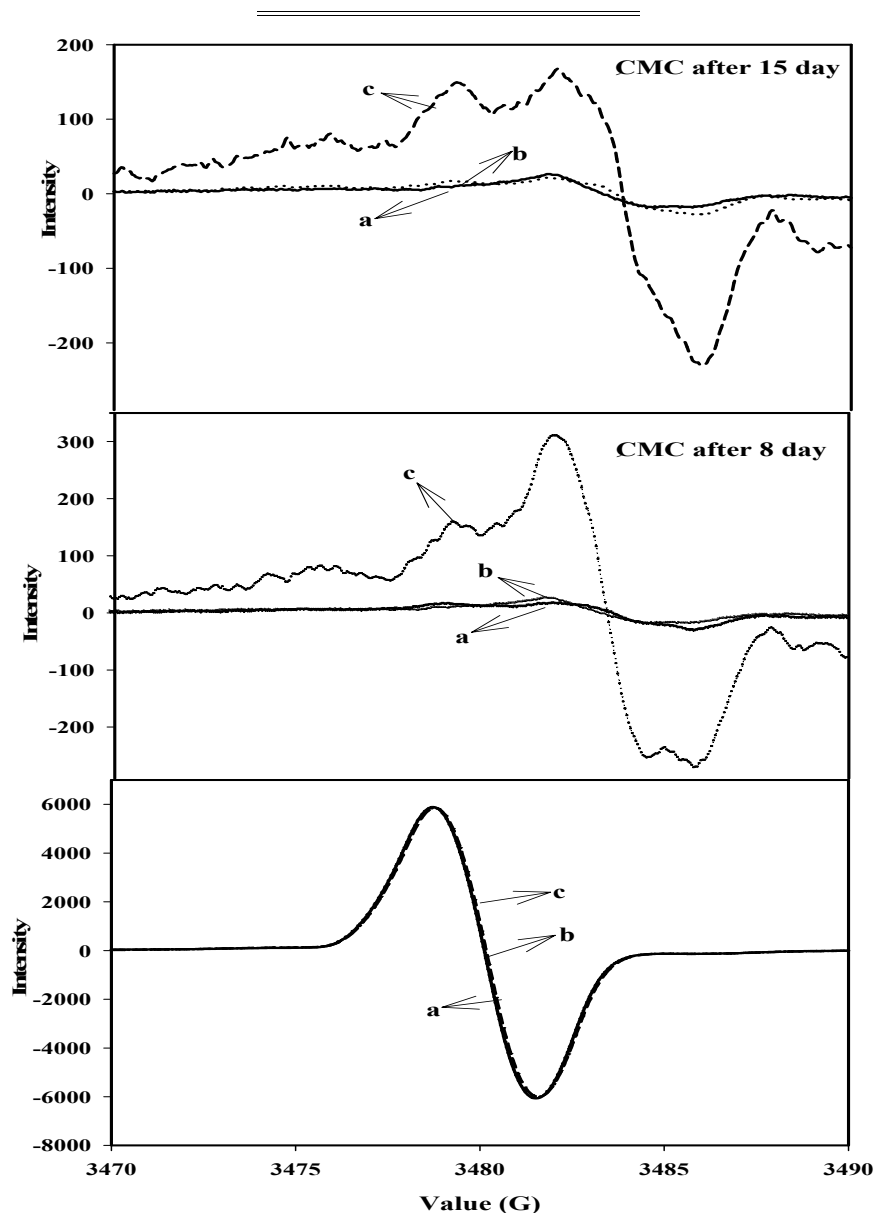


Figure (29): ESR spectrum of (—) pure CMC irradiated at dose of 120 kGy and that mixed with (...) 10 (wt %) APS and (---) 10% H₂O₂ (v/w) at the same dose were measured after 1, 8 and 15 day, dose rate 6.7 kGy/h.

IV.I.7- Applications of Degraded Naturally Occurring Polymers as Growth Promoters in Agricultural Purposes

Degraded sodium alginate and chitosan could be used in agriculture purposes as growth promoters for plants. The growth and other responses of zeamais plants that were treated with irradiated sodium alginate or chitosan of different molecular weights were investigated as in Figures (30, 31, 32 and 33). The test field results in Figure (30) showed that the treatment of the zeamais plant with the irradiated sodium alginate at doses 120, 160, and 200 kGy in the presence of APS results in increasing in plant growth. Meanwhile, the results of the test field in Figure (32) showed that the treatment of the zeamais plant with irradiated chitosan from 80 to 160 kGy enhances not only the plant growth but also the productivity. The increase in plant performance by using degraded alginate or chitosan suggested its possible use in agriculture purposes as growth promoters.

Figures (31 and 33) show the effect of sodium alginate or water soluble chitosan, respectively on the corn cob. It is clear that the zeamais cob size of plant irradiated at 200 kGy in the presence of 10% APS at 200 kGy is much higher than that treated with sodium alginate irradiated at 200 kGy and untreated plant (control)

Tables (10 and 11) describe plant height (cm), ear height (cm), ear length (cm), 100 grain weight (g), grain weight/ ear (g), biological yield fad. (ardab), straw yield fad. (ardab),

grain yield fad. (ardab), total protein (%) and total oil (%) of zea maize yield plants, respectively with spraying the plant by 100 ppm of sodium alginate or water soluble chitosan, respectively. It is obvious from Table (10) that the treatment of zea maize plant by sodium alginate and that mixed with 10 (wt%) APS irradiated at 200 kGy irradiation doses have positive effect on grain yield (ardab/fad) which gives grain yield of 30.41 (ardab/fad) if compared with control plant which gives 21.77 (ardab/fad), high plant height of 229.6 cm if compared with control one which gives 116.5 cm. Also, it is obvious from Table (11) the treatment of maize plant chitosan and that mixed with 10 (wt%) APS irradiated at 120 kGy has positive effect on grain yields (ardab/fad), respectively which gives zea maize grain yield of 25.79 (ardab/fad) if compared with control one which gives 18.58 (ardab/fad), high plant height of 210.1 cm if compared with control plant which gives 113.9 cm.

Also, degraded sodium alginate and chitosan could be used in agriculture purposes as growth promoters for plants. The growth and other responses of faba bean plant that treated with irradiated sodium alginate or chitosan of different molecular weights were investigated as in Figures (34 and 35). The test field results in Figure (34) showed that the treatment of the faba bean plant with the irradiated sodium alginate at doses 120, 160, and 200 kGy in the presence of APS results in increasing in plant growth. Meanwhile, the results of the test field in Figure (35) showed that the treatment of the faba bean plant with

irradiated chitosan from 80 to 160 enhances not only the plant growth but also the productivity. The increase in plant performance by using degraded alginate or chitosan suggested its possible use in agriculture purposes as growth promoters.

Tables (12 and 13) describe plant height (cm), number of pods/ plant, number of pods/ plant/ m², number of plant / m², 100 seed weight (g), biological yield fad. (ardab), straw yield fad. (ardab) and seed yield/ fad.(ardab) of seeds yield of faba bean plants, respectively with spraying the plant by 100 ppm of sodium alginate or water soluble chitosan, respectively.

It is obvious from Tables (12) that the treatment of faba bean by plant sodium alginate and that mixed with 10 (wt%) APS irradiated at 200 kGy irradiation doses have positive effect on seed yield (ardab/fad), respectively which gives seed yield of 11.92 (ardab/fad) if compared with control plant which gives 8.7 (ardab/fad), high plant height of 130.85 cm if compared with control plant which gives 99.51 cm. Also, the treatment of faba bean plant by degraded chitosan and that mixed with 10 (wt%) APS irradiated at 120 kGy has positive effect on seed yields (ardab/fad) which gives faba bean seed yield of 10.72 (ardab/fad) if compared with control plant which gives 8.7 (ardab/fad) , high plant height of 125.18 cm if compared with control plant which gives 99.51 cm.

Nguyen et al. (2000) showed that the growth of rice at various concentrations of degraded alginate that a suitable

range concentration is 20 ± 50 ppm. *Tomoda et al. (1994)* have found much a higher concentration (1000 ppm) of degraded alginate prepared by degradation of enzymatic lyases to obtain the plateau of growth-promotion of barley roots. Also *Natsume et al. (1994)* have also used a very high concentration (600 ppm) to recognize the effect on growth promotion. In addition the chitosan acts as antifungal compound, *Pospieszny et al. (1991)* and *Bautista-Banos et al. (2003)* confirmed unequivocally that a minor amount of chitosan has profound effects on the growth and development of orchid plant tissue. Chitosan has a unique combination of attractive characteristics: it stimulates plant growth, provides plant protection and environmental friendly being of biological origin and is easy biodegradable by soil microorganisms. The unique combination of these properties makes chitosan to be a very useful bio-control agent with a large perspective for horticulture in general and orchid culture in particular.

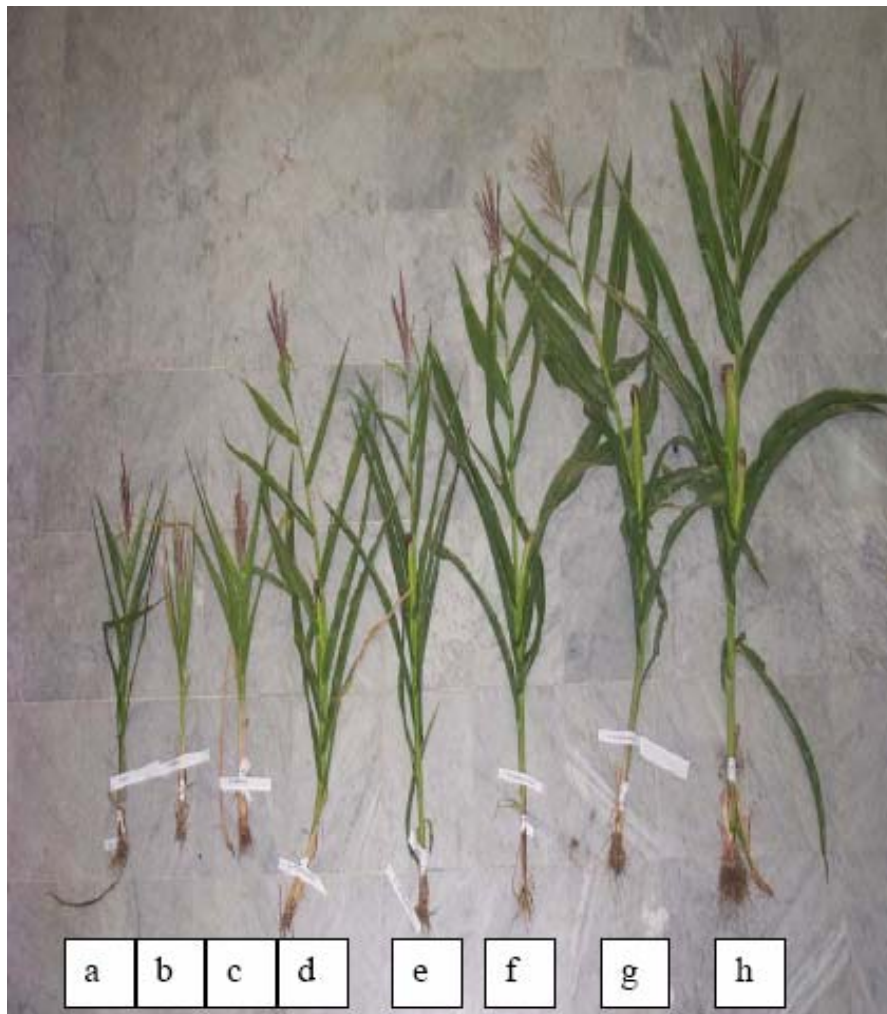


Figure (30): Effect of degraded sodium alginate on growth of zea maize plant: (a) control and spraying the plant by 100 ppm of sodium alginate solution in water, (b) pure one, (c) pure one irradiated at 200 kGy and that mixed with 10 % APS at different irradiation doses of (d) 40 kGy, (e) 80 kGy, (f)

120 kGy, (g) 160 kGy and (h) 200 kGy, (the dose rate is 6.7 kGy/h).



Figure (31): Growth of zea maize cob yield size (a) control and that sprayed by 100 ppm of sodium alginate (b) irradiated at 200 kGy and (c) mixed with 10% APS at 200 kGy, (the dose rate is 6.7 kGy/h).

Table (10): Effect of spraying 100 ppm of sodium alginate and that mixed by 10% wt APS at different irradiation doses on crop yield of zea maize plants.

Factor Treatment	Plant height (cm)	Ear height (cm)	Ear length (cm)	100 grain Wt (g)	Grain wt/ear (g)	Biological yield fad. (ardab)	Straw yield fad. (ardab)	Grain yield/ fad. (ardab)	Total protein %	Total Oil %
Control	116.5	79.03	17.71	27.38	139.7	46.24	24.47	21.77	8.85	4.480
Blank	116.3	78.92	17.69	27.31	139.1	45.61	24.33	21.28	8.73	4.22
40 kGy	116.1	79	17.69	27.24	138.8	45.70	24.27	21.43	7.99	4.55
With APS at 40 kGy	221.4	94.26	19.89	29.42	163.8	52.18	26.97	25.21	9.06	4.58
With APS at 80 kGy	222.4	95.47	20.17	31.11	164.9	53.08	27.43	25.65	9.17	4.61
With APS at 120kGy	223.5	96.47	20.51	32.33	166.7	55.94	29.17	26.77	9.39	4.67
With APS at 160kGy	227.6	98.28	20.89	33.54	170.4	60.43	31.51	28.92	9.43	4.75
With APS at 200kGy	229.6	100.03	21.49	34.85	199.1	63.52	33.11	30.41	9.47	4.87



Figure (32): Effect of degraded chitosan on growth of maize plant: (a) control and spraying the plant by 100 ppm of chitosan solution in water, (b) pure one, (c) pure one irradiated at 200 kGy and that mixed with 10 % APS at different irradiation doses of (d) 40 kGy, (e) 80 kGy, (f) 120 kGy, (g) 160 kGy and (h) 200 kGy, (the dose rate is 6.7 kGy/h).



Figure (33): Growth of zea maize cob yield size (a) control and that mixed with 100 ppm of chitosan, (b) irradiated at 200 kGy and (c) treated with 10% APS at 200 kGy, (the dose rate is 6.7 kGy/h).

Table (11): Effect of spraying 100 ppm of chitosan and that mixed by 10% wt APS at different irradiation doses on crop yield of zea maize plants.

Factor Treatment	Plant height (cm)	Ear height (cm)	Ear length (cm)	100 grain Wt (g)	Grain wt/ear (g)	Biological yield fad. (ardab)	Straw yield fad. (ardab)	Grain yield/ fad. (ardab)	Total protein %	Total Oil %
Control	113.9	70.32	16.55	27.33	128.7	41.97	23.39	18.58	8.73	4.42
Blank	113.3	70.13	16.47	27.09	128.3	41.92	23.55	18.37	8.66	4.33
100 kGy	113.7	70.21	16.51	27.31	128.1	41.71	23.27	18.44	8.47	4.15
With APS at 40 kGy	203.	85.31	17.99	30.45	141.8	45.06	24.19	20.87	9.02	4.5
With APS at 80 kGy	209	87.23	18.99	32.99	155.2	51.04	27.37	23.67	9.36	4.67
With APS at 120kGy	210.1	91.37	19.65	34.01	157.1	54.34	28.55	25.79	9.44	4.71
With APS at 160kGy	204.7	88.91	18.51	31.83	152.2	51.69	27.66	24.03	9.40	4.58
With APS at 200kGy	203.4	86.11	18.32	29.29	142.8	50.09	26.48	23.61	9.13	4.53

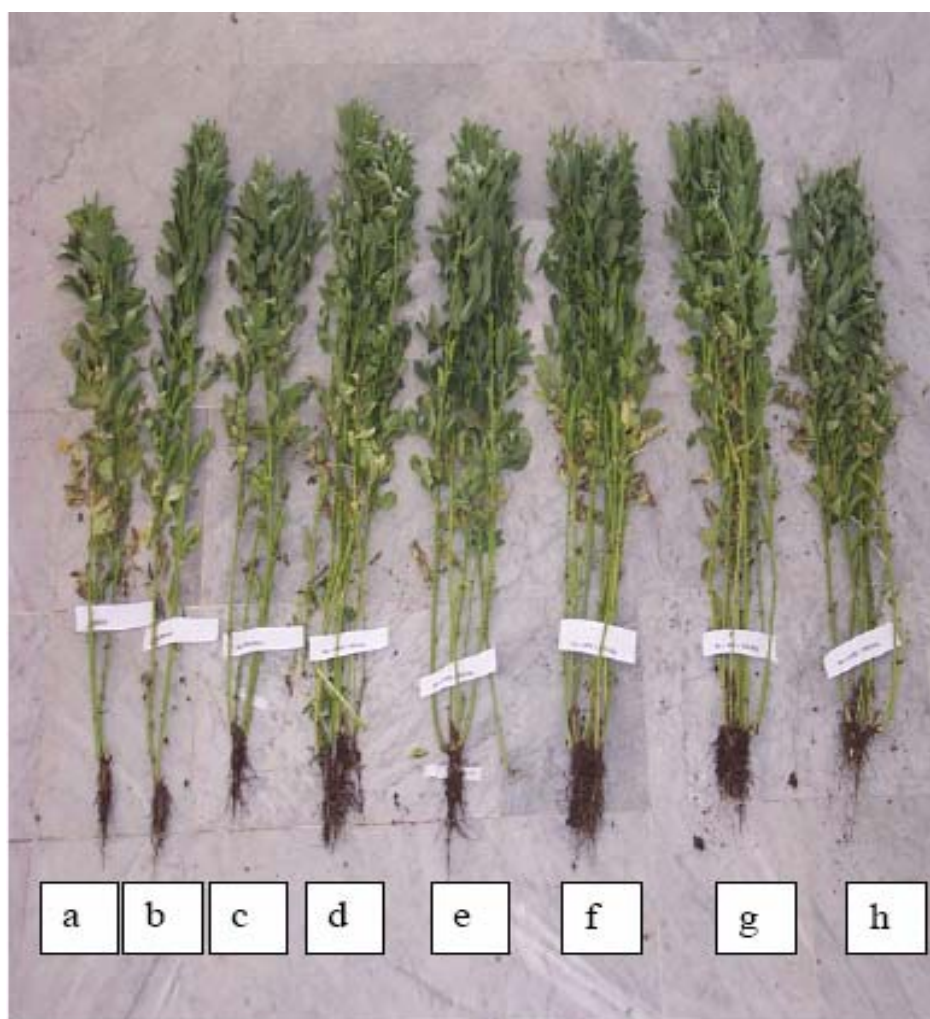


Figure (34): Effect of degraded sodium alginate on growth of soybean plant: (a) control and spraying the plant by 100 ppm of sodium alginate solution in water, (b) pure one, (c) pure one irradiated at 200 kGy and that mixed with 10 % APS at different irradiation doses of (d) 40 kGy, (e) 80 kGy, (f) 120 kGy, (g) 160 kGy and (h) 200 kGy, (the dose rate is 6.7 kGy/h).

Table (12): Effect of spraying 100 ppm of sodium alginate and that mixed by 10 (wt%) APS at different irradiation doses on crops yield of faba bean plants.

Factor Treatment	Plant height (cm)	No. of Pods/ plant	No. of Pods/ Plant/ m ²	No. of plant / m ²	100 seed wt (g)	Biological yield fad. (ardab)	Straw yield fad. (ardab)	Seed yield/ fad. (ardab)
Control	99.51	19.52	183	37.74	57.25	23.9	15.2	8.7
Blank	98.63	19.34	181	37.22	56.73	23.7	15.05	8.65
γ 0.0 kGy	98.57	19.33	181	37.19	56.7	23.77	15.11	8.66
With APS at 40 kGy	105.79	20.75	197	41.45	60.94	25.72	16.31	9.41
With APS at 80 kGy	115.03	22.56	218	46.9	66.38	29.19	19.21	9.98
With APS at 120kGy	126.85	24.88	245	53.88	73.33	31.05	20.63	10.42
With APS at 160kGy	128.14	25.13	248	54.64	74.09	32.75	21.73	11.02
With APS at 200kGy	130.85	27.62	277	62.14	81.56	34.04	22.11	11.92

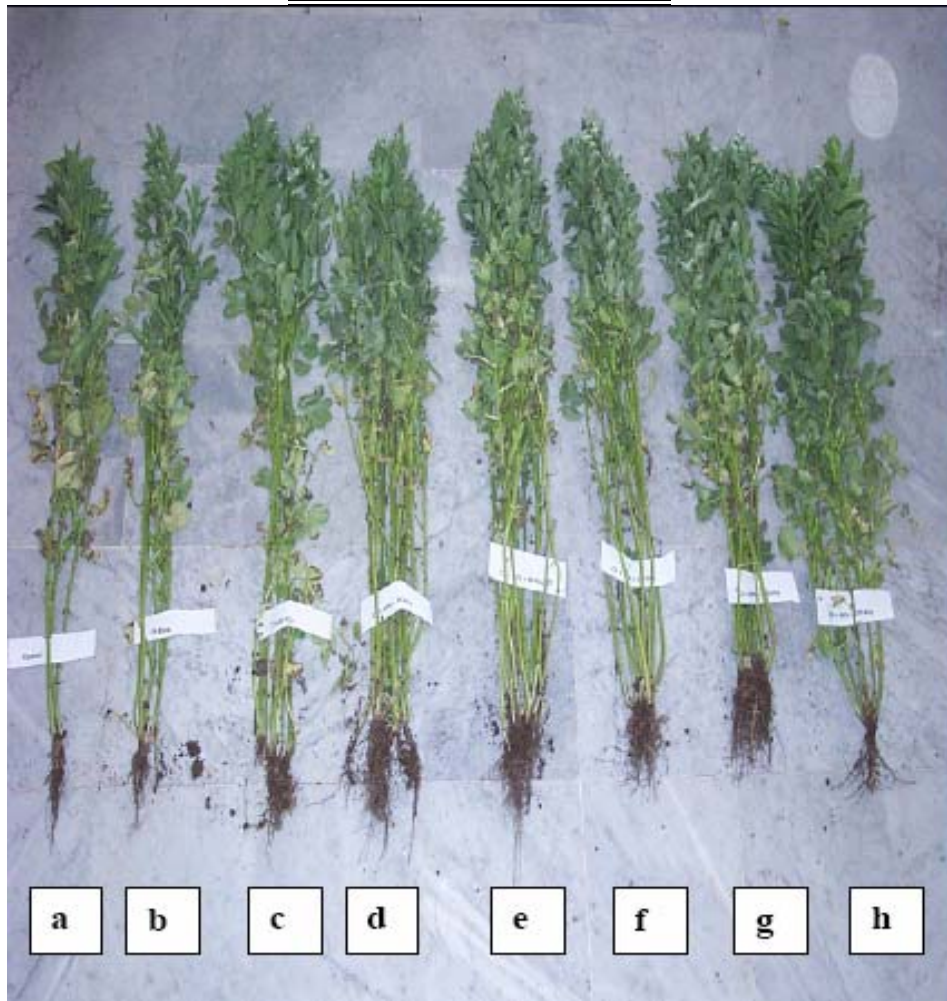


Figure (35): Effect of degraded chitosan on growth of faba bean plant: (a) control and spraying the plant by 100 ppm of chitosan solution in water, (b) pure one, (c) pure one irradiated at 200 kGy and that mixed with 10 % APS at different irradiation doses of (d) 40 kGy, (e) 80 kGy, (f) 120 kGy, (g) 160 kGy and (h) 200 kGy, (the dose rate is 6.7 kGy/h).

Table (13): Effect of spraying 100 ppm of chitosan and that mixed by 10 (wt%) APS at different irradiation doses on crop yield of faba bean.

Factor Treatment	Plant height (cm)	No. of Pods/ plant	No. of Pods/ Plant/ m ²	No. of plant / m ²	100 seed wt (g)	Biological yield fad. (ardab)	Straw yield fad. (ardab)	Seed yield/ fad. (ardab)
Control	99.51	17.92	164	32.94	52.47	22.98	14.87	7.71
Blank	90.13	17.68	162	32.2	51.73	22.83	14.77	8.06
100 kGy	90.24	17.7	162	32.27	51.79	22.82	14.71	8.11
With APS at 40 kGy	111.53	21.87	210	44.84	64.32	24.13	15.19	8.94
With APS at 80 kGy	121.61	23.85	233	50.79	70.25	28.58	18.71	9.87
With APS at 120kGy	125.18	24.55	241	52.9	72.35	32.34	21.62	10.72
With APS at 160kGy	117.91	23.12	225	48.6	68.07	41.31	31.69	9.62
With APS at 200kGy	109.98	21.572	207	43.92	63.41	39.15	30.07	9.08

IV.II- Radiation Graft Copolymerization of VAc/ HEMA Binary Monomer Onto poly(tetraflouroethylene-perflourovinyl ether) (PFA) Films

Grafting of vinyl acetate (VAc), 2-hydroxyethyl methacrylate (HEMA) and their binary monomer onto poly (tetraflouroethylene-perflourovinyl ether) (PFA) films were performed by means of gamma rays from ^{60}Co and a dose rate of 1.85 Gy/s using the direct method. The factors affecting the grafting yield such as type of solvent, inhibitor concentration, monomer and comonomer concentrations, comonomer composition and irradiation dose were investigated.

IV.II.1- Effect of Preparation Conditions on the Grafting Yield***IV.II.1.1- Effect of Solvent***

Figure (36) shows a schematic diagram for the effect of different solvents on the degree of grafting of VAc/HEMA binary monomers onto PFA films using 50% comonomer concentration, (50:50) comonomer composition, irradiation dose 30 kGy, and dose rate 1.85 Gy/s. It is clear that the high degree of grafting is obtained when using methanol as a solvent for this binary monomers/solvent-mixture as compared with the other solvents used.

Solvents are used in radiation grafting experiments to enhance the degree of accessibility of monomer to grafting sites within the polymer and brought about by the ability of the added solvent to swell the base polymer and to enhance the

efficiency and uniformity of the grafting. Almost all solvents are capable of free radical reactions by radiolysis and it is difficult to find inert solvents for radiation-induced polymerization. The formation constant for the solvent-monomer complex may be larger than that for the comonomer complex and would be expected to influence the reactivity of the monomer in the propagation reactions, thus affecting the overall copolymerization behavior **Ratzsch (1988)**.

IV.II.1.2- Effect of Inhibitor Concentration

Figure (37) shows the effect of inhibitor concentration on the degree of grafting of VAc/HEMA binary monomers onto PFA films using methanol as a solvent, 50% comonomer concentration, (50:50) comonomer composition, irradiation dose 30 kGy, and dose rate 1.85 Gy/s.

Attempts were made to use selective inhibitors such as Mohr's salt (ammonium ferrous sulfate) and ferric chloride to minimize the homo-polymerization occurring in the grafting system. Mohr's salt is insoluble in methanol so FeCl_3 can be used. It was observed that the degree of grafting is shown to increase and reach the maximum grafting yield at 0.1 (wt %) then tend to decrease again with increasing the inhibitor concentration.

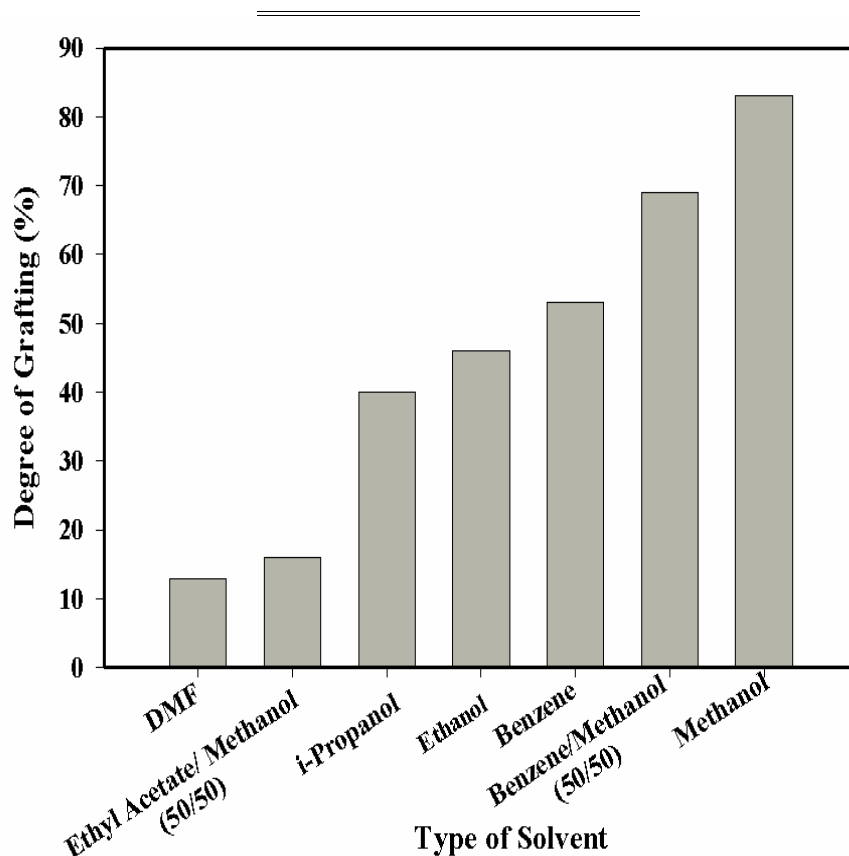


Figure (36): Schematic diagram for the effect of different solvents as a function of the degree of grafting of VAc/HEMA binary monomers onto PFA films using 50% comonomer concentration, (50:50) comonomer composition, irradiation dose 30 kGy, and dose rate 1.85 Gy/s.

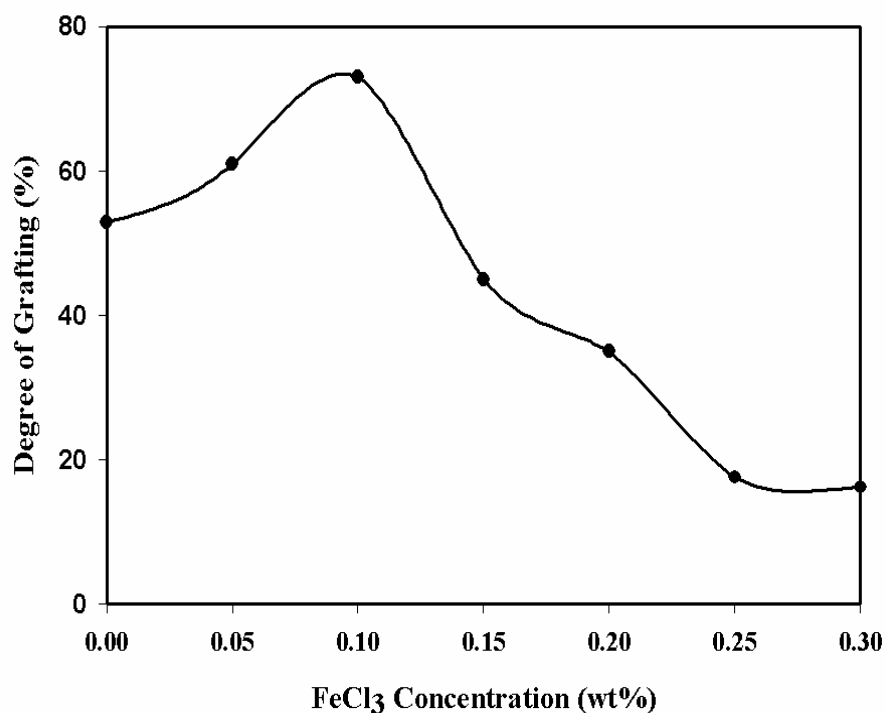


Figure (37): Effect of inhibitor concentration on the degree of grafting of VAc/HEMA binary monomers onto PFA films using methanol as a solvent, 50% comonomer concentration, (50:50) comonomer composition, irradiation dose 30 kGy, and dose rate 1.85 Gy/s.

II.1.3- Effect of Monomer and Comonomer Concentrations***IV.II.1.3.1- Effect of Monomer Concentration***

Figure (38) shows the effect of monomer concentration on the degree of grafting of VAc and HEMA monomers onto PFA films using methanol as a solvent, 0.1 (wt %) FeCl_3 as inhibitor, irradiation dose 30 kGy and dose rate 1.85 Gy/s. It was found that the degree of grafting tend to increase with increasing the VAc and HEMA monomer concentration till reaches the maximum grafting yield at 70% and 50% for VAc and HEMA monomer concentration, respectively.

IV.II.1.3.2. Effect of Comonomer Concentration

Figure (39) shows the effect of comonomer concentration on the degree of grafting of VAc/ HEMA binary monomers onto PFA films using methanol as a solvent, 0.1 (wt%) FeCl_3 as inhibitor, (50:50) comonomer composition, irradiation dose 30 kGy and dose rate 1.85 Gy/s. The influence of comonomer concentration on the grafting process may affect its kinetic parameters. Solvent which will favor the diffusion, might also promote the diffusion of the comonomer to increase the degree of grafting. Diffusibility of the monomers into the polymer matrix has a great effect on the grafting process and grafting yield.

It was observed that the degree of grafting tend to increase with increasing the comonomer concentration with respect to the solvent to reach the maximum grafting yield at 80% comonomer concentration in methanol. Further increase in the

comonomer ratio with respect to solvent leads to a decrease in the degree of grafting. The occurrence of a maximum grafting yield at a certain monomer concentration has been observed in different grafting systems *Beddows et al. (1986)*. This has been attributed to Trommsdorff-type effect *Dilli and Garnett (1967)* whereby, as the viscosity of the grafting medium increases due to monomer being converted to polymer, mutual termination between two growing macroradical chains is inhibited more than in the propagation reaction. The termination reaction involves two long slowly moving chains which can become entangled, while the propagation reaction involves one such long chain and movable monomer molecule. At high concentration of comonomer, propagation tends to decrease whilst termination increases due to the solid homopolymer formation and the grafting yield consequently decreased. This explains the occurrence of maximum in the grafting yield versus comonomer concentration. Also, at high comonomer concentration (80%), a great number of molecules are available to react with the free radicals on backbone of the polymer chains. Alternatively, it also favors the production of large number of growing chains which increase the possibility of H-abstraction via chain transfer to give rise to the substrate macroradicals. This leads to increased chain propagation resulting in a greater degree of grafting.

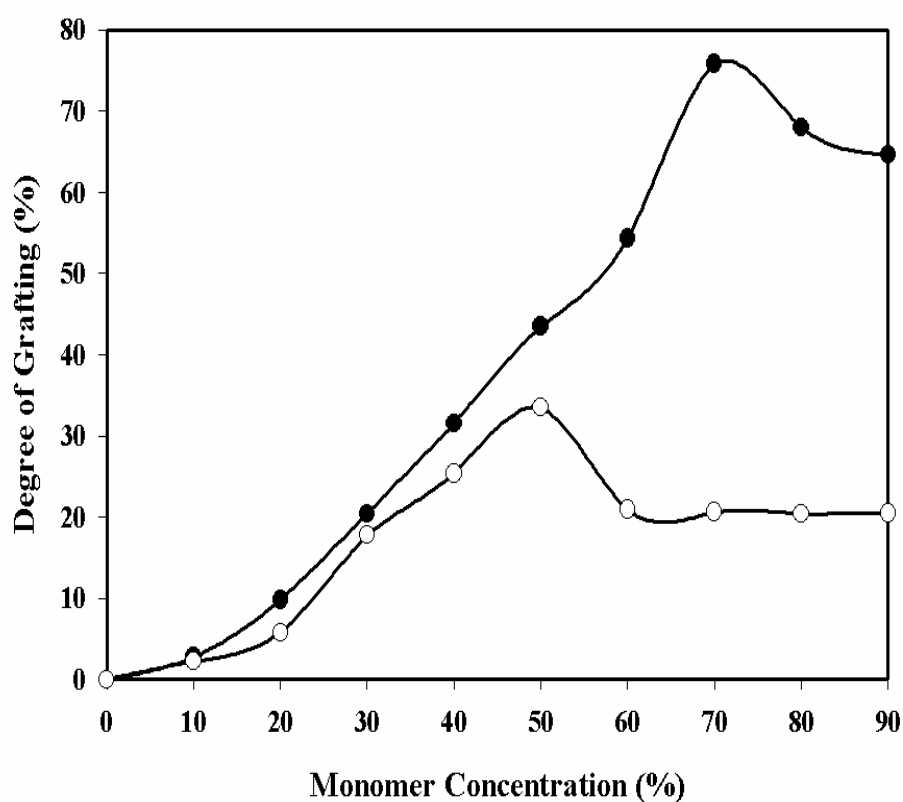


Figure (38): Effect of monomer concentration on the degree of grafting of (●) VAc and (○) HEMA monomers onto PFA films using methanol as a solvent, 0.1 (wt%) FeCl_3 as inhibitor, irradiation dose 30 kGy and dose rate 1.85 Gy/s.

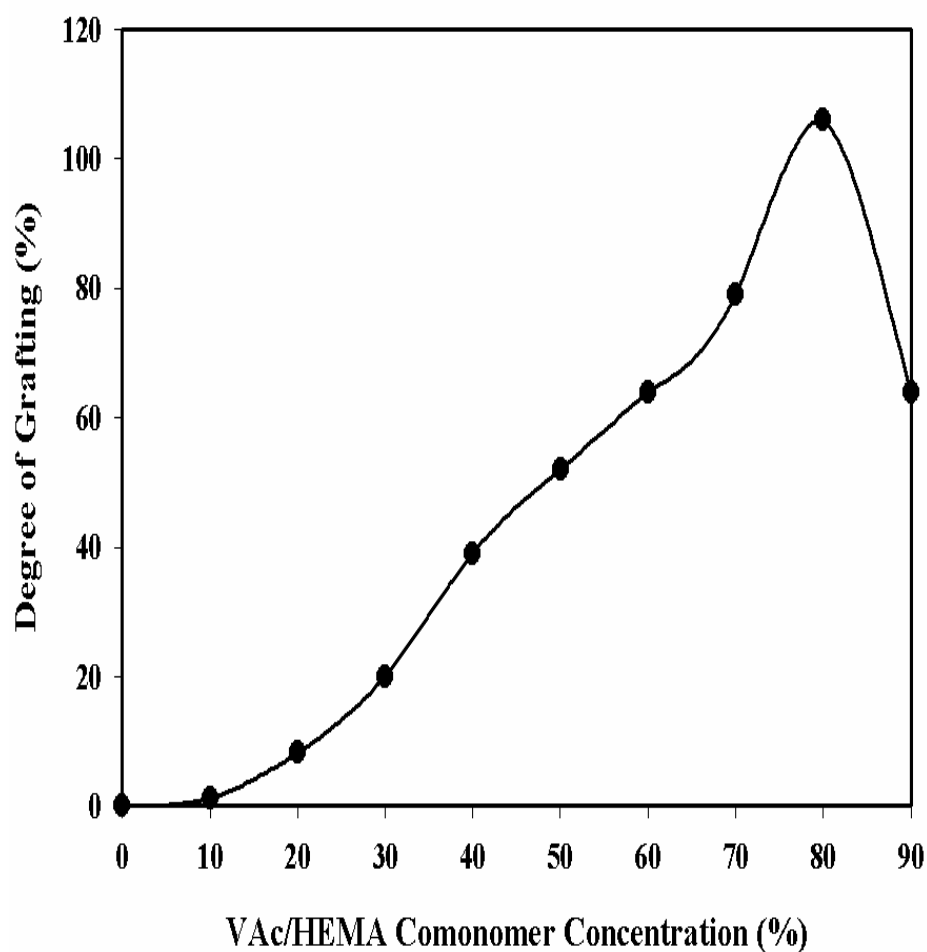


Figure (39): Effect of comonomer concentration on the degree of grafting of VAc/HEMA binary monomers onto PFA films using methanol as a solvent, 0.1 (wt%) FeCl_3 as inhibitor, (50:50) VAc/ HEMA comonomer composition, irradiation dose 30 kGy and dose rate 1.85 Gy/s.

IV.II.1.4- Effect of Comonomer Composition

Figure (40) shows the degree of grafting as a function of VAc / HEMA comonomer composition in methanol at 30 kGy and a dose rate of 1.85 Gy/sec. The degree of grafting is shown to increase with comonomer composition up to 70/30 (v/v) and then tend to decrease with increasing HEMA in VAc / HEMA comonomer composition. Therefore, it is expected that one of binary monomers may enhance the grafting percent. It was found that the maximum grafting yield at VAc / HEMA comonomer composition ratios of 70/30. Thus, the results suggest that the presence of VAc in the comonomer feed solution which enhanced the extent of grafting of HEMA. The magnitude of the enhancement depend on the VAc / HEMA ratio in the comonomer feed solution; the grafting yield was higher when VAc-rich comonomer feed solution is used. Lower grafting yields obtained when the HEMA- rich comonomer feed solutions were used can be interpreted according to the poor tendency of HEMA towards homopolymerization. The excess amount of HEMA acts as a retarding agent for the copolymerization process by trapping the energy of radiation.

IV.II.1.5- Effect of Irradiation Dose

Figure (41) shows the effect of irradiation dose on the degree of grafting of VAc/ HEMA binary monomers onto PFA films using methanol as a solvent, 0.1 (wt%) FeCl₃ as an inhibitor, 50% comonomer concentration, (70:30) comonomer composition and irradiation dose rate 1.85 Gy/s. It was found that the degree of grafting increases with increasing the irradiation dose till reaches 30 kGy and it tends to level off at higher doses. Increasing the grafting yield with the irradiation

dose can be attributed to the increase of active sites. The acceleration occurs at doses ranging from 10 to 30 kGy. The grafting yield tends to level off due to the recombination of free radicals formed without initiating new sites for grafting. Meanwhile, a high homopolymer is formed at such high doses and the diffusion of the comonomer is restricted.

From these results, it can be assumed that the increase in dose resulted in increasing the concentration of free radicals in the polymer substrate as well as in the comonomer binary system. Therefore, a steady increase in the grafting yield is observed for all comonomer compositions, in which the higher the comonomer concentration, the higher the degree of grafting is obtained at a given irradiation dose.

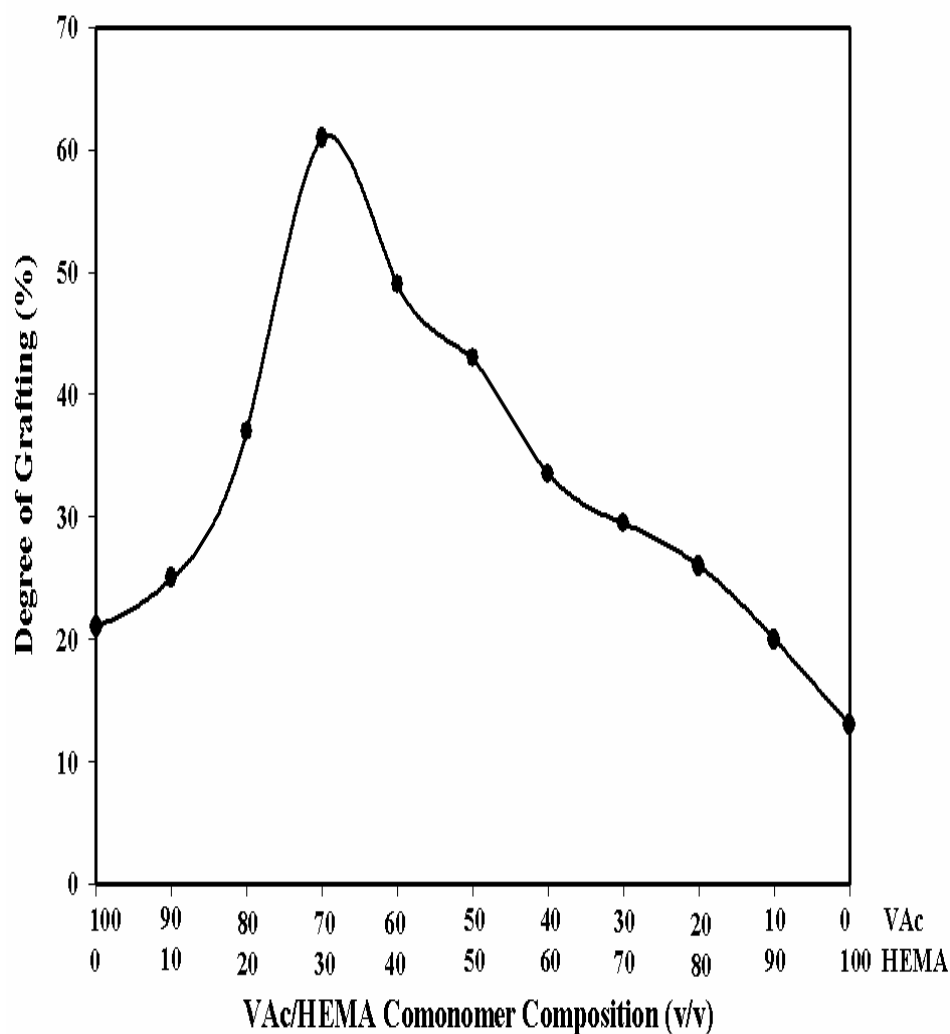


Figure (40): Effect of comonomer composition on the degree of grafting of VAc/HEMA binary monomers onto PFA films using methanol as a solvent, 0.1 (wt %) FeCl_3 as inhibitor, 50% comonomer concentration, irradiation dose 30 kGy and irradiation dose rate 1.85 Gy/s.

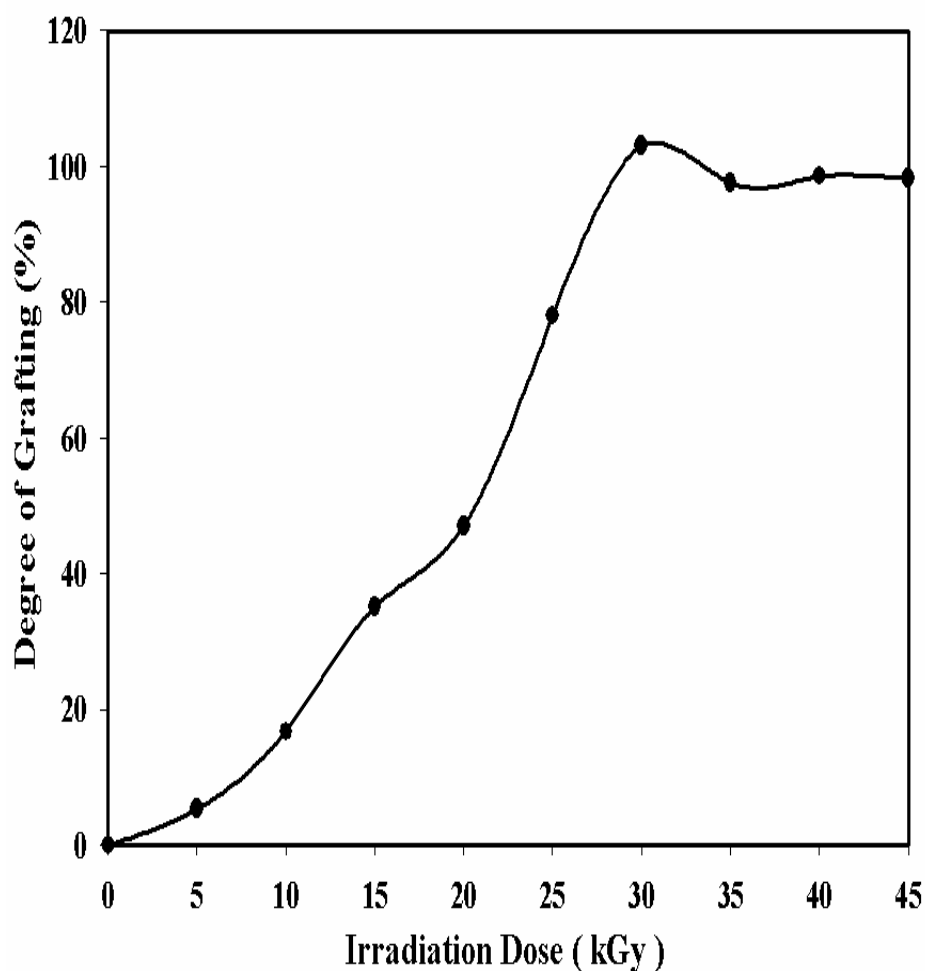


Figure (41): Effect of irradiation dose on the degree of grafting of VAc/HEMA binary monomers onto PFA films using methanol as a solvent, 0.1 (wt %) FeCl_3 as inhibitor, 50% comonomer concentration, (70/ 30) VAc/ HEMA comonomer composition, respectively and irradiation dose rate 1.85 Gy/s.

IV.II.2- Characterization of the Grafted Membranes

To elucidate the possibility of the practical uses of the grafted copolymer membranes obtained by the radiation grafting of VAc/ HEMA binary monomers onto PFA films.

IV.II.2.1- FTIR Spectroscopy

Figure (42) shows the FTIR spectra of trunk PFA (spectrum a), PFA-g-pVAc (spectrum b), PFA-g-pHEMA (spectrum c) and its graft copolymer PFA-g-p(VAc/HEMA) (spectrum d). It was shown that there is a characteristic beak at $1400\text{-}1000\text{ cm}^{-1}$ due to $\nu(\text{C-F})$ bond. Also there is a new characteristic beak at 1730 cm^{-1} due to $\nu(\text{C=O})$ as shown in all spectrum except (spectrum a) due to the grafting by VAc monomer and this absorption band increased with the grafting by HEMA monomer (spectrum b, c, and d). The absorption band at 2950 cm^{-1} is due to the $\nu(\text{C-H})$ stretching and there is broad band at $3600\text{-}3200\text{ cm}^{-1}$ due to hydroxyl group of HEMA monomer (spectrum c) and this broad band increased by the increase in grafting yield of copolymer (spectrum d).

IV.II.2.2- Mechanical Analysis

Figure 43 (A and B) shows the change in elongation at break percent and tensile strength (MPa), respectively as a function of monomer concentration of grafted PFA films by VAc and HEMA using methanol as a solvent, 0.1 (wt %) FeCl_3 inhibitor, irradiation dose 30 kGy and dose rate 1.85 Gy/s. It is obvious from Figure (43A) that the elongation at break percent increase with increasing the concentration VAc monomer and decreasing with increasing the HEMA

concentration in the grafting process till reach elongation at break percent 118 and 3.32 % at 90 % VAc and/or HEMA monomer concentration, respectively. Also Figure (43B) show the tensile strength (MPa) increases with increasing the monomer concentration then decrease again at 50% and 30% monomer concentration for VAc and MEHA monomers, respectively.

Figure 44 (A and B) shows the changes in elongation at break percent and tensile strength (MPa), respectively with VAc/HEMA comonomer composition of grafted PFA films. It is obvious from that elongation at break percent and tensile strength increase with increasing the VAc concentration in VAc/HEMA comonomer composition till reach elongation 289 % and 28.6 MPa tensile strength at (90/10) VAc/HEMA comonomer composition, respectively. The results suggest that the grafting of VAc/HEMA onto PFA matrix results in crosslinked materials of network structure and improving both elongation at break percent and tensile strength (MPa).

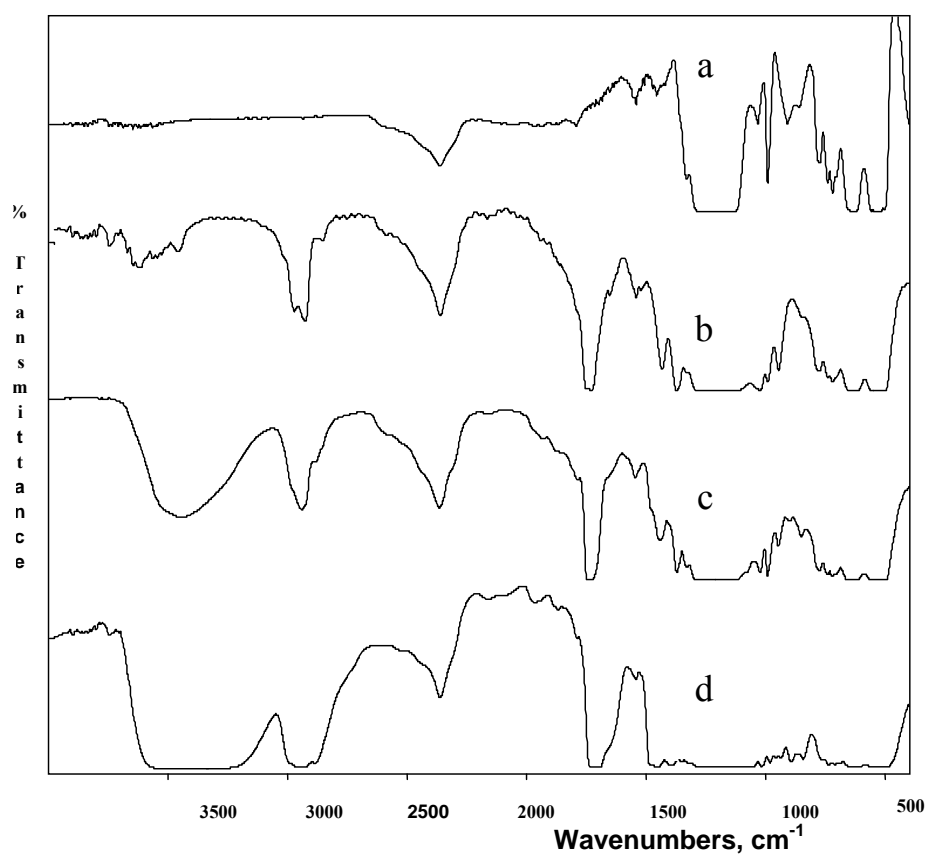


Figure (42): FTIR spectra of (a) trunk PFA, (b) PFA-g-pVAc, (c) PFA-g-pHEMA and (d) its graft copolymer PFA-g-p(VAc/HEMA).

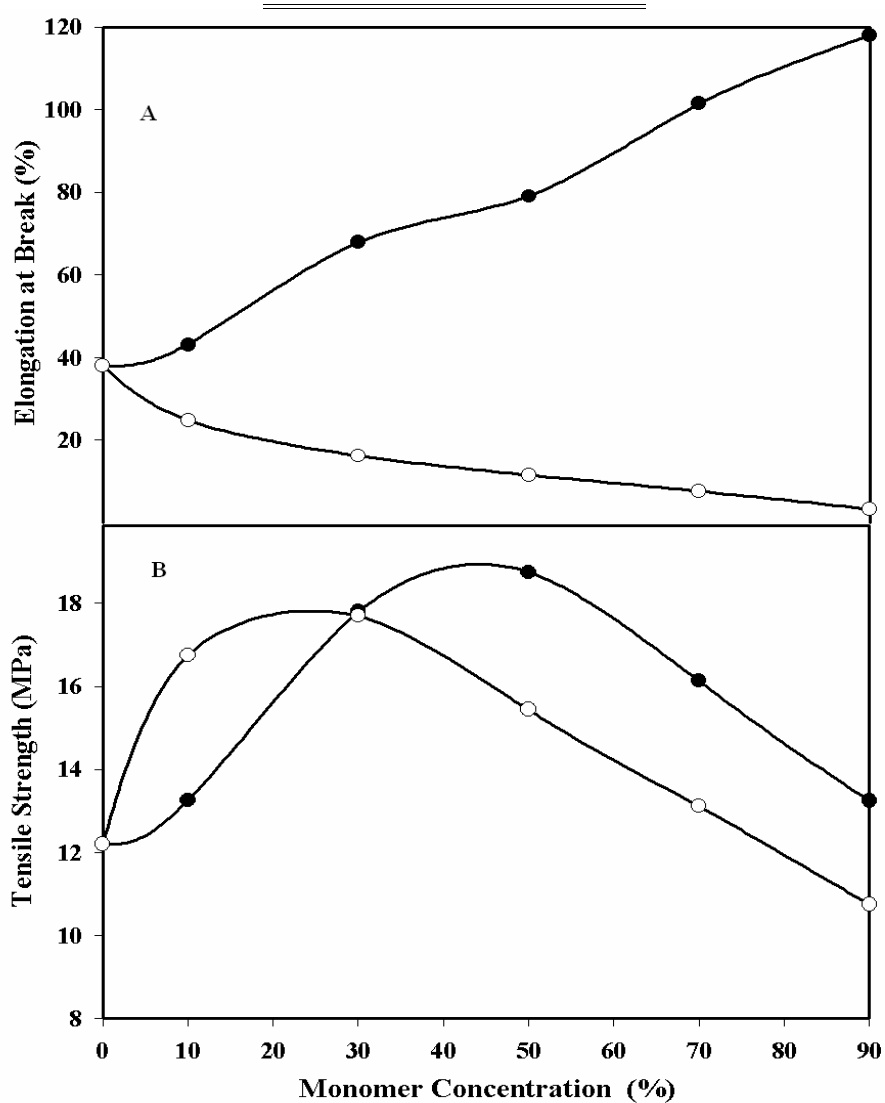


Figure (43): The change in elongation at break percent and tensile strength, respectively with monomer concentration of grafted PFA films by (●) VAc and (○) HEMA using methanol as a solvent, 0.1 (wt%) FeCl_3 inhibitor and irradiation dose 30 kGy and dose rate 1.85 Gy/s.

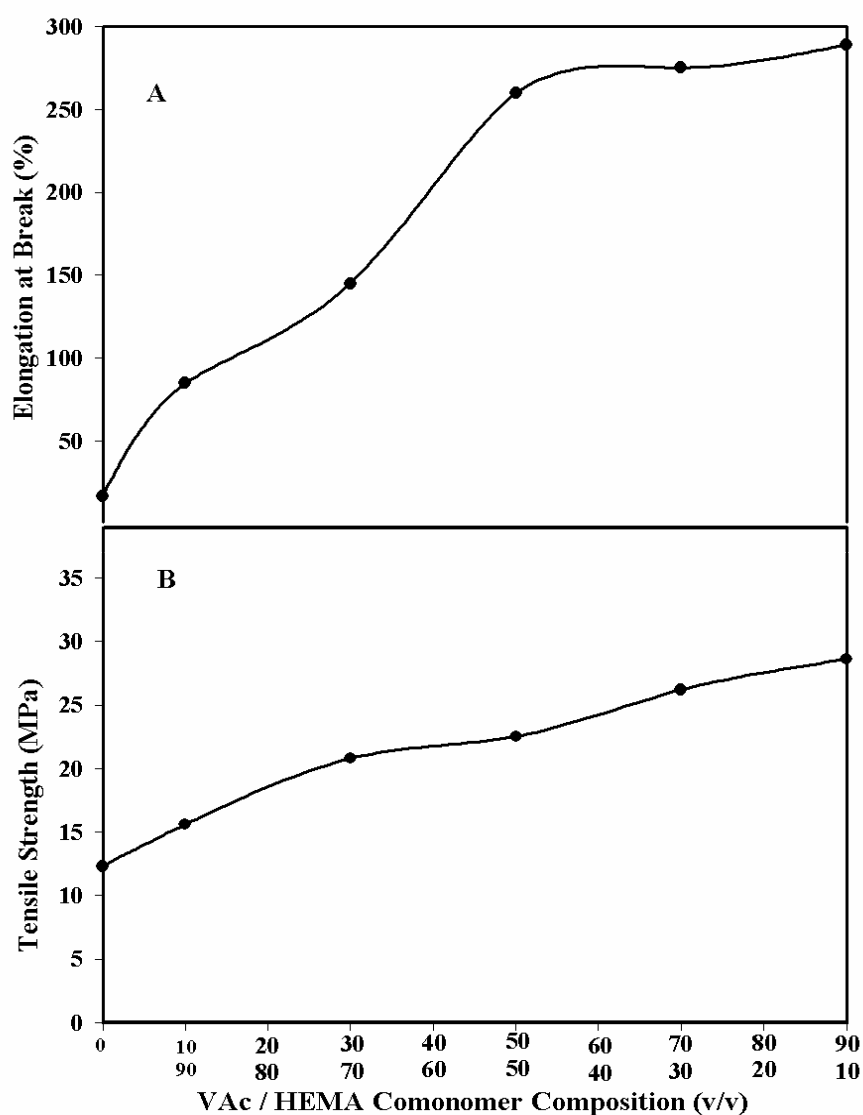


Figure (44): The change in elongation at break percent and tensile strength, respectively with VAc/HEMA comonomer composition of grafted PFA films using methanol as a solvent, 0.1 (wt%) FeCl_3 inhibitor, 50% comonomer concentration, irradiation dose 30 kGy and dose rate 1.85 Gy/s.

IV.II.2.3- Thermal Gravimetric Analysis (TGA)

Figure (45) shows the TGA spectra as a function of temperature of (a) trunk PFA, (b) PFA-g-pVAc, (c) PFA-g-pHEMA and its graft copolymer (d) PFA-g-p(VAc/HEMA). The thermal stability of the radiation-grafted PFA membranes was measured by TGA at the range of 25-600 °C under N₂ atmosphere and heating rate of 10 °C/min. Table (14) indicates that, the weight loss percent of the first stage starting at a room temperature up to 500 °C for trunk PFA, PFA-g-pVAc, PFA-g-pHEMA and its graft copolymer PFA-g-p(VAc/HEMA), respectively. The thermal stability of the trunk PFA is stable up to 500 °C. However, the grafted films at the early stages due to the departure of physicosorbed water at 100-200°C. The grafting brought about a marked decrease in the thermal stability of the films because of a faster rate of degradation of the grafted chains and so the PFA-g-pHEMA shows the lower thermal stability to 250 °C of 13.8 weight loss %. Also it can be observed that there is a sharp decrease in thermal stability of PFA-g-pVAc films up to 400°C of 40.2 weight loss %. It was found that the thermal stability of grafted copolymer film, PFA-g-p(VAc/HEMA), was nearly the same as that of PFA-g-pHEMA and greater than that of PFA-g-pVAc up to 350°C. Also, the thermal stability of PFA-g-p(VAc/HEMA) at elevated temperature up to 500°C became 33 weight loss % lower than that of PFA-g-pHEMA and still greater than that of PFA-g-pVAc. This means that the copolymerization grafting of VAc/HEMA binary monomers onto PFA matrix improve the thermal stability than grafting by VAc monomer alone. Consequently, the degradation of the polymeric grafted chains increased with elevating the temperature up to 400-500 °C.

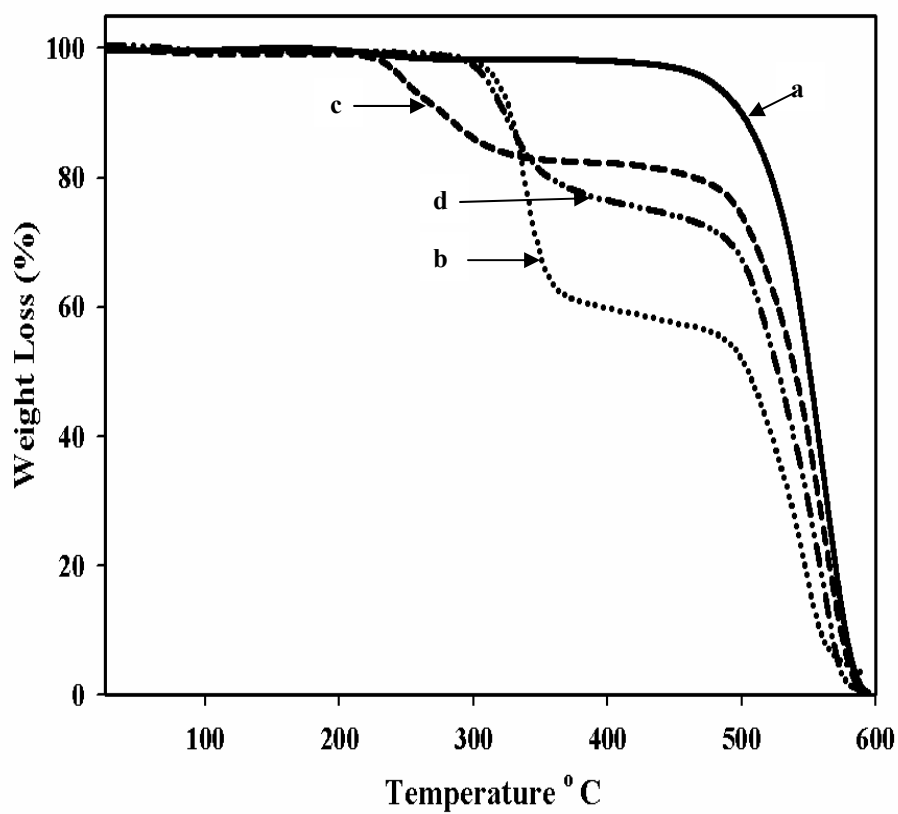


Figure (45): TGA spectra of (a) trunk PFA, (b) PFA-g-pVAc, (c) PFA-g-pHEMA and its graft copolymer (d) PFA-g-p(VAc/HEMA).

Table (14): The weight loss (%) for trunk PFA, PFA-g-pVAc, PFA-g-pHEMA and PFA-g-p(VAc/HEMA) in nitrogen atmosphere and heating rate of 10°C /min.

Sample	Weight loss (%)					
	25-100 °C	100-200 °C	200-300 °C	300-350 °C	350-400 °C	400-50 °C
Trunk PFA	-	0.3	1.7	1.8	2	11.1
PFA-g-pVAc	0.3	1.6	2	32	40.2	48.3
PFA-g- pHEMA	0.8	1	13.8	17.2	17.75	26
PFA-g-p(VAc/HEMA)	0.33	0.51	2.8	19	23.5	33

IV.II.2.4- Morphological Structure

Figure (46) shows the SEM micrographs of (a) trunk PFA (b) PFA-g-pVAc, (c) PFA-g-pHEMA and (d) PFA-g-p(VAc/HEMA). The scanning electron micrograph depicted in Figure (46 a) for the trunk PFA film, the surface texture showed smooth surface. While the micrograph depicted in Figure (46 b) for PFA-g-pVAc shows formation of large texture with regular shape. The micrograph depicted in Figure (46 c) for PFA-g-pHEMA showed high spots aggregates distributed randomly on the surface. The micrograph depicted in Figure (46 d) for PFA-g-p(VAc/HEMA) showed a tough surface like osmotic cells characteristic of the HEMA graft copolymer system.

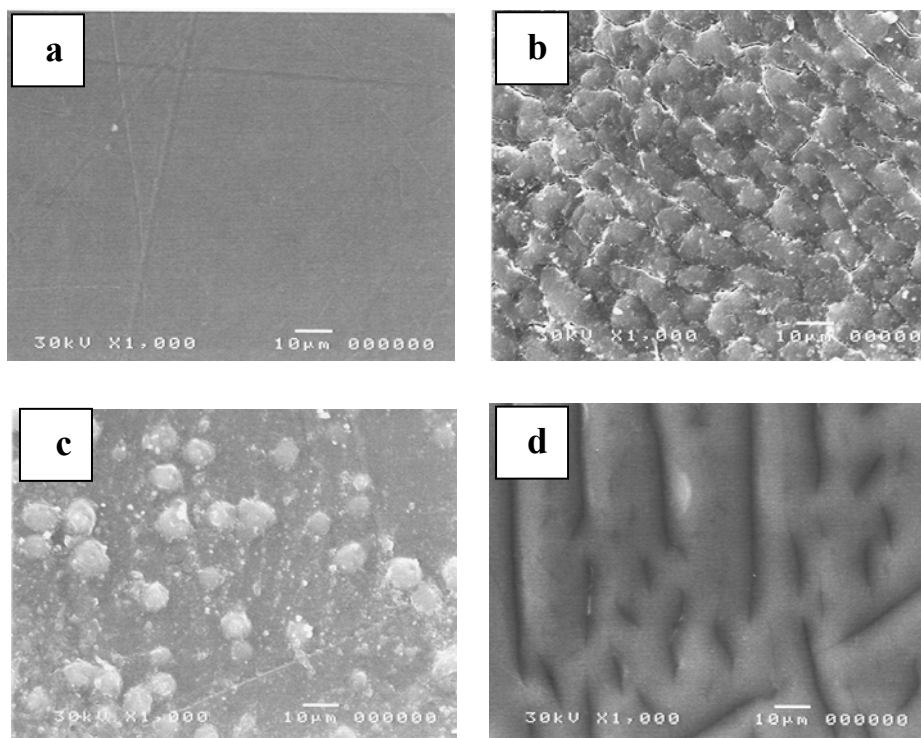


Figure (46): The SEM micrographs of (a) trunk PFA (b) PFA-g-pVAc, (c) PFA-g-pHEMA and (d) PFA-g-p(VAc/HEMA).

IV.II.3- Applications of Grafted Membranes

IV.II.3.1- Platelet Adhesion Assessment

Figure (47) The SEM micrographs before treatment by platelet adhesion of (a) trunk PFA and PFA-g-p(VAc/HEMA) with different grafting yield of (b) 5.3 (c) 21.2 (d) 31.5 and (e) 42 %, respectively. The scanning electron micrograph depicted in Figure (47 a) for the trunk PFA film, the surface texture showed smooth surface while increasing the degree of grafting a tough surface is appeared as shown in the micrographs of Figure (47 b), while the micrograph depicted in Figure (47 c) and Figure (47 d) showed a tough surface like osmotic cells characteristic of the HEMA graft copolymer system. The micrograph depicted in Figure (47 e) showed smooth surface as that of the trunk PFA film due to increasing the ratio of HEMA monomer in the VAc/HEMA comonomer composition ratio which can fill the osmotic cells formed.

Figure (48) shows the SEM micrographs of platelet adherent on (a) trunk PFA and PFA-g-p(VAc/HEMA) with comparison of platelet adhesion at different grafting yield of (b) 5.3, (c) 21.2, (d) 31.5 and (e) 42 %. Scanning electron micrographs were used to show the changes in surface morphology of the grafted films due to changes in the physiological functions of blood and clotting system with the thrombus formation on the surface polymers and also selective for adsorption of blood plasma proteins The scanning electron micrograph depicted in Figure (48 a) for the trunk PFA film

was found to be transparent, clear, smooth and have no platelets on its surface due to anti-thrompogenicity **Chen et al. (2004)**. Meanwhile, The scanning electron micrograph depicted in Figure (48 b) shows some changes in the morphology, the platelets appeared singular and such changes increase with presence of distinct sphere with the typical rounded shape in the grafted films as shown in micrograph depicted in Figures (48 c and d) due to adhesion of blood platelets on the surface embedding with VAc and HEMA chains onto the PFA matrix. The adhesion of blood platelets increase with increasing the grafting yield up to 31.5% as shown in micrograph of (48 d), then the surface of grafted membrane having grafting yield of 42% micrograph of (48 e) become smooth as trunk PFA. This means that the platelets can be adhered only onto the tough surfaces and the amount of platelets appeared depend on the toughness of the surface. The results suggest that the presence of VAc and HEMA chains in the grafted copolymer matrix enhance the adhesion of platelets and by increasing the grafting yield the platelets adhesion increases as well.

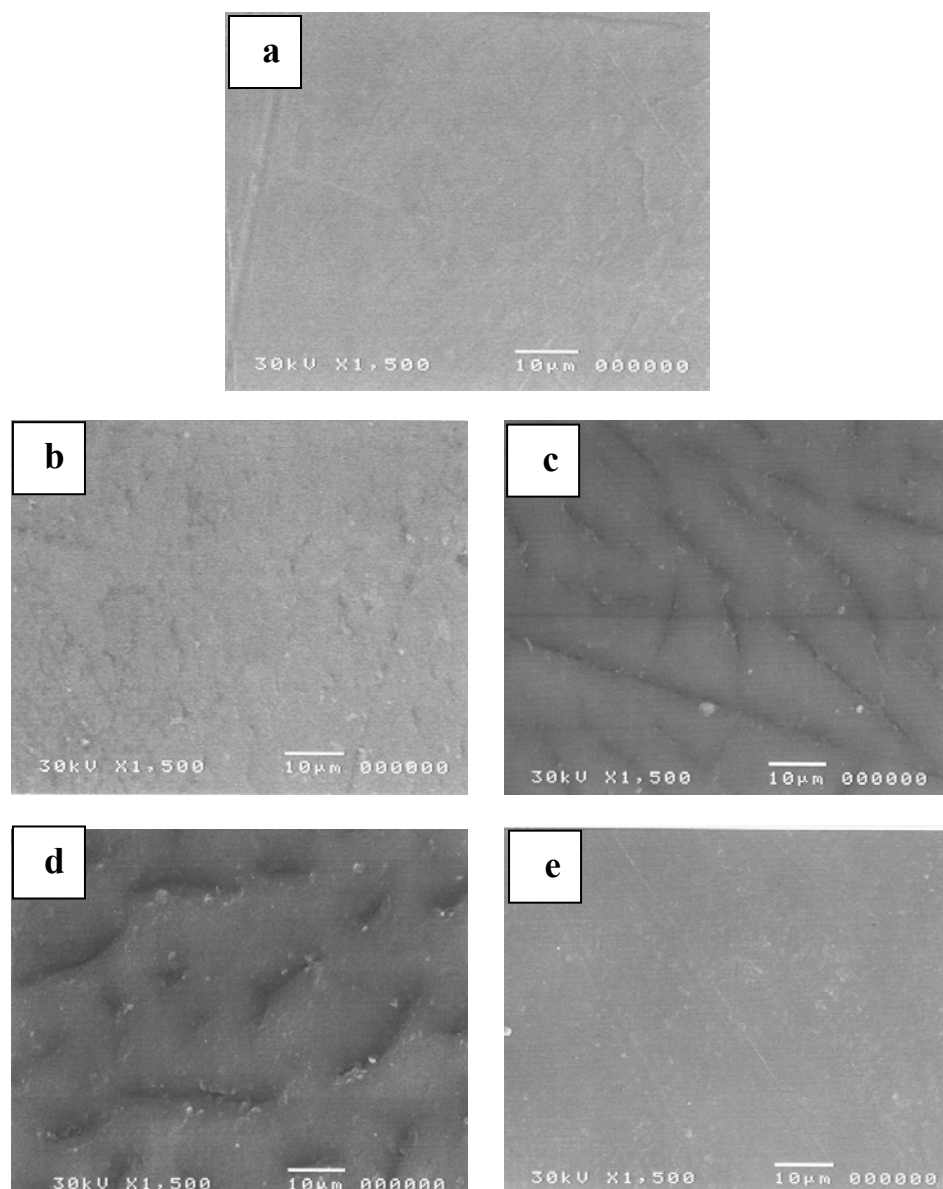


Figure (47): The SEM micrographs before treatment by platelet adhesion of (a) trunk PFA and PFA-g-p(VAc/HEMA) with different grafting yield of (b) 5.3, (c) 21.2, (d) 31.5 and (e) 42%, respectively.

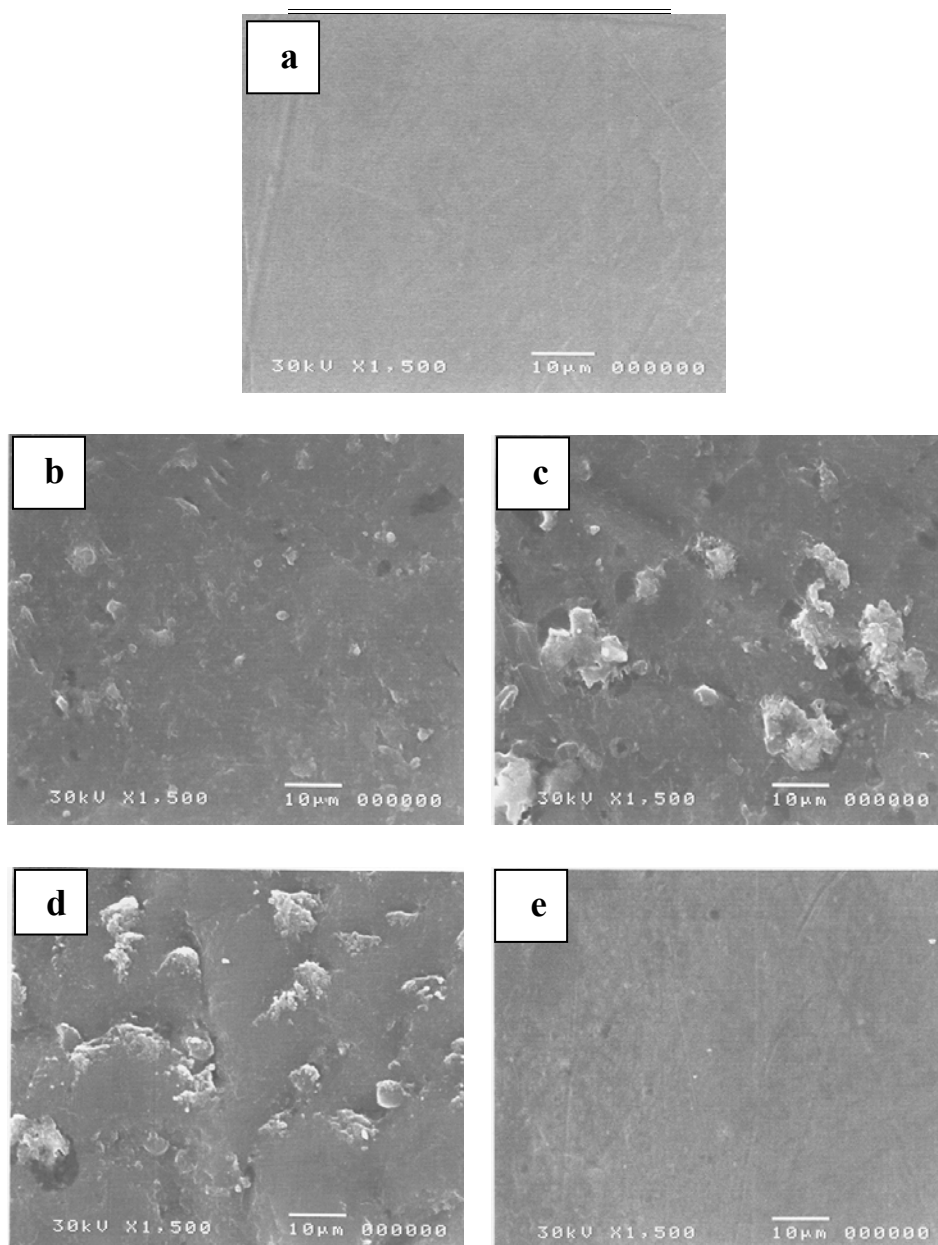


Figure (48): The SEM micrographs of platelet adherent on (a) trunk PFA and PFA-g-p(VAc/HEMA) with comparison of platelet adhesion at different grafting yield of (b) 5.3, (c) 21.2, (d) 31.5 and (e) 42%, respectively.

IV.II.3.2- Polymer Metal - Complex Membranes

The tendency of the graft copolymer to absorb and/ or bind Cu^{2+} and Cr^{3+} ions from aqueous solutions is of promising use in the field of waste treatment of heavy metals in the environmental industrial wastes and these membranes can be characterized as follows:

IV.II.3.2.1- FTIR Spectroscopy

Figure (49) shows the FTIR spectra of (a) PFA-g-p(VAc/HEMA) and its graft copolymer complexed with (b) Cu^{2+} and (c) Cr^{3+} ions, having the same grafting yield of 5.3 %. The broad band of hydroxyl group appeared at $3200\text{-}3600\text{ cm}^{-1}$ due to the grafting by HEMA monomer in the VAc/HEMA comonomer composition. It was observed that there is decrease in this band due to the complexation with Cu^{2+} and Cr^{3+} ions, respectively. While, the band appeared at 1730 cm^{-1} is represent the carbonyl groups of grafted VAc/HEMA chains via the complexation by Cu^{2+} and Cr^{3+} ions.

IV.II.3.2.2- UV- Vis Measurements

Figure 50 (I and II) shows the relationship between the relative absorbance and wavelength (nm) of $\text{Cu}(\text{NO}_3)_2$ and $\text{Cr}(\text{NO}_3)_3 \cdot 9\text{H}_2\text{O}$, respectively, at 1.0 wt % aqueous solutions (curve a and b) before and after reactions respectively, and (curve c) PFA-g-p(VAc/HEMA) complexed with Cu^{2+} ions (Figure 50 I) and Cr^{3+} ions (Figure 50 II), having a grafting yield of 42 %. Such measurements were made to determine the absorbance bands of each metal ion before and after reactions (curve a and b). The very broad centered band on 680 nm

appeared to result from the absorbance of Cu^{2+} ions as shown in Figure (50 I curve c) whereas Cu^{2+} ions in aqueous before the complex formation solution appeared at 810 nm as shown in Figure (50 I curve a and b). While the shoulder band which appeared at around 558 nm may be due to the absorbance of Cr^{3+} ions resulting from the complexation of Cr^{3+} ions as shown in Figure (50 II curve c). The Cr^{3+} ions in aqueous solutions exhibits two d-d bands at 412 and 580 nm, respectively, before complex formation as shown in Figure (50 II curve a and b). This is in a good agreement with the results obtained in a previous study *El-Sawy (2000)*.

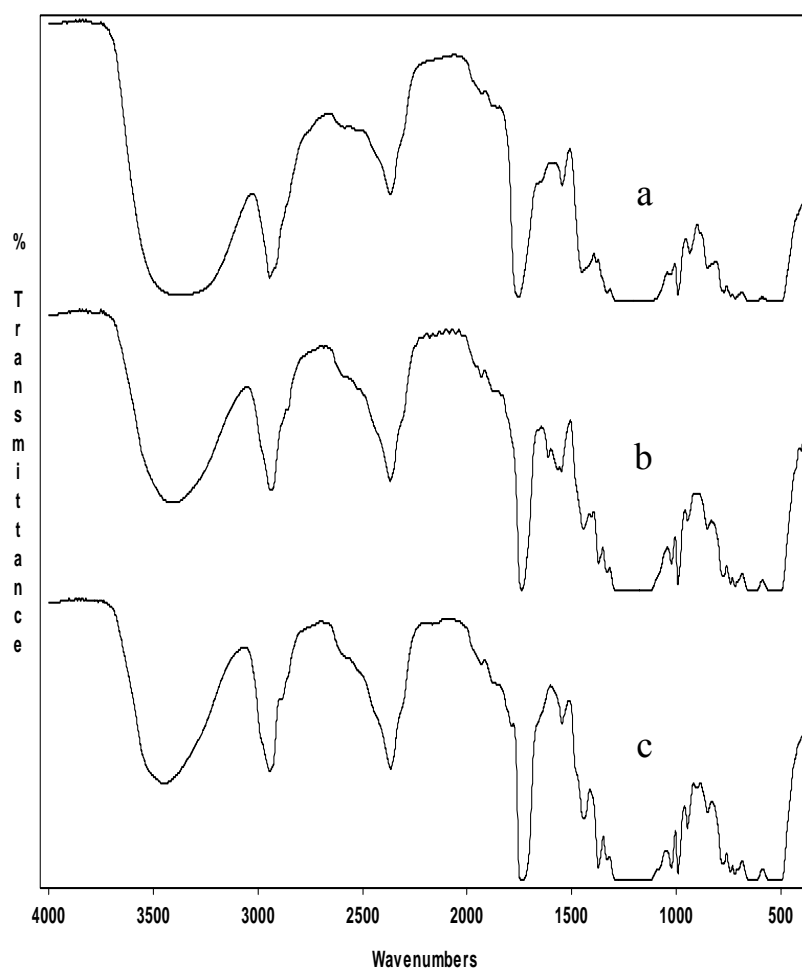


Figure (49): FTIR spectra of (a) PFA-g-p(VAc/HEMA) and its graft copolymer complexed with (b) Cu^{2+} and (c) Cr^{3+} ions, having the same grafting yield of 5.3 %.

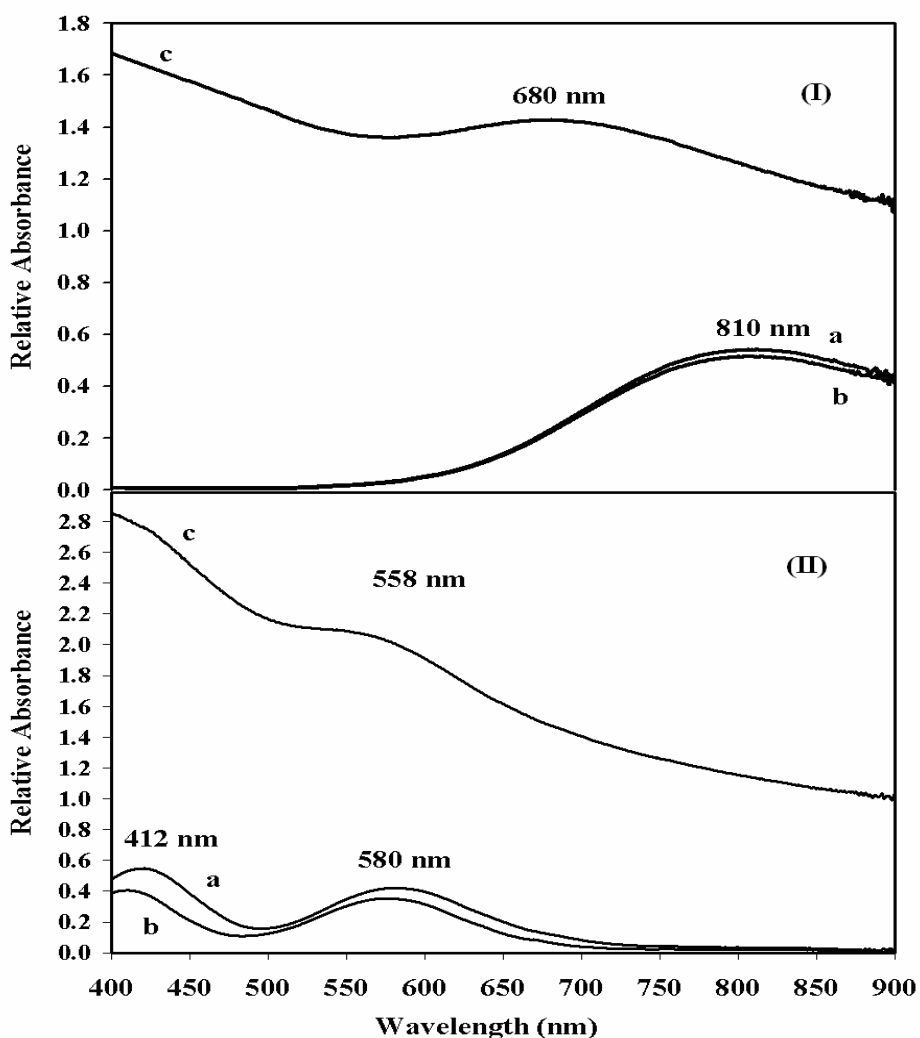


Figure (50): Change in the relative absorbance with wavelength (nm) for (I) $\text{Cu}(\text{NO}_3)_2$ and (II) $\text{Cr}(\text{NO}_3)_3 \cdot 9\text{H}_2\text{O}$ in aqueous solutions (curve a and b) before and after reactions respectively, and (curve c) PFA-g-p(VAc/HEMA) complexed with Cu^{2+} (Fig.50 I) and Cr^{3+} (Fig.50 II) ions, having the same grafting yield of 42%.

IV.II.3.2.3- X-ray Fluorescence Measurements

Figure 51 (a and b) shows the intensity (cps) spectra as a function of energy (keV) for PFA-g-p(VAc/HEMA) complexed with Cu^{2+} ions (curve a) and Cr^{3+} ions (curve b). The peaks of Cu^{2+} and Cr^{3+} ions revealed chelation of the grafted chains during the complexation process. The results suggest that the absorption of metal ions through the grafted chains of copolymer depends on the nature of metal ions and so the absorption value of Cu^{2+} ions is higher than that of Cr^{3+} ions and appear at 8 and 5.4 keV, respectively.

IV.II.3.2.4- Electron Spin Resonance (ESR)

Figure (52) shows ESR spectra of PFA-g-p(VAc/HEMA) complexed with Cu^{2+} and Cr^{3+} ions at room temperature and having the same grafting yield of 42%. The coordination structure of a polymer-metal complex can be determined from the ESR spectrum in which an interaction occurs between the spin of the central metal ion and a coordinated ligand, the strength of which is given by its g value (spectroscopic splitting). The spectrum of Cu^{2+} ions has the parameters $g_{\parallel} = 2.312$, $g_{\perp} = 2.068$. The results for Cu^{2+} ions are the axial type with $g_{\perp} = 2.068$ and $g_{\parallel} = 2.312$ and it may represent a square planar environment. The results are good agreement with a previous study *El-Sawy (2000)*. The spectrum of the graft copolymer –Cr complex exhibits a very broad signal of one- g type; $g = 2.03$. This result reflects perfect octahedral environment or grossly misaligned set tetragonal axes, rather than Cr–Cr interaction and confirms the electronic spectral results given in UV-Vis measurements which are consistent with previous studies *El-sawy (2000)* and *El-sawy and Al-Sagheer (2001)*.

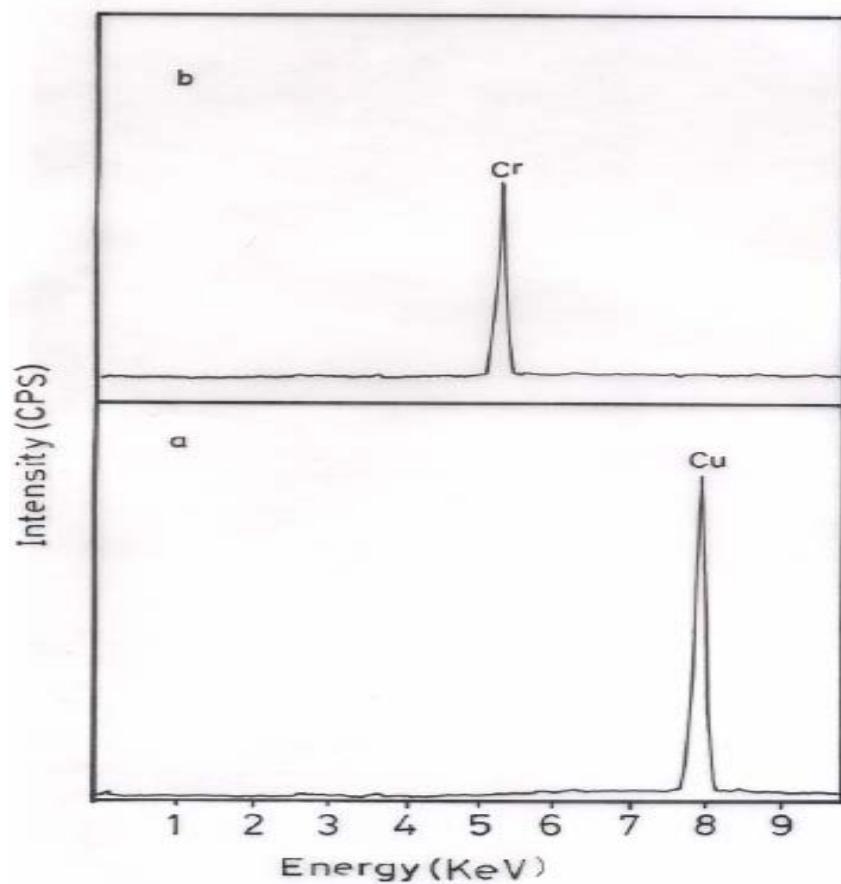


Figure (51): X-ray fluorescence spectra of PFA-g-p(VAc/HEMA) complexed with (a) Cu^{2+} and (b) PFA-g-p(VAc/HEMA) complexed with Cr^{3+} ions, having the same grafting yield of 42%.

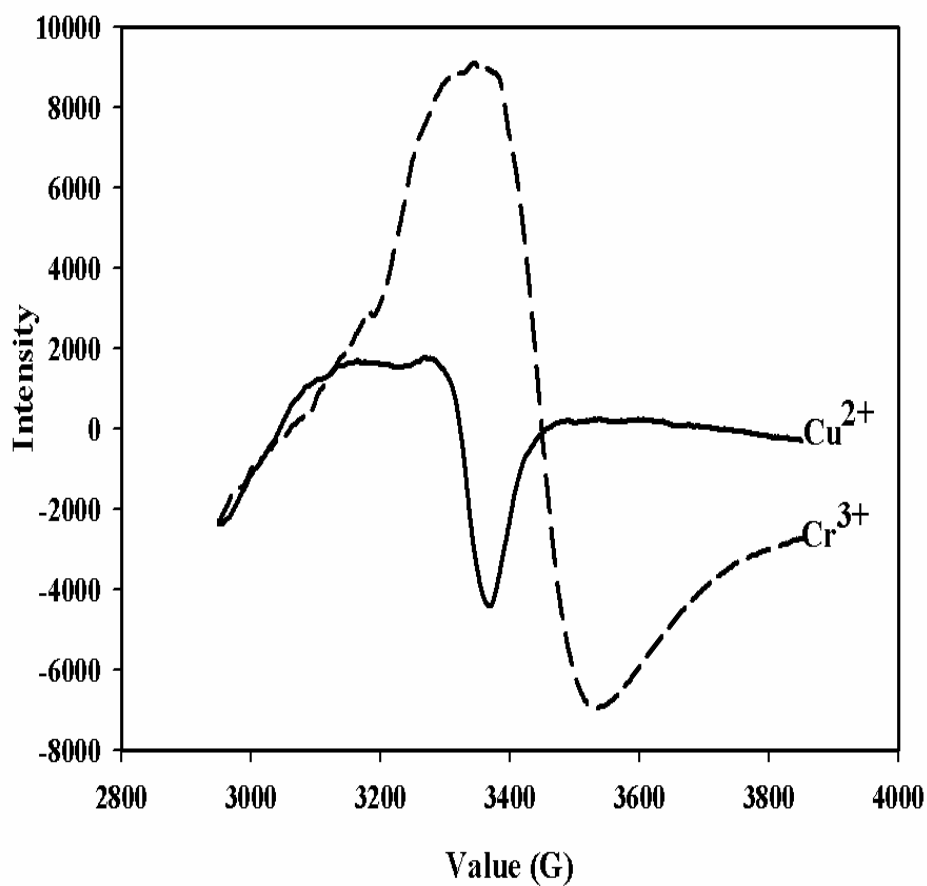


Figure (52): ESR spectra of PFA-g-p(VAc/HEMA) complexed with (—) Cu^{2+} ions and (---) PFA-g-p(VAc/HEMA) complexed with Cr^{3+} ions at room temperature, having the same grafting yield of 42%.

IV.II.3.2.5- TGA Analysis

Figure (53) shows the TGA spectra of (a) PFA-g-p(VAc/HEMA), (b) PFA-g-p(VAc/HEMA) complexed with Cu^{2+} ions and (c) PFA-g-p(VAc/HEMA) complexed with Cr^{3+} ions, having the same grafting yield of 42% measured at the range of 25-600 °C under a nitrogen atmosphere and heating rate of 10 °C/min. Table (15) indicates the weight loss (%) of the first stage starting at a room temperature up to 600°C for grafted and metal-treated grafted membranes with Cu^{2+} and Cr^{3+} ions. The thermal stability of the grafted PFA matrix is higher than those of the complexed films at the early stages of heating up to 300 °C. It can be observed that the decrease in thermal stability of PFA film occurred upon grafting of VAc/HEMA chains due to the departure of physicosorbed water at 100-200°C. However, the introduction of Cu^{2+} or Cr^{3+} ions through the grafted layer during complex formation may increase the rate of degradation of grafted copolymer chains. Consequently, the degradation of the polymeric grafted chains increased with elevating the temperature up to 400-500 °C, the complexed films of either Cu^{2+} or Cr^{3+} are degradable with increasing temperature, but the weight loss is less than that of the grafted membrane because of the presence of metal throughout the complex structure which may retard degradation until some bonds of the complex structure are broken at elevated temperature. Thus, the complexed metal ions suppress the degradation of the membranes.

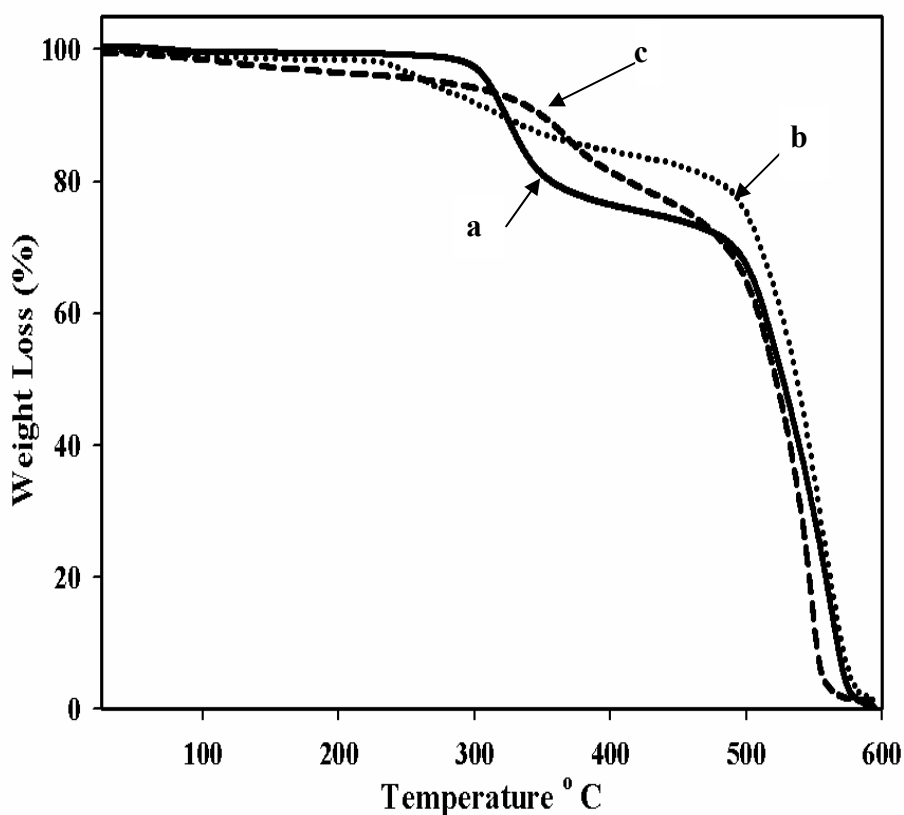


Figure (53): TGA spectra of (a) PFA-g-p(VAc/HEMA), (b) PFA-g-p(VAc/HEMA) complexed with Cu^{2+} ions and (c) PFA-g-p(VAc/HEMA) complexed with Cr^{3+} ions, having the same grafting yield of 42%.

This is in a good agreement with the results obtained in previous studies *El-Sawy and Ali (2007)* and *El-Sawy (2000)*.

The sequence of the stability of various membranes is as follows: $-\text{Cu}^{2+} \geq -\text{Cr}^{3+}$. Such a sequence seems to be reasonable, from the view point of the effective ionic radii of the investigated ions.

Table (15): The weight loss (%) for PFA-g-p(VAc/HEMA), PFA-g-p(VAc/HEMA) complexed with Cu^{2+} and Cr^{3+} ions in nitrogen atmosphere, having the grafting yield of 42%.

Sample	Weight loss (%)				
	25-100 °C	100-200 °C	200-300 °C	300-400 °C	400-500 °C
PFA-g-p(VAc/HEMA)	0.33	0.51	2.8	23.5	33
PFA-g-p(VAc/HEMA)- Cu^{2+}	0.95	2.53	8	15.4	24.85
PFA-g-p(VAc/HEMA)- Cr^{3+}	1.5	3.5	5.8	18.6	35.3

IV.II.3.2.6- Electrical Conductivity Measurements

Figure (54) shows the electrical conductivity of PFA-g-p(VAc/HEMA) and PFA-g-p(VAc/HEMA) complexed with Cu^{2+} and Cr^{3+} ions as a function of degree of grafting. It is clear that the electrical conductivity increases with increasing the degree of grafting. It is obvious that the graft copolymer metal complexes show much higher electrical conductivity values as compared with that of the grafted films. The electrical conductivity for PFA-g-p(VAc/HEMA)- Cr^{3+} complex films is much higher than PFA-g-p(VAc/HEMA)- Cu^{2+} complex films under the same conditions. This effect may be attributed to the fact that the electrolytic groups

introduced by the complexation process result in an increase in the mobility and freedom of the ionic species, leading to an increase in the electrical conductivity which may lead them to being considered for use as semiconductor materials (10^{-3} - 10^{-10} ohm⁻¹ cm⁻¹) *Hegazy et al. (1993)* and *El-Sawy and Al-Sagheer (1998)*.

IV.II.3.2.7- - Surface Morphology

Figure (55) shows the micrographs of (a) PFA-g-p(VAc/HEMA), (b) PFA-g-p(VAc/HEMA) complexed with Cu²⁺ ions and (c) PFA-g-p(VAc/HEMA) complexed with Cr³⁺ ions recorded at room temperature and having the same grafting yield of 42%. The scanning electron micrograph depicted in Figure (55 a) for PFA-g-p(VAc/HEMA) the surface texture showed a tough surface with osmotic cells as characteristic of the HEMA graft copolymer system. The micrograph in Figure (55 b), which is due to the treated membranes of grafted PFA with Cu²⁺ ions gives a clearly smooth and translucent shape due to complete adsorption of Cu²⁺ ions the surface. The micrograph in Figure (55 c) shows that the modified grafted PFA with Cr³⁺ ions cause some changes and granular formations of pores and chaps on the surface of the grafted layer.

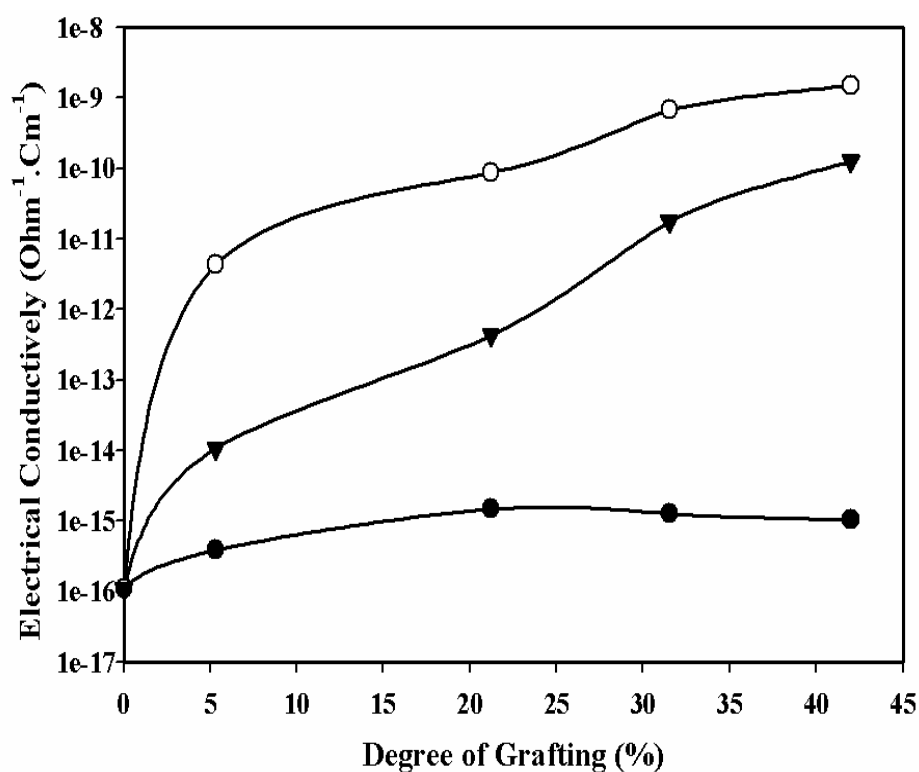


Figure (54): Electrical conductivity of (●) PFA-g-p(VAc/HEMA) and (▼) PFA-g-p(VAc/HEMA) complexed with Cu²⁺ ions and (○) PFA-g-p(VAc/HEMA) complexed with Cr³⁺ ions as a function of degree of grafting.

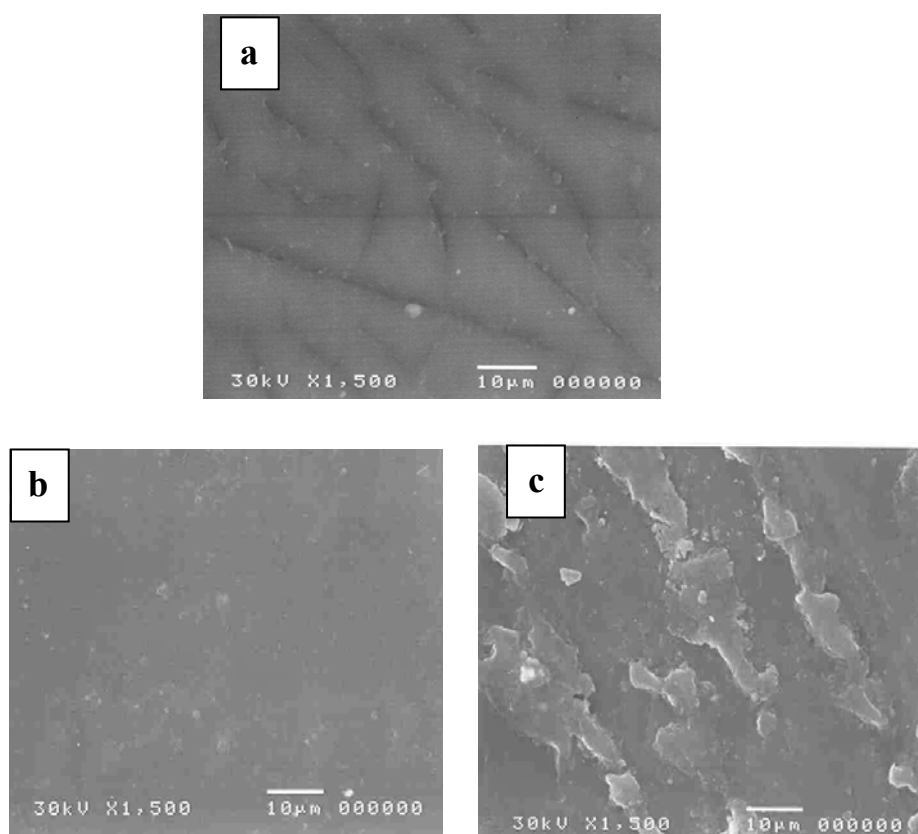


Figure (55): The SEM micrographs of (a) PFA-g-p(VAc/HEMA), (b) PFA-g-p(VAc/HEMA) complexed with Cu^{2+} ions and (c) complexed with Cr^{3+} ions, having the same grafting yield of 42%.

Summary and Conclusion

The present study divided into two parts. First part focused on the effect of the radiation on some naturally occurring polymers such as chitosan, sodium alginate and carboxymethylcellulose for controlling the degradation process of these polymers. These polymers of low molecular weights can be used as growth promoters for plants in the agriculture field. Second part focused on the radiation grafting of VAc/HEMA binary monomers onto PFA films using γ -irradiation was carried out to synthesize the graft copolymer membranes by direct method. The complexing ability with some selected transition metal ions such as Cu^{2+} and Cr^{3+} ions was investigated. These graft copolymer membranes can be used in the field of blood biocompatibility and in waste treatment of some heavy metals in the environmental industrial wastes. The results obtained can be summarized as follows:

I- Controlling the Radiation-Induced Degradation Process of Naturally Occurring Polymers

1- The changes in the viscosity average molecular weights of chitosan, sodium alginate and CMC when exposed to various gamma irradiation doses in the solid form was investigated. The chitosan, sodium alginate and CMC molecules undergo degradation reactions resulting in the reduction of its viscosity average molecular weights. Meanwhile, as the irradiation dose increases, the viscosity average molecular weight of chitosan, sodium alginate and

CMC molecules decreases. The decrease in molecular weight is very fast up to 80 kGy.

2- The effect of irradiation on degradation of sodium alginate, chitosan and CMC in the presence of some initiators at 80 kGy as a function of molecular weight changes was investigated. It is observed that the addition of ammonium per-sulfate, potassium per-sulfate and hydrogen-peroxide to sodium alginate chitosan and CMC during the irradiation process accelerates the degradation process.

3- The rate of radiation degradation of sodium alginate in the presence of such additives is much higher if compared with the degradation rate of the natural polymer using gamma irradiation only.

4- The effect of APS concentration on degradation process of chitosan, sodium alginate and CMC irradiated at 80 kGy was investigated. It was found that with increasing the concentration of APS the degradation rate of natural polymers under investigation increases.

5- The effect of treatment time on the degradation of chitosan, sodium alginate and CMC, treated by H₂O₂ and APS using gamma irradiation or thermal heating at 70°C was studied. It was found that the rate of degradation of these polymers using gamma irradiation is higher than that by thermal heating at 70°C.

6- The changes in the viscosity average molecular weights of pure chitosan, sodium alginate and CMC, respectively and those mixed with (w/w) 10% H₂O₂, 20% H₂O₂, 10% KPS and 10% APS with the irradiation dose were studied. With increasing the irradiation dose, the decrease in the viscosity average molecular weight of chitosan, sodium alginate and CMC, the increase in the rate of degradation process was observed.

6- The UV-Vis studies of irradiated chitosan, sodium alginate, were investigated. It was found that the peak intensity for carbonyl groups increases with increasing the irradiation dose.

7- The XRD analysis of irradiated chitosan, sodium alginate, CMC was investigated. It was found that the crystallinity decreased with increasing the irradiation dose.

8- The TGA diagram and the weight loss percent of irradiated chitosan, sodium alginate, CMC was investigated. It was observed that the thermal stability of pure polymers is higher than for irradiated samples.

9- ESR studies for the irradiated samples revealed that the decay rate of the radicals formed during irradiation for the samples irradiated in the presence of hydrogen peroxide is much lower than that for samples irradiated in the presence of Ammonium per-sulfate.

10- The effects of degraded sodium alginate or chitosan on the growth of maize and bean plants were investigated. It was found that by spraying 100 ppm of low molecular weights of degraded sodium alginate or chitosan to orchid plant results in a considerable positive effect not only on plant growth but also its productivity. This suggested the possible use of such degraded polymers in agriculture purposes as growth promoters for plants.

II- Radiation Graft Copolymerization of VAc/HEMA Binary Monomer onto PFA Films

Grafting of VAc, HEMA and their binary monomer onto PFA films were performed by means of gamma rays from ^{60}Co using the direct method. The factors affecting the grafting process such as type of solvent, inhibitor concentration, monomer and comonomer concentrations, comonomer composition and irradiation dose on the grafting yield were investigated.

11- The factors affecting the preparation conditions on the grafting yield of VAc/HEMA binary monomers onto PFA films such as type of solvent, inhibitor concentration, monomer and comonomer concentrations, comonomer composition and irradiation dose were investigated. It was found that the higher grafting yield can be obtained when methanol used as solvent, 0.1 wt% FeCl_3 as an inhibitor, 70 and 50% monomer concentration for grafting by VAc and HEMA, respectively, 80% comonomer concentration, 70/30

(v/v) of VAc/HEMA comonomer composition ratios, respectively at 30 kGy irradiation dose.

12- The FTIR spectra of trunk PFA, PFA-g-pVAc, PFA-g-pHEMA and PFA-g-p(VAc/HEMA) membranes were investigated. It was shown that there is a characteristic bands at 2370 cm^{-1} due to $\nu(\text{C-F})$ bond and new characteristic bands at 1730 cm^{-1} due to $\nu(\text{C=O})$, 2950 cm^{-1} due to the $\nu(\text{C-H})$ stretching and broad band at $3200\text{--}3600\text{ cm}^{-1}$ due to hydroxyl groups.

13- The change in elongation at break percent and tensile strength (MPa) for trunk PFA, PFA-g-pVAc, PFA-g-pHEMA and PFA-g-p(VAc/HEMA) membranes were studied. The results revealed that the increasing of the VAc ratio in VAc/HEMA comonomer composition, the increase in the elongation at break percent (E_b) and tensile strength (T_b) were obtained.

14- The thermal stability of trunk PFA, PFA-g-pVAc, PFA-g-pHEMA and PFA-g-p(VAc/HEMA) membranes were examined. It was found that the thermal stability decreased with increasing grafting yield.

15- The SEM micrographs of trunk PFA, PFA-g-pVAc, PFA-g-pHEMA and PFA-g-p(VAc/HEMA) membranes were investigated.

16- The applicability of grafted membranes in blood biocompatibility especially platelet adhesion was investigated. The SEM was used to show the changes in surface morphology of the grafted films by the adherent platelets.

17- The complexing ability of graft copolymer membranes with some selected transition metal ions such as Cu^{2+} and Cr^{3+} ions was investigated.

18- The complex formation of these graft copolymer-metal complexes was studied by FTIR, UV-Vis, XRF, SEM, TGA and ESR was investigated. The results revealed that the tendency of the graft copolymer to absorb and/ or bind Cu^{2+} and Cr^{3+} ions from aqueous solutions is of promising use in the field of waste treatment of heavy metals in the environmental industrial wastes. Also, the electrical conductivity increases with increasing the degree of grafting where the electrical conductivity for PFA-g-p(VAc/HEMA)- Cr^{3+} complex films is much higher than PFA-g-p(VAc/HEMA)- Cu^{2+} complex films is much higher than PFA-g-p(VAc/HEMA) films under the same conditions.

References

- 1- Abad L.V., Nasimova I. R., Relleve L. S., Aranilla C. T., De la Rosa A. M., Shibayama M., *Int. J. Biolog. Macromole.*, 34, 81 (2004).
- 2- Abd El-Reheim H. A., *J. of Bioactiv. and Compat. Polym.*, 20, 51-75 (2005).
- 3- Abd El-Rehim H. A. , El-Hag Ali A., Mostafa T.B., Hala A. Farrag, *Eur. Polym. J.*, 40, 2203 (2004).
- 4- Abd El-Rehim H. A. and El-Arnaouty M. B., *J Biomed. Mater. Res. Part B: Appl. Biomat.*, 68, 209 (2004).
- 5- Abd El-Rehim H. A., Hegazy E. A., Ali A. M., *J. of Appl. Polym. Sci.*, 74, 806 (1999).
- 6-Abd El-Rehim H. A., Hegazy E. A., El-Hag Ali A., *React. and Funct. Polym.*, 43, 105 (2000).
- 7- Abd El-Rehim H. A., Mostafa T. B., Abd El-Monem Bashindy, *J. of Macromolecul. Sci., Part A: Pure and Appl. Chem.*, 42, 853 (2005).
- 8- Abdel-Ghaffar M., Hegazy E. A., Dessouki A. M., El-Assy N. B. and El-Sawy N. M., *Radiat. Phys. Chem.*, 38(4), 369 (1991).
- 9-Adaoha Mbanaso E. N. and Roscoe D. H., *Plant Sci. Letter.*, 25, 61 (1982).
- 10- Adem E., Avalos-Borja M., Bucio E., Burillo G., Castillon F. F., Cota L., *Nucl. Instrum. and Meth. in Phy. Res.*, B 234, 471 (2005).
- 11- Ait Si Mamuar S. And Hadjadj A., *Radiat. Phys. Chem.*, 35, 451 (1990).

- 12- Ajay K. Singh, Rachna Varshney, Manu Sharma, Shyam S. Agarwal, Kailash C. Bansal, *J. of Plant Physiol.*, 163 , 220 (2006).
- 13- Akiyama H., Endo T., Nakakita R., Murata K., Yonemoto Y., Okayama K., *Biosci. Biotech. Biochem.* 56, 335 (1992).
- 14- Alla V. Ilyina, Natalya Yu. Tatarinova, Valery P. Varlamov, *Proc. Biochem.*, 34, 875 (1999).
- 15- Andrzej G. Chmielewski, Mohammad Haji-Saeid, Shamshad Ahmed, *Nuclear Instrum. and Meth. in Phys. Res.*, 236, 44 (2005).
- 16- Barillon R., Yamauchi T., *Nucl. Instrum. and Meth. in Phy. Res.*, 208, 336 (2003).
- 17- Bautista-Banos S., Hernandez-Lopez M., Bosquez-Molina E., Wilson C. L., *Crop Protect.*, 22, 1087 (2003).
- 18- Beddows C. G., Gil M. H., Guthrie J. T., *Polym. Photochem.*, 7, 213 (1986).
- 19- Benson R. S., *Nucl. Instr. and Meth., B*, 191, 752 (2002).
- 20- Bersch P. C., Nies B., and Liebendorfer A., *J. of Material Sci., Mater. in Medic.*, 6(2), 231 (1995)..
- 21- Bhuvanesh Gupt, Rachna Jain, Nishat Anjum, Harpal Singh, *Radi. Phy. and Chem.*, 75, 161 (2006).
- 22- Biji Balakrishnan, D.S. Kumar, Yasuhiko Yoshida, A. Jayakrishnan, *Biomater.* 26 3495 (2005).
- 23- Bin Fei, Radoslaw A. Wach, Hiroshi Mitomo, Fumio Yoshii, Tamikazu Kume., *J. of Appl. Polym. Sci.*, 78, 278 (2000).
- 24- Bin Kang, Yao-dong Dai, Hai-qian Zhang, Da Chen, *Polym. Degrad. and Stab.*, 92, 359 (2007).

- 25- Bradley T. D. and Mitchell J. R., *Carbohy. Polym.* 9, 257 (1988).
- 26- Bucio E., Burillo G., *Radi. Phy. and Chem.*, 76, 1724 (2007).
- 27- Buddy D. Ratner, *j. of Biomedi. Mater. Res.*, 14, 665 (2004).
- 28- Carenza M., Lora S., Palma G., Pezzin G. and Caliceti P., *Radiat. Phys. Chem.*, 48, 231 (1996).
- 29- Casimiro M. H., Botelho M. L., Leal J. P., Gil M. H., *Radiat. Phys. Chem.*, 72, 731 (2005a).
- 30- Casimiro M. H., Leal J. P., Gil M. H., *Nucl. Instrum. and Meth. in Phy.Res.*, B 236, 482 (2005b).
- 31- Chandy T. and Sharma C. P., *Biomater.*, 13, 949 (1992).
Chirachanchai S., Lertworasiriku A. and Tachaboonyakiat W., *Carbohyd. Polym.*, 46, 19 (2001).
- 32- Chao A. C., Shyu S. S., Lin Y. C. and Mi F. L., *Bioresource Technol.*, 91(2), 157 (2004).
- 33- Cheung A. K., Parker C. J., Janatova J., Brynda E., *J. Am. Soc. Nephrol.*, 2, 1328 (1992).
- 34- Chmielewski A. ., Migdal W., Swietoslawski J., Swietoslawskid J., Jakubaszek U., Tarnowski T., *Radiat. Phys. and Chem.*, 76, 1840 (2007).
- 35- Chuanlun Cai, Qiang Shi, Lili Li, Lianchao Zhu, Jinghua Yin, *Radia. Phys. and Chem.*, 77, 370 (2008).
- 36- Chun Mao, Jiang Yuan, Hua Mei, Aiping Zhu, Jian Shen, Sicong Lin, *Mater. Sci. and Engin.*, 24, 479 (2004).
- 37- Clough R. L, Gillen K. T., *Appl. Sci.*, 79, 156 (1991).

- 38- Czechowska-Biskup R., Rokita B., Ulanski P., Rosiak J. M., *Nucl. Instrum. and Meth. in Phy. Res. B*, 236, 383 (2005).
- 39- Dilli S., Garnett J. L., *J. Appl. Polym. Sci.*, 11, 859, (1967).
- 40- Dong Wook Lee, Won Seok Chol, Myung Woo Byun Hyun Jin Park, Yong-Man Y. U. and Chong M. Lee, *J. Agric. Food Chem.*, 51, 4819 (2003).
- 41- Dong-Hong Li, Liang-Ming Liu, Kun-Lun Tian, Jian-Chang Liu, Xiao-Qing Fan, *Carbohydr. Polym.*, 67, 40 (2007).
- 42- Dumitriu S., *New York: Marcel Dekker*; Polysaccharides in medical applications, 631-649 (1996).
- 43- El-Hag Ali A., Shawky H. A. , Abd El Rehim H. A., Hegazy E.A., *Eur. Polym. J.* 39, 2337 (2003).
- 44- El-Sawy N. M. and Al Sagheer F., *Eur. Polym. J.*, 37, 161 (2001).
- 45- El-Sawy N. M. and Al Sagheer F., *J. of Appl. Polym. Sci.*, 85, 2692 (2002).
- 46- El-Sawy N. M. and Al Sagheer F., *Polym. Int.*, 47, 324 (1998).
- 47- El-Sawy N. M. and Ali Z. I., *J. Appl. Polym. Sci.*, 103, 4065 (2007).
- 48- El-Sawy N. M., Abdel-Ghaffar M., Hegazy E. A., Dessouki A. M., *Eur. Polym. J.*, 28, 825 (1992).
- 49- El-Sawy N. M., Hegazy E. A., Rabie A. M., Hamed A. and Miligy G. A., *Polym. Int.*, 33, 285 (1994).
- 50- El-Sawy N. M., *J. Appl. Polym. Sci.*, 67, 1449 (1998).
- 51- El-Sawy N. M., *Polym. Int.*, 49, 533 (2000).

-
- 52- El-Sawy N. M., *Polym. Int.*, 53, 212 (2004).
 - 53- Ershov B. G., Isakova O. V., Rogoshin S. V., Gamazazade A. I., Leonova E. U., *Dokl. Akad. Nauk. SSSR*, 295, 1152 (1987).
 - 54- Fadel M. A., Khalil W. A. and Abd-Alla R. A., *Nucl. Instr. and Meth.in Phy. Res.*, 236, 178 (1985).
 - 55- Fang Yuae and Shi Tianyi, *J. of Membr. Sci.* , 39, 1 (1988).
 - 56- Fedoseeva E. N., Smirnova L. A., Sorokina M. A., and Pastukhov M. O., *Macromole. Chem. and Polym. Mater.* 79, 857 (2006).
 - 57- Felse P. A. and Panda T., *Bioproc., Engineer.*, 20, 505 (1999).
 - 58- Ferreira L. M., Falcao A. N. , Gil M. H., *Nucl. Instrum. and Meth. in Phy. Res. B* 236, 513 (2005).
 - 59- Greenway T. M. *New York: Honser*; Water soluble derivatives and their commercial use. In: Gilbert DR, editor. *Cellulosic polymers*, 173-188 (1994).
 - 60- Gronroos A., Pirkonen P., Ruppert O., *J. Ultrasonics Sonochem.*, 11, 9 (2004).
 - 61- Guo J. H., Skinner G. W., Harcum W. W., Barnum P. E., *Pharm. Sci. Technol.*, 1, 254 (1998).
 - 62- Haiyang Yang, Pingping Zhu, Chunlin Peng, Shengli Ma, Qingren Zhu, Chenggao Fan, *Eur. Polym. J.*, 37, 1937 (2001).
 - 63- Hasegawa M., Isogai A., Onabe F., Usuda M., & Atalla R. H., *J. of Appl. Polym. Sci.*, 45, 1873 (1992).

- 64- Hegazy E. A., Abd E., Ali A.M.I., Nowiev H.G., Aly H.F., *Nucl. Instrum. Meth. Phys. Res.*, B 151, 393 (1999).
- 65- Hegazy E. A., Abd El-Rehim H. A., Khalifa N.A., El-Hag Ali A., *Radi. Phy. and Chem.*, 55, 219 (1999).
- 66- Hegazy E. A., Abd El-Rehim H. A., Nevien A. Khalifa, Atwa S. M. and Shawky H. A., *Polym. Int.*, 43, 321 (1997).
- 67- Hegazy E. A., Abd El-Rehim H. A., Shawky H. A., *Radi. Phy. and Chem.*, 57, 85 (2000).
- 68- Hegazy E. A., Dessouki A., El-Sawy N., El-Ghaffar M., *J. Polym. Sci., A: Polym. Chem.*, 31, 527 (1993).
- 69- Hegazy E. A., Kamal H., Maziad N., Dessouki A., *Instrum. Meth. Phys. Res.*, B 151, 386 (1999).
- 70- Hegazy E. A., Massarat B. S. Osman, Mokhtar S. M. and Abo El-Khair B. Mostafa, *polym.*, 33, 4230 (1992).
- 71- Hilde K. Holme, Karine Lindmo, Kristiansen A., Olav Smidsrød, *Carbohydr. Polym.*, 54, 431 (2003).
- 72- Hong Kyoon No, Na Young Park, Shin Ho Lee, Samuel P. Meyers, *Int. J. of Food Microbiol.*, 74, 65 (2002).
- 73- Hong Kyoon No, Soon Dong Kim, Witoon Prinyawiwatkul and Samuel P Meyers, *J Sci. Food Agric.*, 86, 1365 (2006).
- 74- Hui Liu, Jianguo Bao, Yumin Du, Xuan Zhou and John F. Kennedy, *Carbohydr. Polym.*, 64, 553 (2006).
- 75- Iwasaki Y., Mikami A., Kurita K., Yui N., Ishihara K., Nakabayashi N., *J. Biomed. Mater. Res.*, 36, 508 (1997).

-
- 76- Jaroslaw M. Wasikiewicz, Fumio Yoshii, Naotsugu Nagasawa, Radoslaw A. Wach, Hiroshi Mitomo, *Radi. Phy. and Chem.*, 73, 287 (2005).
- 77- Jianhua Zu, Minghong Wu, Haiying Fu, Side Yao, *Rad. Phy. and Chem.*, 72, 759 (2005).
- 78- Jin Li, Yumin Du, Hongbo Liang, *Polym. Degrad. and Stab.*, 92, 515 (2007).
- 79- Jin Li, Yumin Du, Jianhong Yang, Tao Feng, Aihua Li and Ping Chen, *Polym. Degrad. and Stab.*, 87, 441 (2005).
- 80- Jinhua Chen, Masaharu Asano, Tetsuya Yamaki, Masaru Yoshida, *J. of Membr. Sci.*, 269, 194 (2006).
- 81- Jo S. and Park K., *Biomaterial.* 21, 605 (2000).
- Juan Carlos Cabrera, Pierre Van Cutsem, *Biochem. Engineer. J.*, 25, 165 (2005).
- 82- Kamath K. R., Park H., Shim H.S., Park K., *Colloids Surf.*, 2, 471 (1994).
- 83- Kaneko M. and Isuchida E., *J. Polym. Sci. Macromol. Rev.*, 16, 397 (1981).
- 84- Keelara V. Harish Prashanth, Shylaja M. Dharmesh, Kosagi S. Jagannatha Rao and Rudrapatnam N. Tharanathan *Carbohydr. Res.*, 342, 190 (2007).
- 85- Khin Lay Nge, Nitar Nwe, Suwalee Chandkrachang, Willem F. Stevens, *Plant Sci.*, 170, 1185 (2006).
- 86- Kim J. H., Lee Y. M., *Polym.*, 34, 1952 (1993).
- 87- Köll P., Borchers G. and Metzger J. O., *J. of Analyt. and Appl. Pyrolys.*, 19, 119 (1991).
- 88- Köll P., Borchers G. and Metzger J. O., *J. of Analyt. and Appl. Pyrolys.*, 17, 319 (1990).

- 89- Kume T., Nagasawa N., Yoshii F., *Radi. Phy. and Chem.*, 63, 625 (2002).
- 90- Lam N. D., Nagasawa N., Kume T., *Radiat. Phys. Chem.*, 59, 393 (2000).
- 91- Le Hai, Tran Bang Diep, Naotsugu Nagasawa, Fumio Yoshii, Tamikazu Kume, *Nucl. Instrum. and Meth. in Phy. Res.*, 208, 466 (2003).
- 92- Le Q. L., Nguyen Q. H., Nagasawa N., Kume T., Yoshii F., Nakanishi T. M., *Biotechnol. Appl. Biochem.*, 38, 283 (2003).
- 93- Le Xuan Tham, Naotsugu Nagasawa, Shinpei Matsuhashi, Noriko S. Ishioka, Takehito Ito, Tamikazu Kume, *Radi. Phy. and Chem.*, 61, 171 (2001).
- 94- Lee J. H., Lee H. B., Andrade J. D., *Prog. Polym. Sci.*, 20, 1043 (1995).
- 95- Lee-Yong Lim, Eugene Kho, Otilia Koo, *J. Biomed. Mater. Res.*, 43: 282 (1998).
- 96- Leonhardt J., Arnold G., Baer M., Langguth H., Gey M. and Hgbert S., *Radi. Phys. Chem.*, 25, 899 (1985).
- 97- Li Z. F. and Ruckenstein E., *J. of Colloid and Interface Sci.*, 269, 62 (2004).
- 98- Lian-Ying Zheng, Jiang-Feng Zhu, *Carbohydr. Polym.*, 54, 527 (2003).
- 99- Ling Huang, Jing Peng, Maolin Zhai_, Jiuqiang Li, Genshuan Wei, *Radiat. Phys. and Chem.*, 76, 1679 (2007a).
- 100- Ling Huang, Maolin Zhai, Jing Peng, Jiuqiang Li, Genshuan Wei, *Carbohy. Polym.*, 68, 109 (2007b).

- 101- Ling-Shu Wan, Zhi-Kang Xu, Xiao-Jun Huang, Zhen-Gang Wang, Jian-Li Wang, *Polym.*, 46, 7715 (2005).
- 102- Luan le Q., Ha V.T., Nagasawa N., Kume T., Yoshii F., Nakanishi T.M. , *Biotechnol. Appl. Biochem.*, 41, 49 (2005).
- 103- Malesic J., Kolar J., Strlic M., Kocar D., Fromageot D., Lemaire J., Haillant O., *Polym. Degrad. and Stabi.*, 89, 64 (2005).
- 104- Mao C., Zhu J. J., Hu Y. F., Ma Q. Q., Qiu Y. Z., Zhu A. P., Zhao W.B., Shen J., *Colloid. and Surf. B: Biointerfaces*, 38, 47, (2004).
- 105- Martel B., Devassine M., Crini G., Weltrowski M., Bourdonnaeu M. and Morcellet M., *J. of Polym. Sci., Part-A: Polym. Chem.*, 39(1), 169 (2001).
- 106- Matsushashi S. and Kume T., *J. Sci. Food Agric.*, 73, 237 (1997).
- 107- Min Larng Tsaih, Rong Huei Chen, *J. of Appl. Polym.Sci.*, 90, 3526 (2003).
- 108- Mitomo H., Watanabe Y., Ishigaki I., Saito T., *Polym. Degrad. and Stab.*, 45, 11 (1994).
- 109- Mukherjee A. K. and Gupta B. D., *J. Appl. Polym. Sci.*, 30, 2253 (1985).
- 110- Muzzarelli R. A. A., *Cell Molecular and Life Science*, 53, 131 (1997).
- 111- Naotsugu Nagasawa, Hiroshi Mitomo, Fumio Yoshii, Tamikazu Kume, *Polym. Degrad. and Stab.*, 69, 279 (2000).

- 112- Nasef M. M., Hegazy E. A., *Prog. Polym. Sci.*, 29, 499 (2004).
- 113- Natsume, M., Kamo, Y., Hirayama, M., Adachi, J., *Carbohydr. Res.*, 258, 187 (1994).
- 114- Nguyen Quoc Hien, Naotsugu Nagasawa, Le Xuan Tham, Fumio Yoshii, Vo Huy Dang, Hiroshi Mitomo, Keizo Makuuchi, Tamikazu Kume, *Radi. Phy. and Chem.*, 59, 97 (2000).
- 115- Nho Y. C, Kwon O. H. and Chen H., *Radiat. Phys. Chem.*, 64, 67 (2002).
- 116- Nieto, J. M., Peniche-Covas, C. And Padron, G., *Thermochimica Acta*, 176, 63 (1991).
- 117- Nitzel K., *J. of Indust. Irradi Technol.*, 2, 11 (1984).
- 118- Nunes S. P. and Peinemann K. V. (eds), *Membrane Technology : In the Chemical Industry*, Wiley-Interscience, Weinheim, New York (2001).
- 119- Pankaj R. Rege, Lawrence H. Block, *Carbohydr. Res.* 321, 235 (1999).
- 120- Park P. J., Je J. Y. and Kim S. W., *Carbohydr. Polym.*, 55, 17 (2004).
- 121- Pedro L. Granja, Bernard De Jeso, Reine Bareille, Francois Rouais, Charles Baquey, Mario A. Barbosa, *React. & Funct. Polym.*, 66, 728 (2006).
- 122- Pekna M., Larsson R., Formgren B., Nilsson U.R., Nilsson B., *Biomaterial.*, 14, 189 (1993).
- 123- Pengfei Liu, Maolin Zhai, Jiuqiang Li, Jing Peng, Jilan Wu, *Radi. Phy. and Chem.*, 63, 525 (2002).

- 124- Petryayev Y. P., Boltromeyul V. V., Kovalenko and N. I., Shadyro O. I., *Polym. Sci. U.S.S.R.*, 30, 2208 (1988).
- 125- Pospieszny H., Chirkov S., Atabekov J., *Plant Sci.* 79, 63 (1991).
- 126- Prime K. L., Whitesides G. M., *Sci.*, 252, 1164 (1991).
- 127- Qin C.Q., Du Y.M., Xiao L., *Polym. Degrad. and Stab.*, 76, 211-218 (2002).
- 128- Qun Zeng Huang, Li Hong Zhuo, Ying Chen Guo, *Carbohydr. Polym.*, 72, 500 (2008).
- 129- Qun Zeng Huang, Shi Ming Wang, Jin Feng Huang, Li Hong Zhuo, Ying Chen Guo, *Carbohydr. Polym.* 68, 761 (2007).
- 130- Radoslaw A. Wach, Hisaaki Kudoh, Maolin Zhai, Naotsugu Nagasawa, Yusa Muroy, Fumio Yoshii, Yosuke Katsumur, *Polym.*, 45, 8165 (2004).
- 131- Rangrong Yoksan, Mitsuru Akashi, Mikiji Miyata and Suwabun Chirachanchai, *Radi. Res.*, 161, 471 (2004).
- 132- Rangrong Yoksan, Mitsuru Akashi, Siriratana Biramontri and Suwabun Chirachanchai, *Biomacromole.*, 2, 1038 (2001).
- 133- Ratzsch M., *Prog. Polym. Sci.*, 13, 277 (1988).
- 134- Reichmanis E., Frank C., O'Donnell J., Hill D., O'Donnell J., *Washington, DC: American Chemical Society*, 2 (1993).
- 135- Relleve L., Nagasawa N., Luan L.Q., Yagi T., Aranilla C., Abad L., Kume T., Yoshii F., De la Rosa A., *Polym. Degrad. and Stab.*, 87 405 (2005).
- 136- Renata Czechowska-Biskup, Bozena Rokita, Salah Lotfy,

-
- Rinaudo M., Milas M., Le Dung P., *Int. J. Biol. Macromol.*, 15, 281 (1993).
- 137- Ronge Xing, Song Liu, Huahua Yu, Quanbin Zhang, Zhien Li and Pengcheng Li, *Carbohydr. Res.*, 339, 2515 (2004).
- 138- Ronge Xing, Song Liu, Huahua Yu, Zhanyong Guo, Pibo Wang, Cuiping Li, Zhien Li and Pengcheng Li, *Carbohydr. Res.*, 340, 2150 (2005).
- 139- Sankholkar S. and Deb B. D., *J. Appl. Polym. Sci.*, 39, 1681 (1990).
- 140- Satio H., Tabeta R., *Macromol.*, 20, 2424 (1987).
- 141- Shailesh M. Kolhe, Ashok Kumar, *Radiat. Phys. and Chem.*, 74, 384 (2005).
- 142- Shari Baxter, Svetlana Zivanovic and Jochen Weiss, *Food Hydrocolloid.*, 19, 821 (2005).
- 143- Shih-Chang Hsu, Trong-Ming Don, Wen-Yen Chiua, *Polym. Degrad. and Stab.*, 75, 73 (2002).
- 144- Shi-Ming Wang, Qun-Zeng Huang and Qiong-Sheng Wang *Carbohydr. Res.*, 340, 1143 (2005).
- 145- Shirui Mao, Xintao Shuai, Florian Unger, Michael Simon, Dianzhou Bi, Thomas Kissel, *Int. J. of Pharmac.*, 281, 45 (2004).
- 146- Tanyarut Boonthekul, Hyun-Joon Kong, David J. Mooney *Biomater.* 26, 2455 (2005).
- 147- Tao Sun, Dongxiang Zhou, Fang Mao and Yingna Zhu, *Eur. Polym. J.*, 43, 652 (2007).
- 148- Tirkistani F. A. A., *Polym. Degrad. and Stab.*, 60, 67 (1998).

- 149- Tomoda Y., Umemura K., Adachi T., *Biosci. Biotech. Biochem.*, 58, 203 (1994).
- 150- Ulanski p. and Rosiak J. , *Carbohydr. Polym.*, 60, 175 (2005).
- 151- Ulanski p. and Rosiak J., *Radiat. Phys. Chem.*, 39, 53 (1992).
- 152- Wanichpongpan P., Suriyachan K., Chandkrachang S., in: T. Uragami, K. Kurita, T. Fukamizo (Eds.), *Chitin and Chitosan in Life Science*, Yamaguchi, 198 , (2001).
- 153- Won-Seok Choi, Kil-Jin Ahn, Dong-Wook Lee, Myung-Woo Byun, *Polym. Degrad. and Stab.*, 78, 533 (2002).
- 154- Woods R. T. and Pikaev A. K., *Appl. Radi. Chem.*, 341, 352 (1994).
- 155- Wuling Lin, Xiangyang Hu, Wenqing Zhang, W. John Rogers, Weiming Cai, *J. of Plant Physiol.*, 162, 937 (2005).
- 156- Yamada K, Gondo T, Hirata M., *J. Appl. Polym. Sci.*, 81, 1595 (2001).
- 157- Yessica S. Ramirez-Fuentes, Emilio Bucio, Guillermina Burillo, *Nucl. Instrum. and Meth. in Phys. Res. B*, 265 183 (2007).
- 158- Young Chang Nho and Oh Hyun Kwon, Chen Jie, *Radi. Phy. and Chem.* 64, 67 (2002).
- 159- Young Chang Nho and Oh Hyun Kwon, *Radi. Phy. and Chem.* 66, 299 (2003).
- 160- Zhao Wenwei, Zhong Xiaoguang, Yu Li, Zhang Yuefang and Sun Jiazhen, *Polym. Degrad. and Stab.*, 41, 83 (1993).

-
- 161- Zhi-Kang Xu, Fu-Qiang Nie, Chao Qu, Ling-Shu Wan, Jian Wu, Ke Yao, *Biomater.*, 26, 589 (2005).
 - 162- Zou X. P., Kang E. T., Neoh K. G., *Surf. Coat. Technol.*, 149, 119 (2002).